

Biases in the estimation of the hydrostatic mass of the Virgo simulated CLONE

Théo Lebeau

Supervisors : Nabila Aghanim and Jenny Sorce

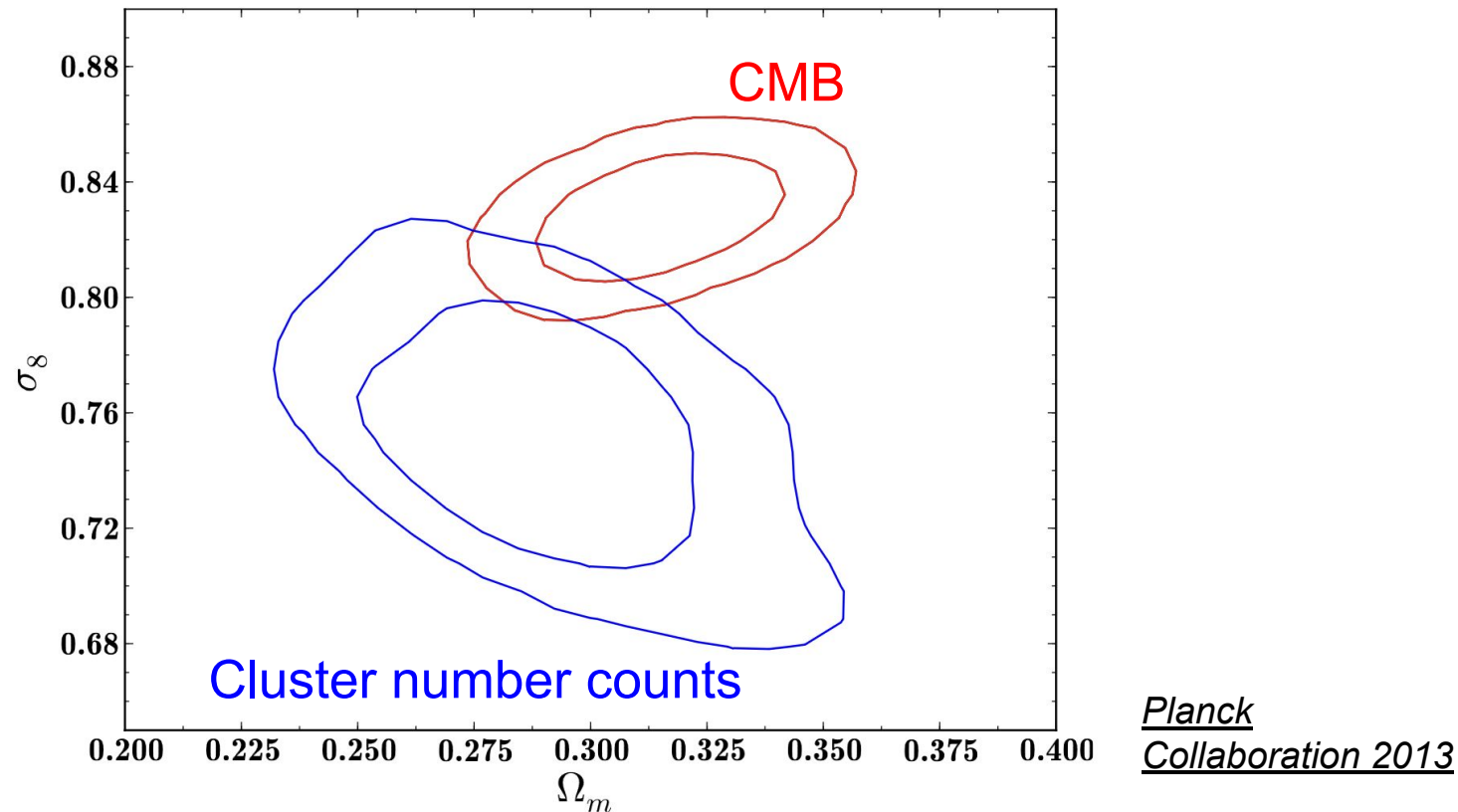


Clusters as cosmological probes

- Clusters formed by gravitational collapse, tracers of the matter distribution in the Universe depending on σ_8 and Ω_m

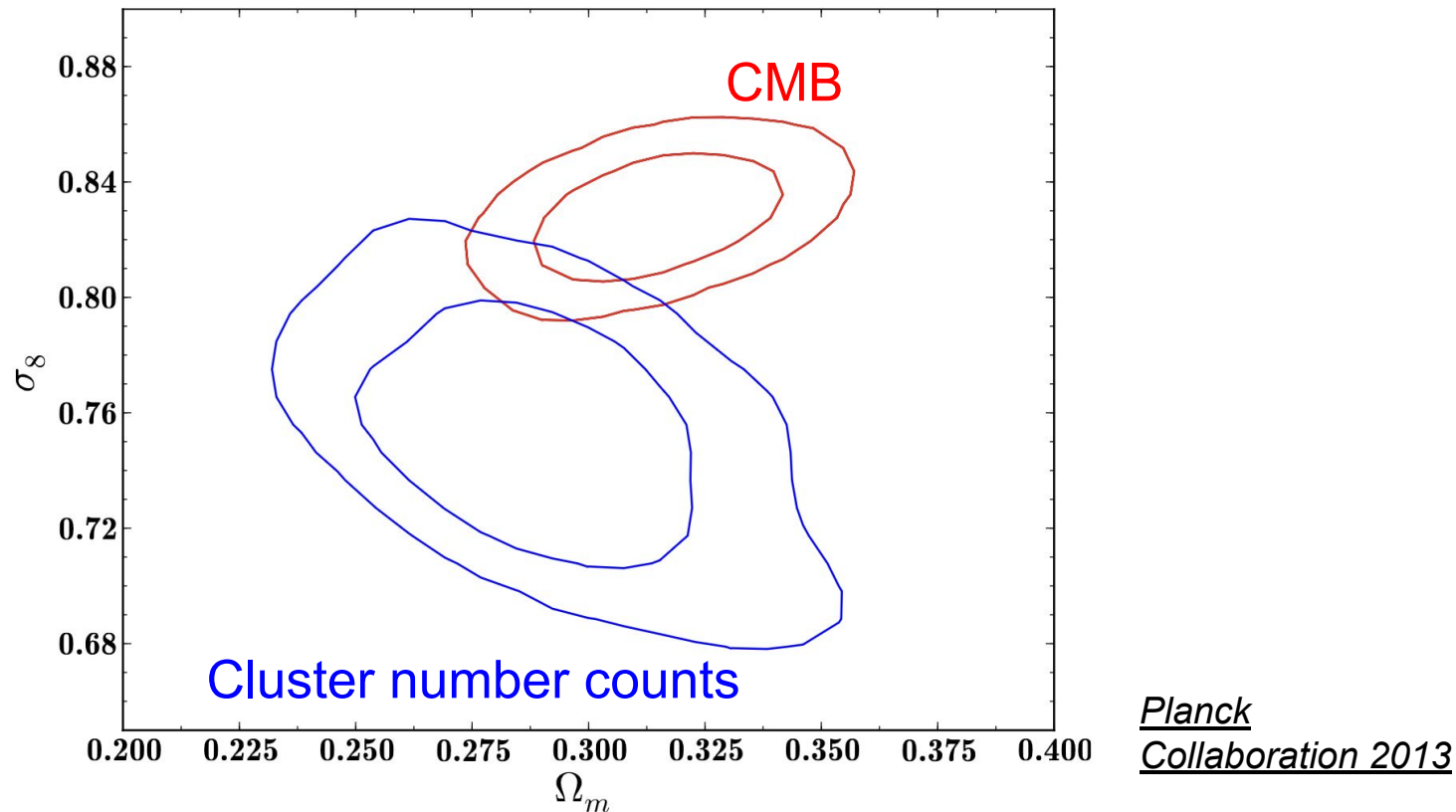
Clusters as cosmological probes

- Clusters formed by gravitational collapse, tracers of the matter distribution in the Universe depending on σ_8 and Ω_m
- Constraints on the cosmological parameters using the cluster number counts



Clusters as cosmological probes

- Clusters formed by gravitational collapse, tracers of the matter distribution in the Universe depending on σ_8 and Ω_m
- Constraints on the cosmological parameters using the cluster number counts



- The tension can be resolved by introducing the mass bias $(1-b) \in [0.5, 1.2]$

Calculating cluster masses with the ICM

Hypothesis :

- **Hydrostatic equilibrium** between the intra-cluster medium (ICM) and the **gravitational potential well** (dark matter + baryons)
- Spherical symmetry
- No turbulent or magnetic pressure

Calculating cluster masses with the ICM

Hypothesis :

- **Hydrostatic equilibrium** between the intra-cluster medium (ICM) and the **gravitational potential well** (dark matter + baryons)
- Spherical symmetry
- No turbulent or magnetic pressure

$$\frac{dP}{dr} = -\frac{Gm\rho}{r^2}$$

Hydrostatic Mass

$$M_{\text{HE}}(< r) = -\frac{rP_{\text{th}}(r)}{G\mu m_p n_e(r)} \frac{d \ln P_{\text{th}}(r)}{d \ln r}$$

$$M_{\text{HE}}(< r) = -\frac{rk_B T(r)}{G\mu m_p} \left[\frac{d \ln n_e(r)}{d \ln r} + \frac{d \ln T(r)}{d \ln r} \right]$$

$$P = \frac{\rho k_B T}{\mu m_p} = n_e k_B T$$

Equation of state of a perfect gas

Calculating cluster masses with the ICM

Hypothesis :

- **Hydrostatic equilibrium** between the intra-cluster medium (ICM) and the **gravitational potential well** (dark matter + baryons)
- Spherical symmetry
- No turbulent or magnetic pressure

$$\frac{dP}{dr} = -\frac{Gm\rho}{r^2}$$

Hydrostatic Mass

$$M_{\text{HE}}(< r) = -\frac{rP_{\text{th}}(r)}{G\mu m_p n_e(r)} \frac{d \ln P_{\text{th}}(r)}{d \ln r}$$

$$M_{\text{HE}}(< r) = -\frac{rk_B T(r)}{G\mu m_p} \left[\frac{d \ln n_e(r)}{d \ln r} + \frac{d \ln T(r)}{d \ln r} \right]$$

Total Mass

$$M_{\text{tot}} = M_{\text{DarkMatter}} + M_{\text{gas}}$$

$$P = \frac{\rho k_B T}{\mu m_p} = n_e k_B T$$

Equation of state of a perfect gas

Calculating cluster masses with the ICM

Hypothesis :

- **Hydrostatic equilibrium** between the intra-cluster medium (ICM) and the **gravitational potential well** (dark matter + baryons)
- Spherical symmetry
- No turbulent or magnetic pressure

$$\frac{dP}{dr} = -\frac{Gm\rho}{r^2}$$

Hydrostatic Mass

$$M_{\text{HE}}(< r) = -\frac{rP_{\text{th}}(r)}{G\mu m_p n_e(r)} \frac{d \ln P_{\text{th}}(r)}{d \ln r}$$

Total Mass

$$M_{\text{tot}} = M_{\text{DarkMatter}} + M_{\text{gas}}$$

$$P = \frac{\rho k_B T}{\mu m_p} = n_e k_B T$$

Equation of state of a perfect gas

$$M_{\text{HE}}(< r) = -\frac{rk_B T(r)}{G\mu m_p} \left[\frac{d \ln n_e(r)}{d \ln r} + \frac{d \ln T(r)}{d \ln r} \right]$$

$$M_{\text{tot}} = \frac{M_{\text{HE}}}{(1 - b)}$$

Hydrostatic mass bias

Towards bias-free mass calibration of galaxy clusters ...

Possible contributions to the mass bias

- Turbulence, magnetic pressure
- Local environnement
- Dynamical state
- **Projection effects**

Towards bias-free mass calibration of galaxy clusters ...

Possible contributions to the mass bias

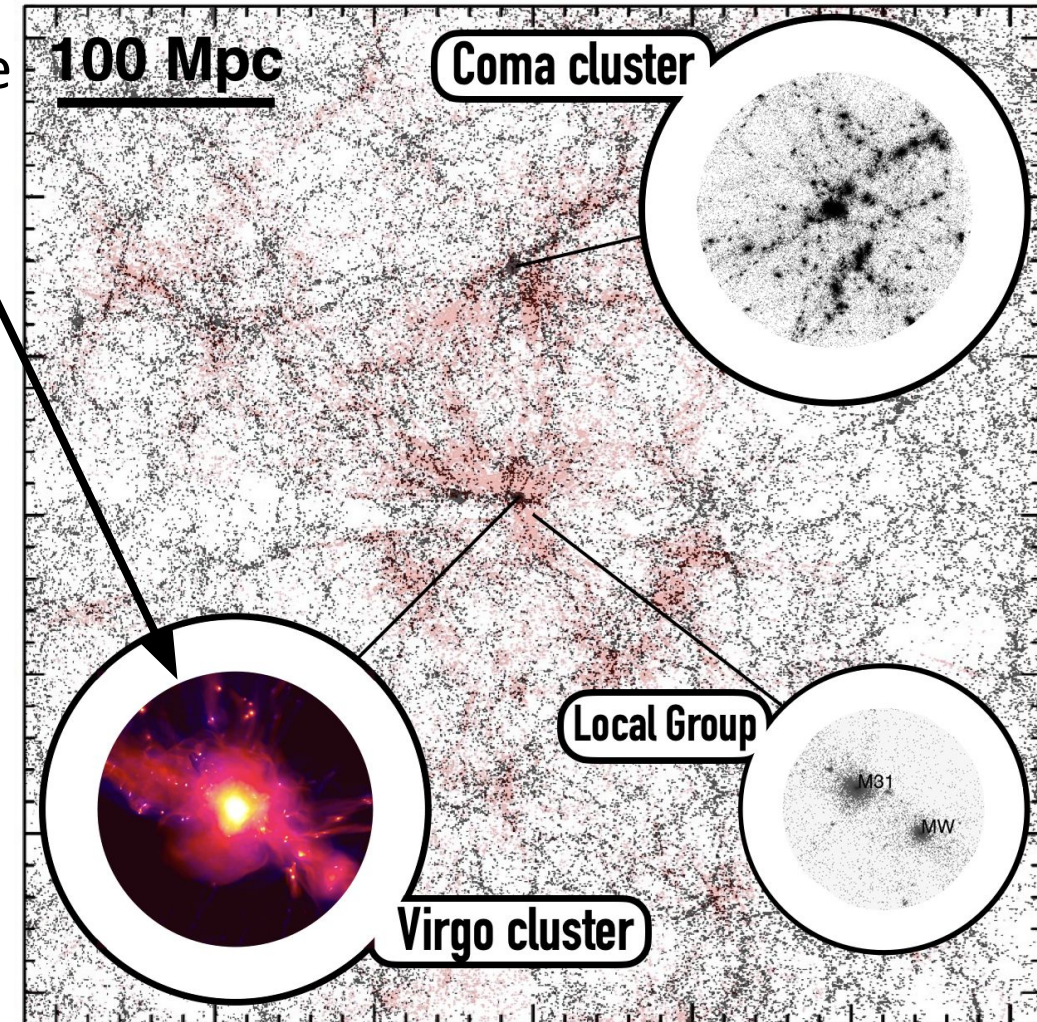
- Turbulence, magnetic pressure
- Local environnement
- Dynamical state
- **Projection effects**

The objectives:

- Quantify contributions to the bias and their impact on cluster mass estimates
- Propose a physically-motivated parametrization of the bias
- Eventually improve constraints on the cosmological parameters using galaxy clusters

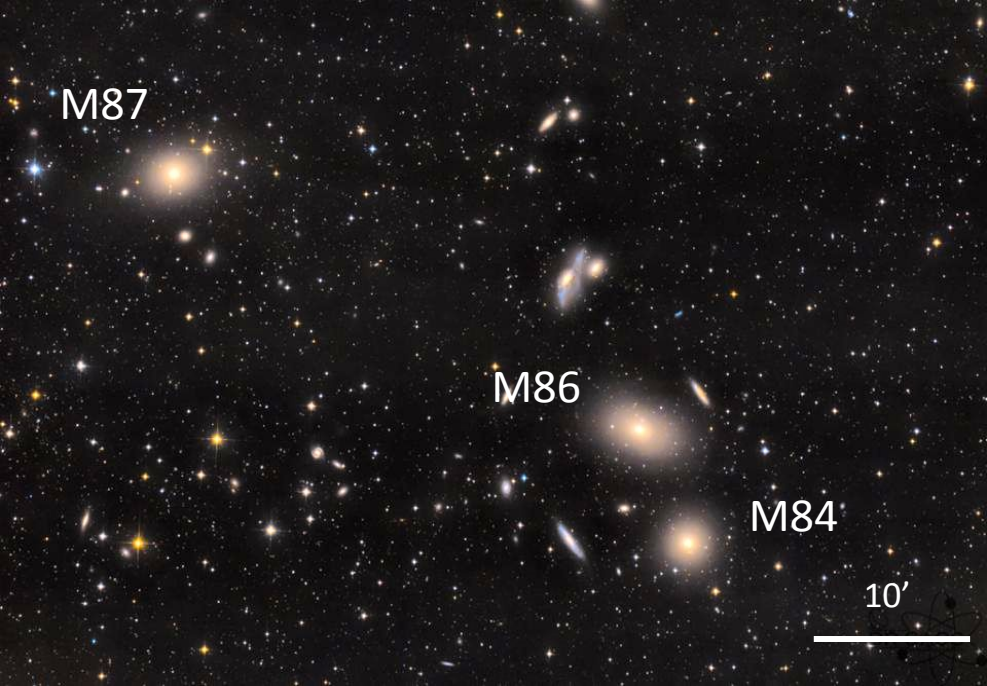
...using constrained cosmological simulations

- Cosmological simulation reproducing the Local Universe
 - Dark matter simulation on the full box
 - Hydrodynamical zoom on the Virgo cluster
 - Hydrodynamical simulation on the full box (upcoming)
 - Around 1500 cluster with a mass superior to $10^{14} M_{\odot}$ in 300Mpc around the Milky Way
- To be compared to observations and typical cosmological simulations

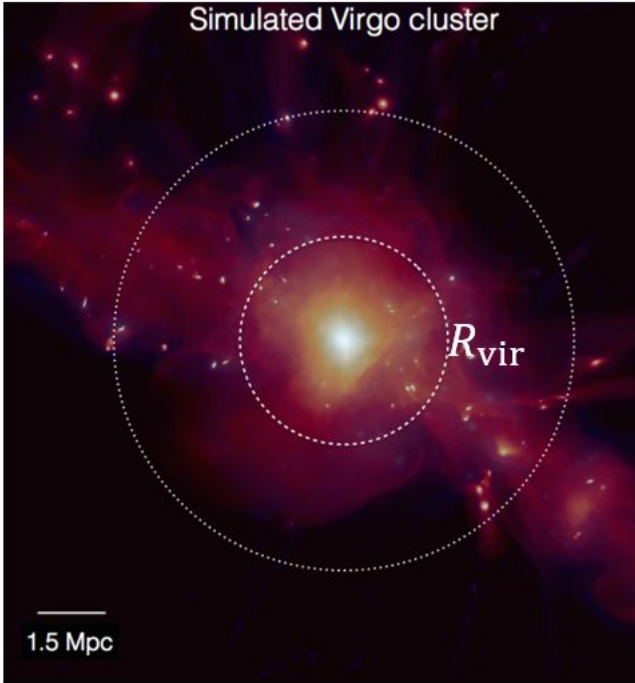


Developing the method with the Virgo cluster

Closest cluster from the Local Group , $M_{200} = 5.7 \pm 0.6 \cdot 10^{14} M_{\odot}$, $R_{200} = 1.7 \pm 0.2$ Mpc, $z = 0.00428 \pm 0.00002$ *Sorce et al. (2019)*



Astrophotography of the Virgo Cluster, Fernando Pena

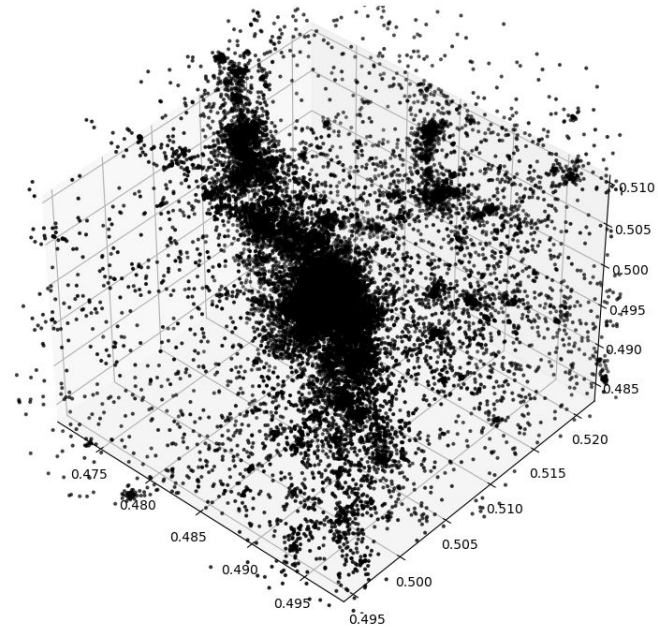


Hydrodynamical simulation of 15 Mpc radius centered on the Virgo Cluster *Sorce et al. (2021)*

Quantify the projection effects on the mass bias

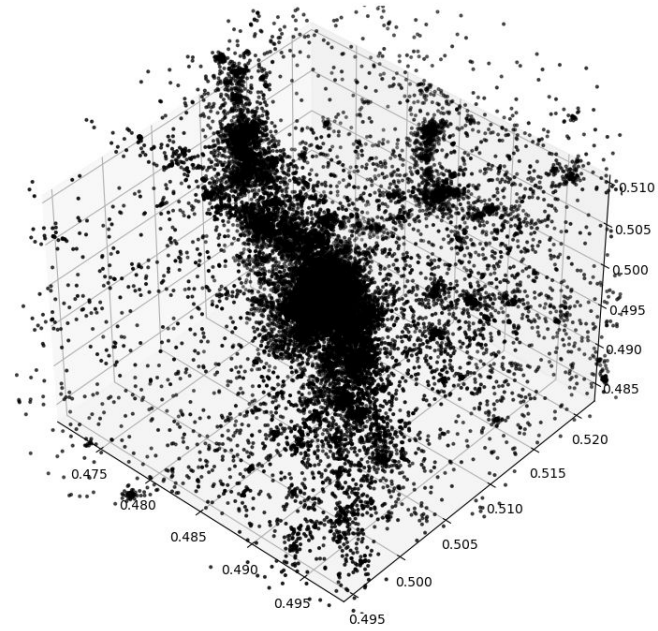
Methodology

- Select the ICM cells in the simulation dataset



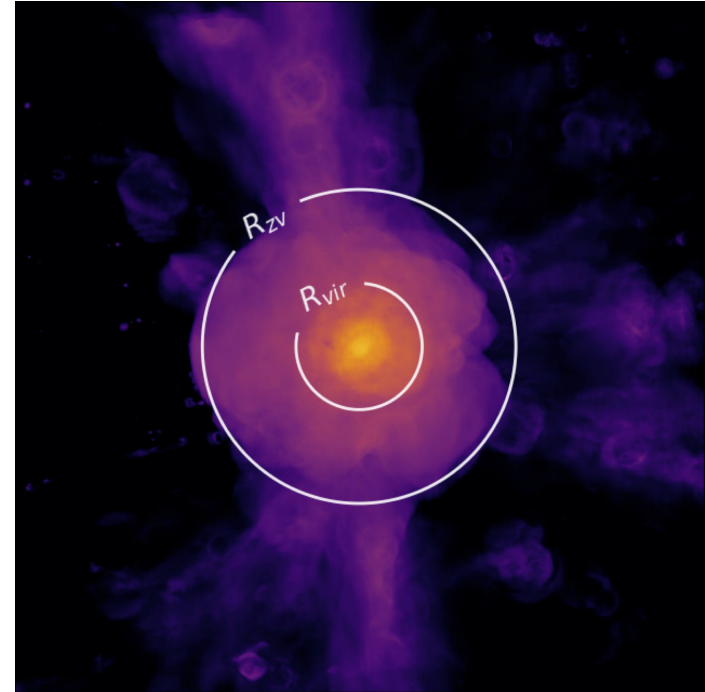
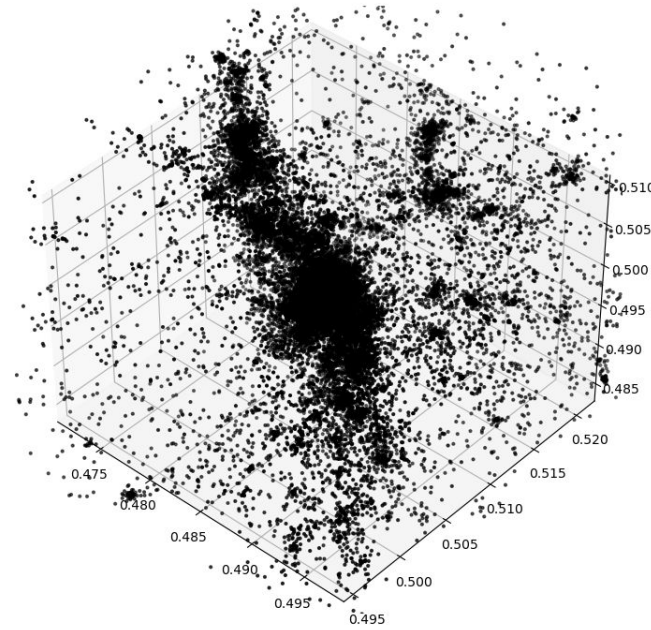
Methodology

- Select the ICM cells in the simulation dataset
- Compute pressure, electron density and temperature 3D radial profiles



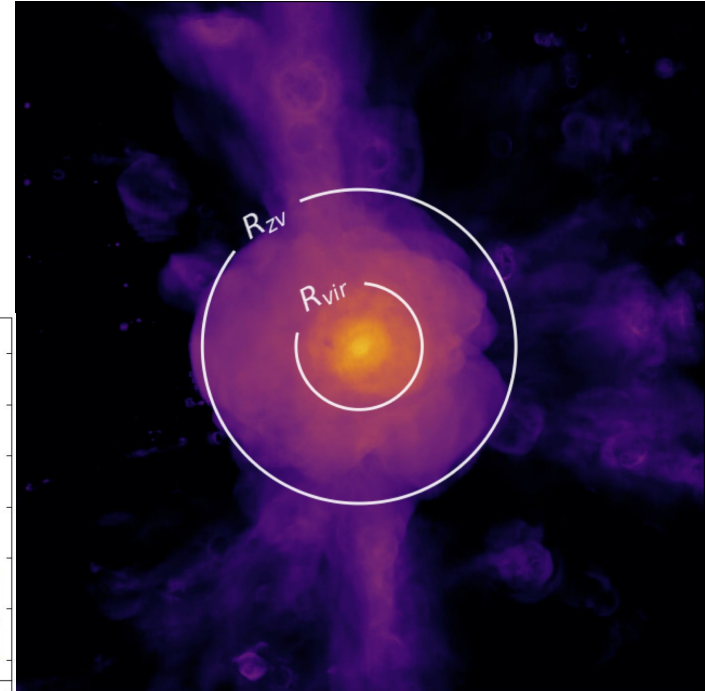
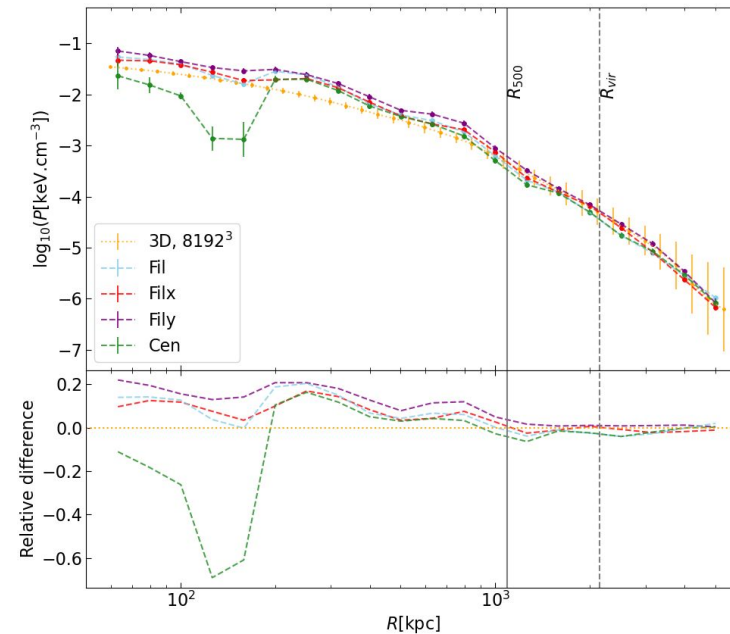
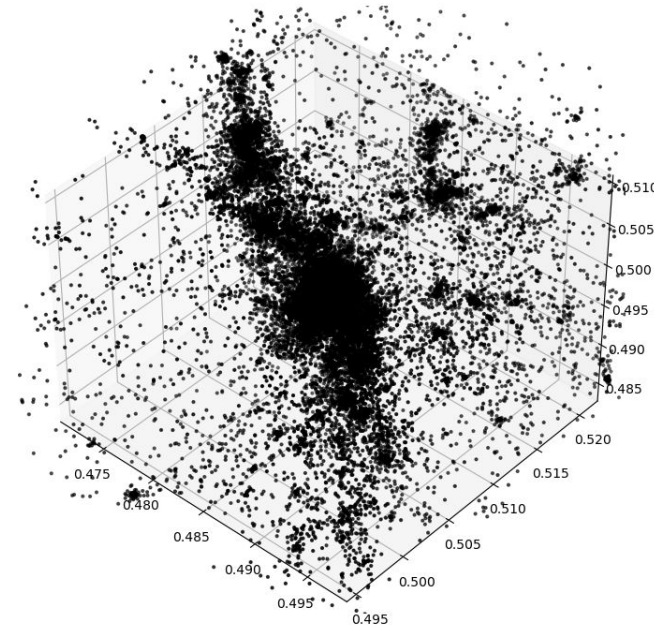
Methodology

- Select the ICM cells in the simulation dataset
- Compute pressure, electron density and temperature 3D radial profiles
- Construct maps of the same quantities in several projections



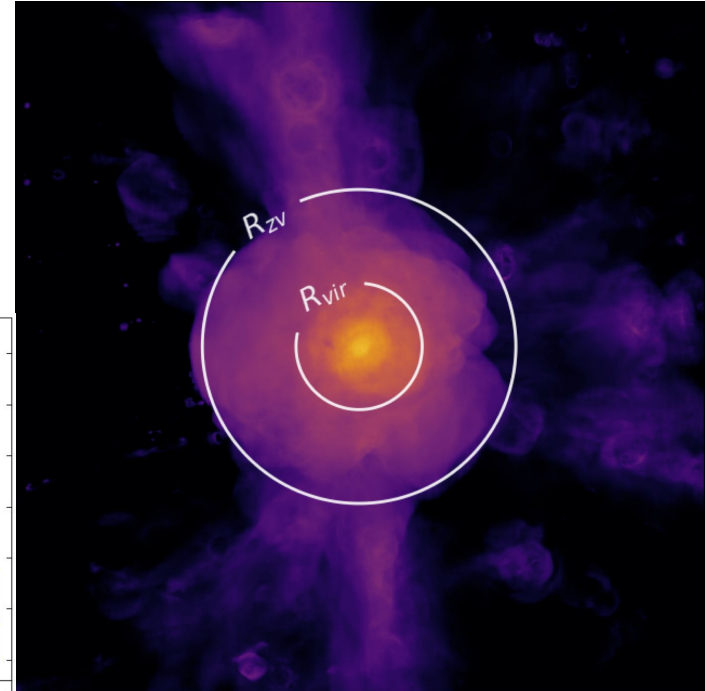
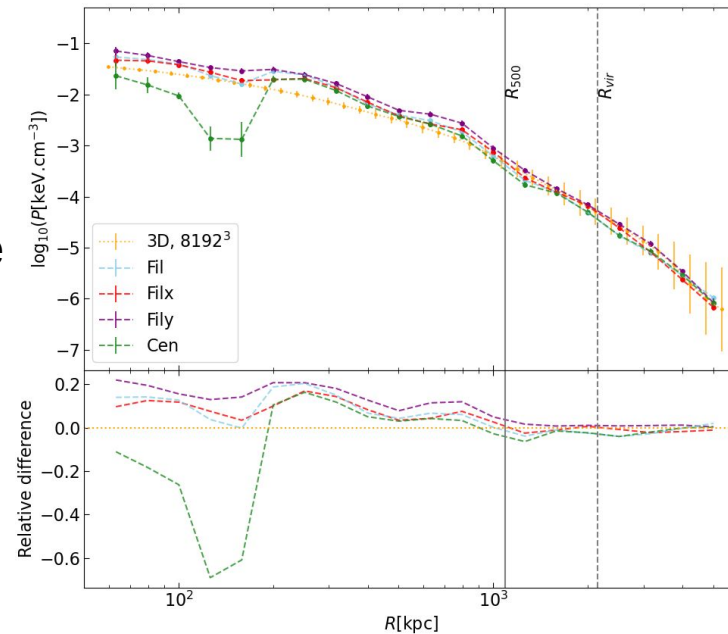
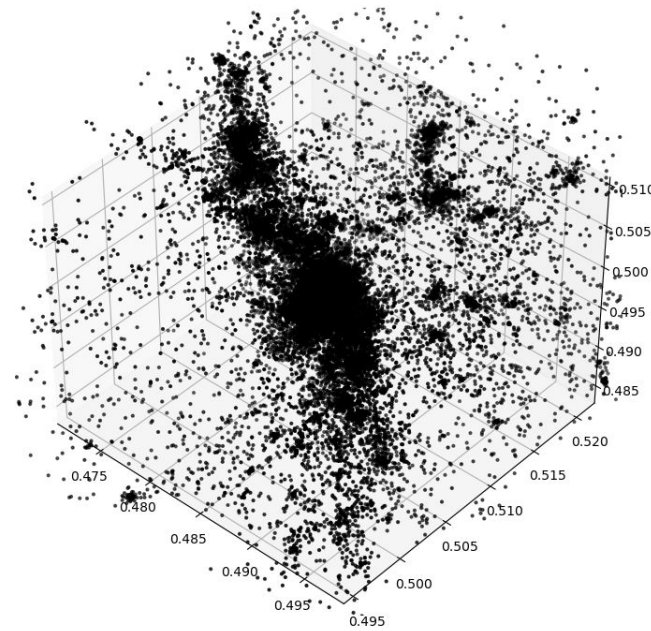
Methodology

- Select the ICM cells in the simulation dataset
- Compute pressure, electron density and temperature 3D radial profiles
- Construct maps of the same quantities in several projections
- Use a deprojection method to recover the 3D radial profiles from the 2D projected profile



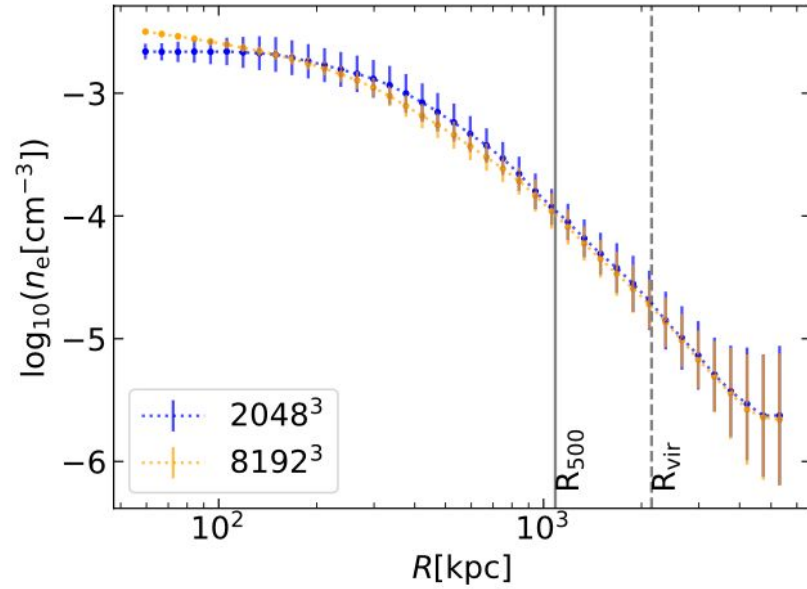
Methodology

- Select the ICM cells in the simulation dataset
- Compute pressure, electron density and temperature 3D radial profiles
- Construct maps of the same quantities in several projections
- Use a deprojection method to recover the 3D radial profiles from the 2D projected profile
- Derive the hydrostatic mass bias and compare it to the bias derived from 3D profiles

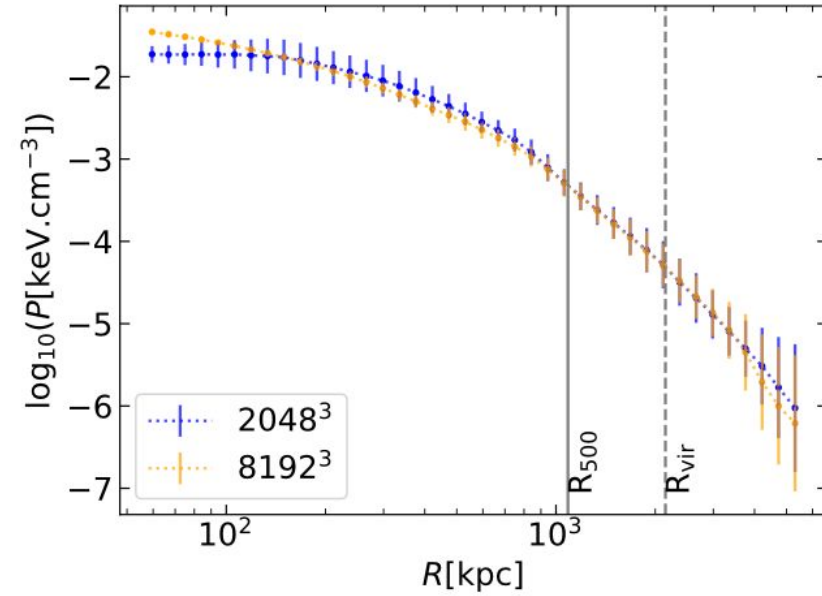


3D profiles

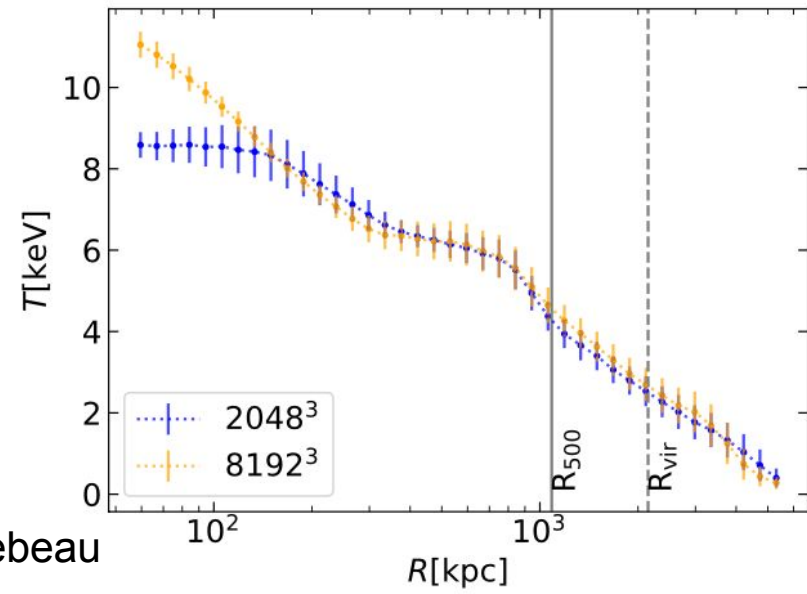
Electron density



Pressure

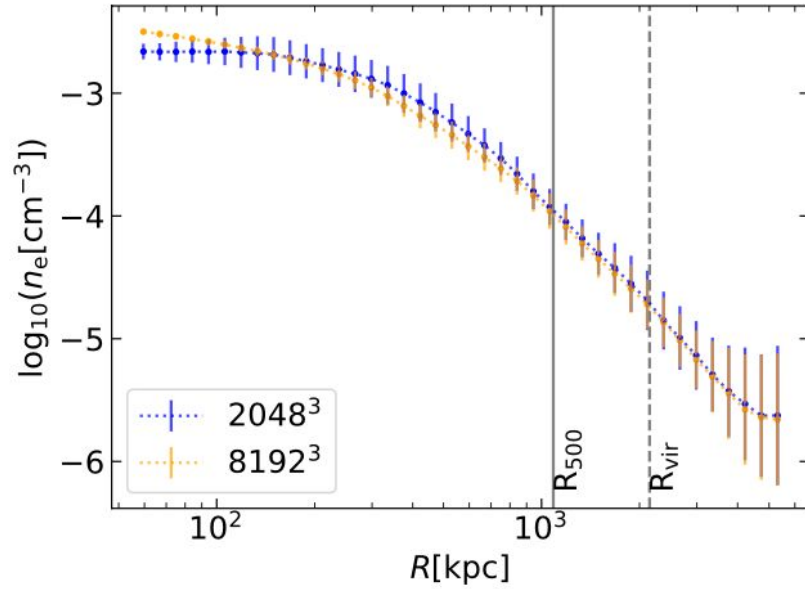


Temperature

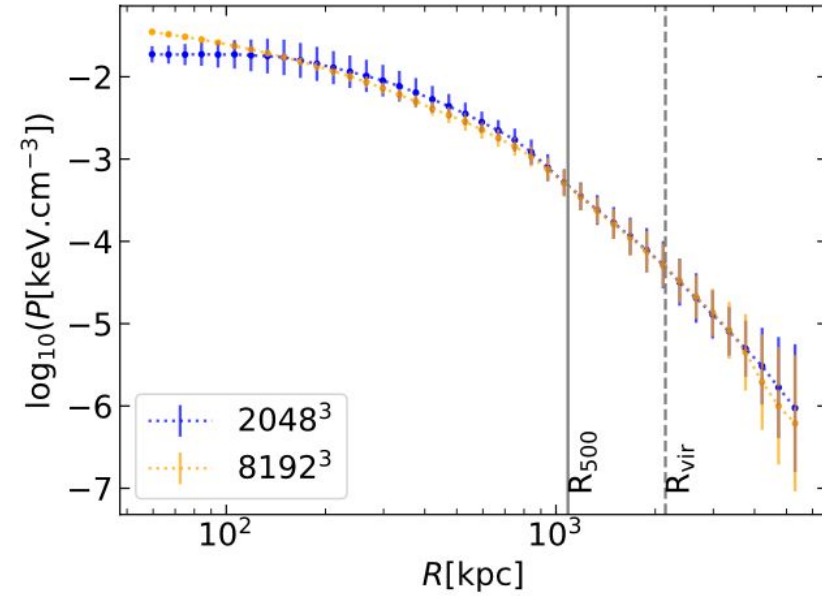


3D profiles

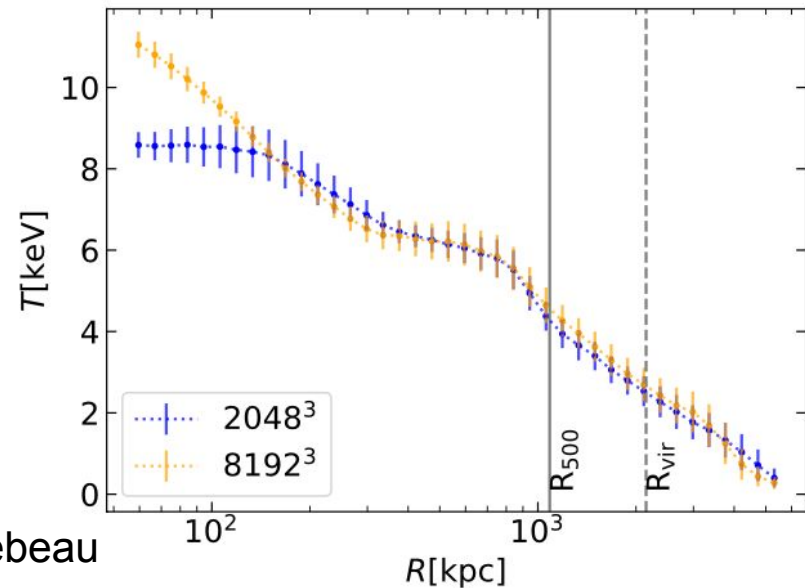
Electron density



Pressure



Temperature



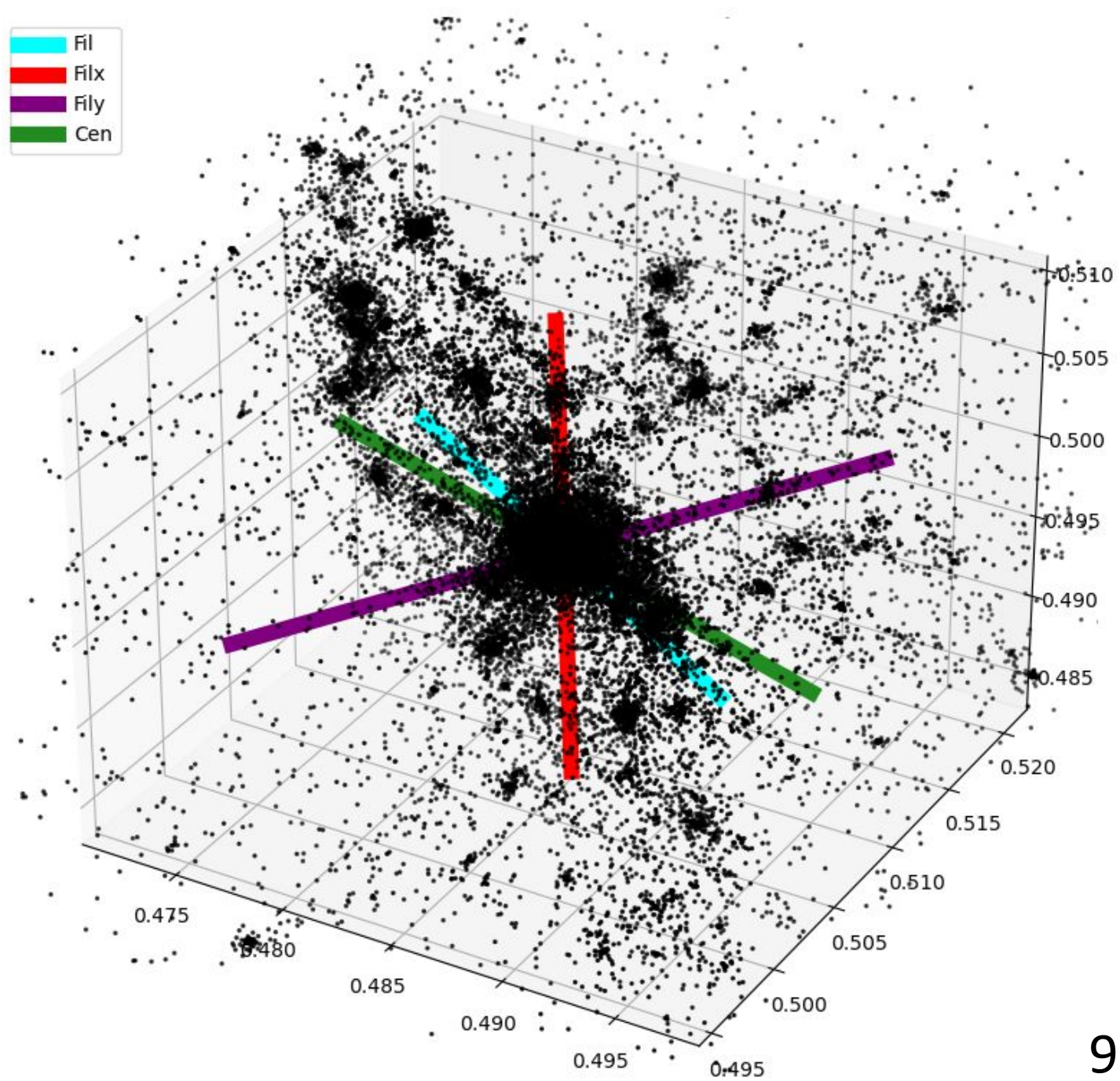
Probe of the convergence of the 2048^3 simulation for future works:
(The large scale hydro simulation will be a 2048^3)

The radial profiles are similar from $\sim 150\text{kpc}$ to the outskirts




The 2048^3 resolution can be used to study the clusters at R_{500} or R_{vir}

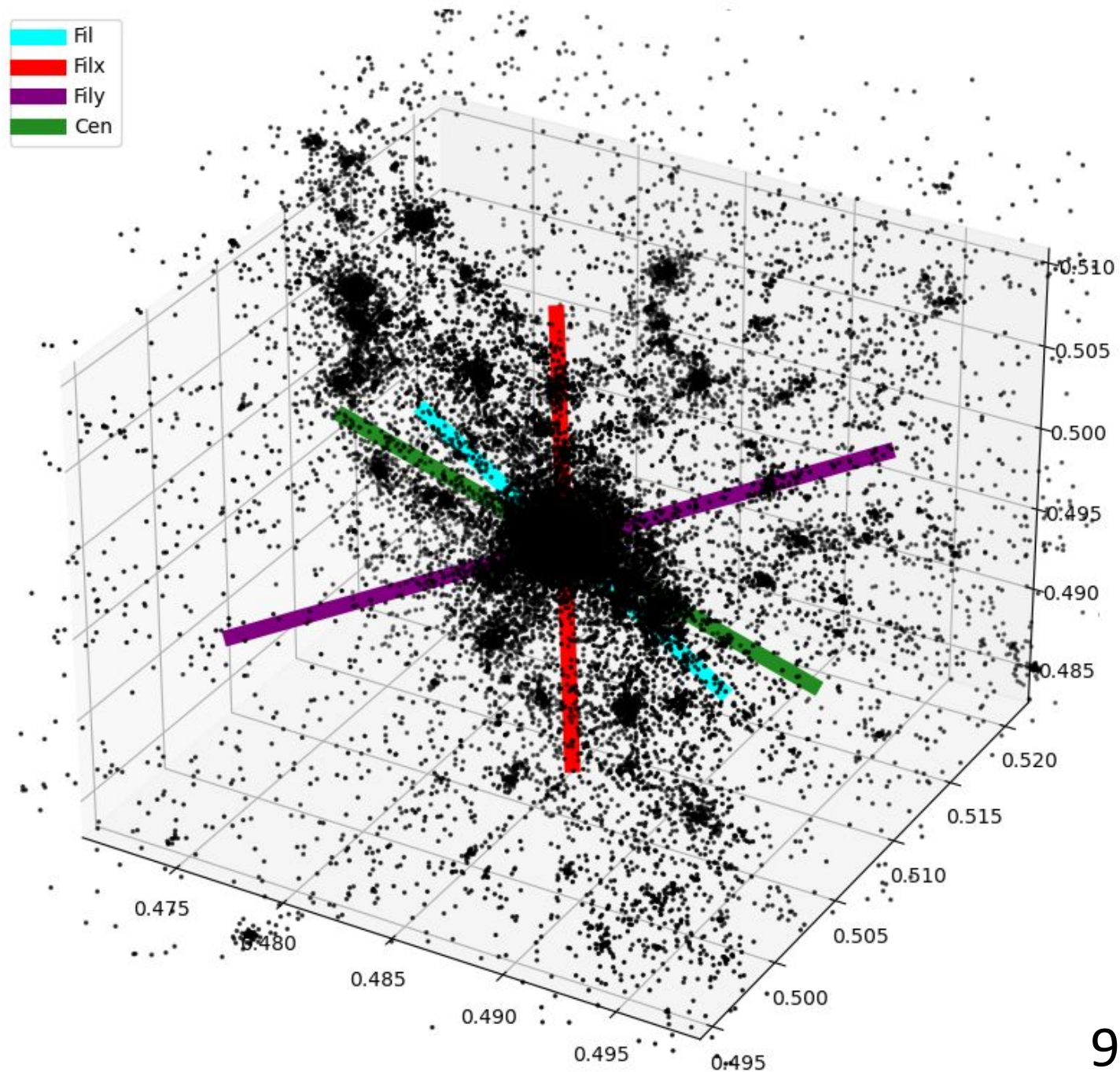
The simulated box



On next slides : LoS = Line of Sight



The simulated box

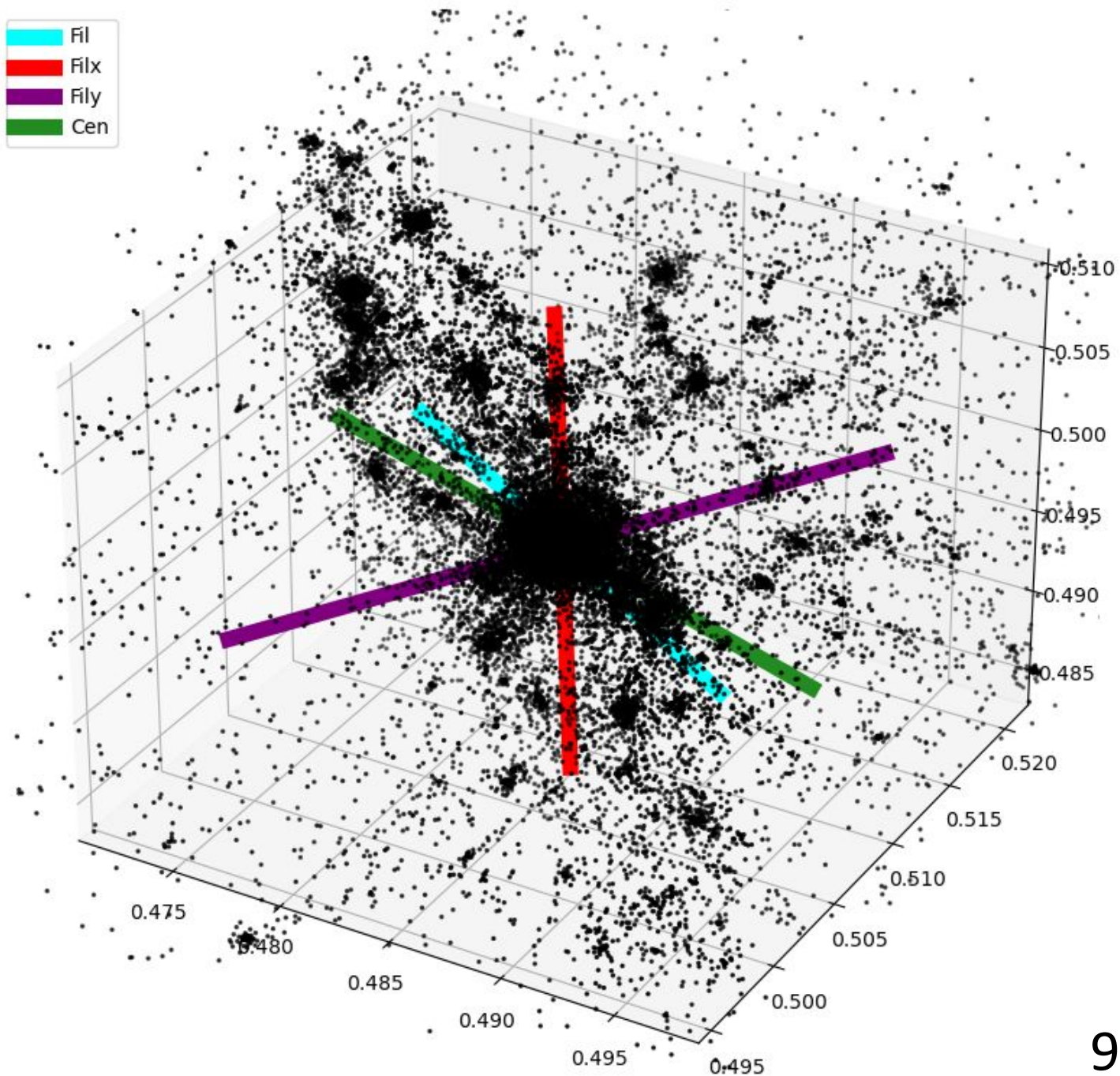
 Main filament axis (**Fil**): *should integrate the most mass*



On next slides : LoS = Line of Sight

The simulated box


-  Main filament axis (**Fil**): *should integrate the most mass*
-  Perpendicular to the main filament (x axis rotation: **Filx**): *the opposite, should integrate less mass*





On next slides : LoS = Line of Sight

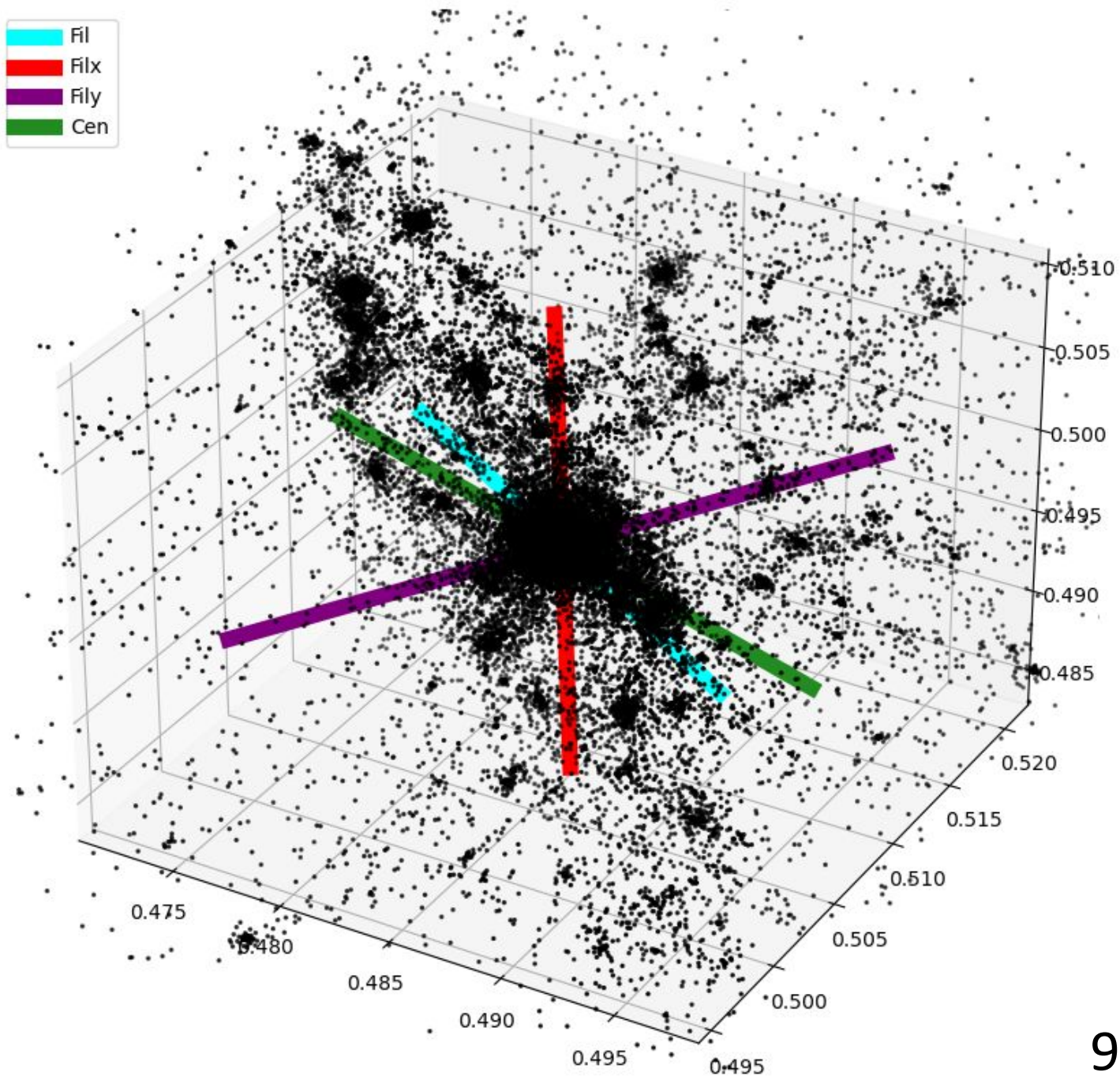
The simulated box



 Main filament axis (**Fil**): *should integrate the most mass*

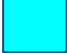



 Perpendicular to the main filament (x axis rotation: **Filx**): *the opposite, should integrate less mass*

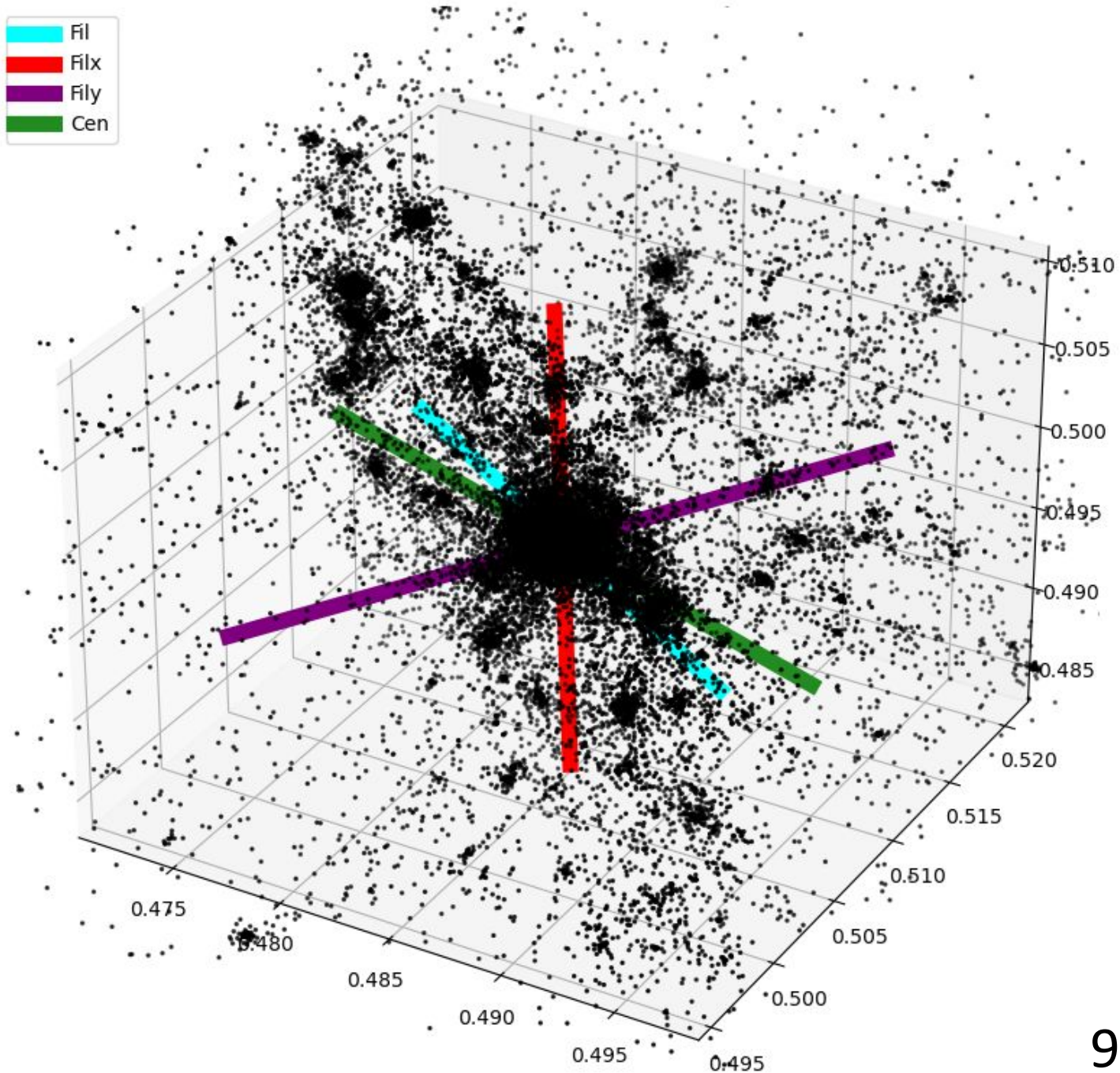
 Perpendicular to the main filament (y axis rotation : **Fily**): *the opposite, should integrate less mass*



On next slides : LoS = Line of Sight

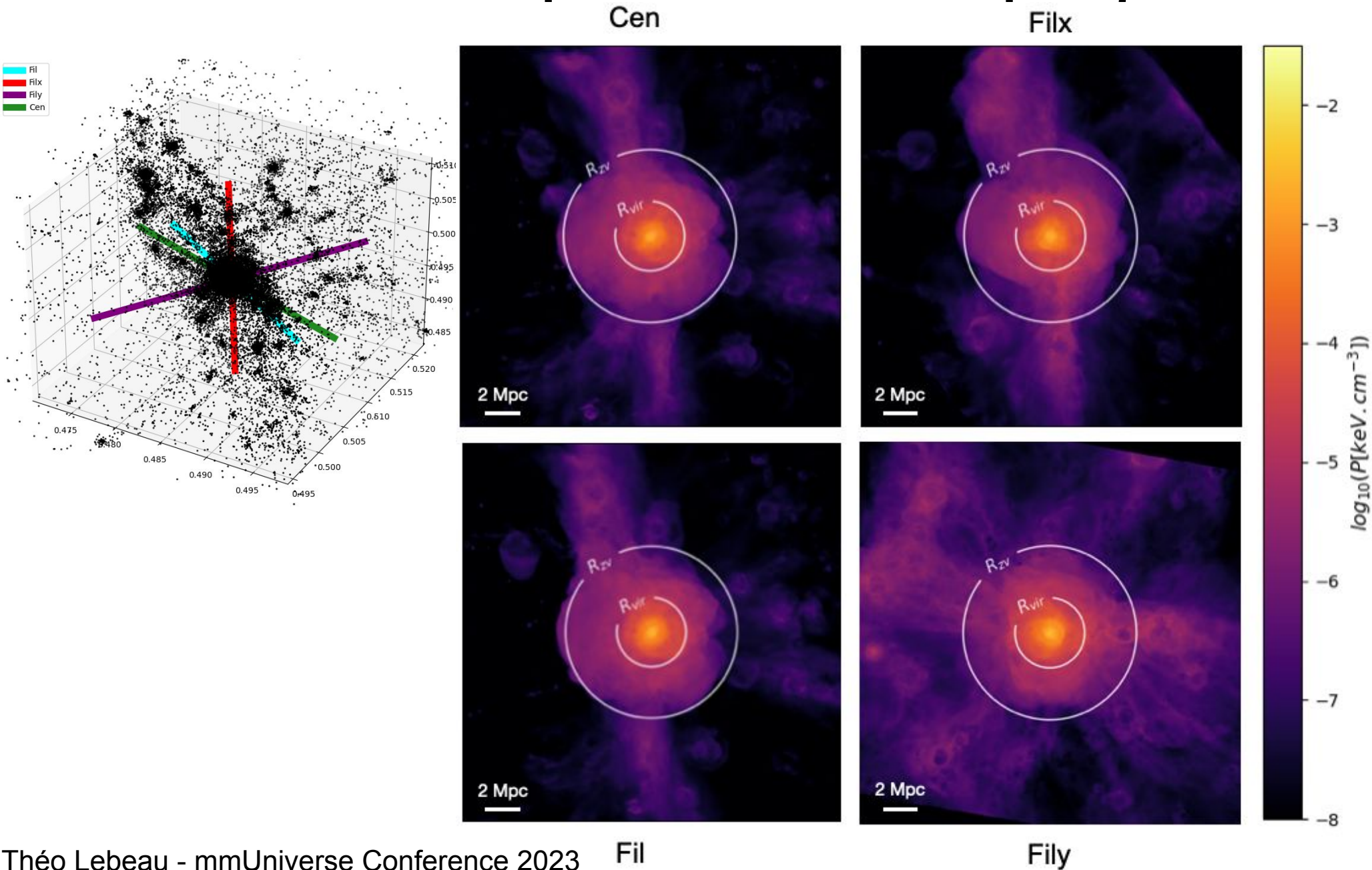
The simulated box

-  Main filament axis (**Fil**): *should integrate the most mass*
-  Perpendicular to the main filament (x axis rotation: **Filx**): *the opposite, should integrate less mass*
-  Perpendicular to the main filament (y axis rotation : **Fily**): *the opposite, should integrate less mass*
-  Virgo-center of the box axis (**Cen**): *Assuming it is close to the real line of sight*

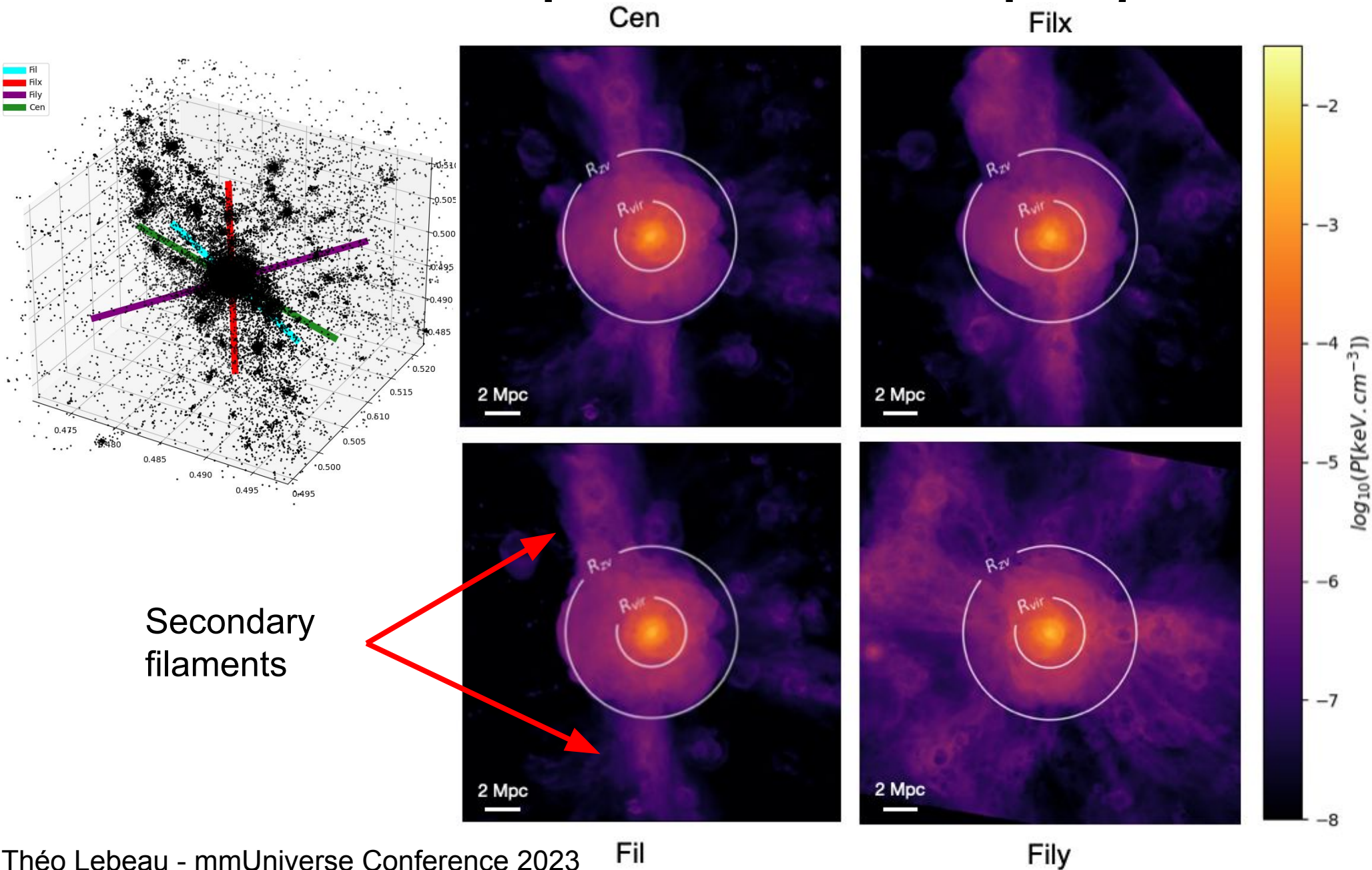


On next slides : LoS = Line of Sight

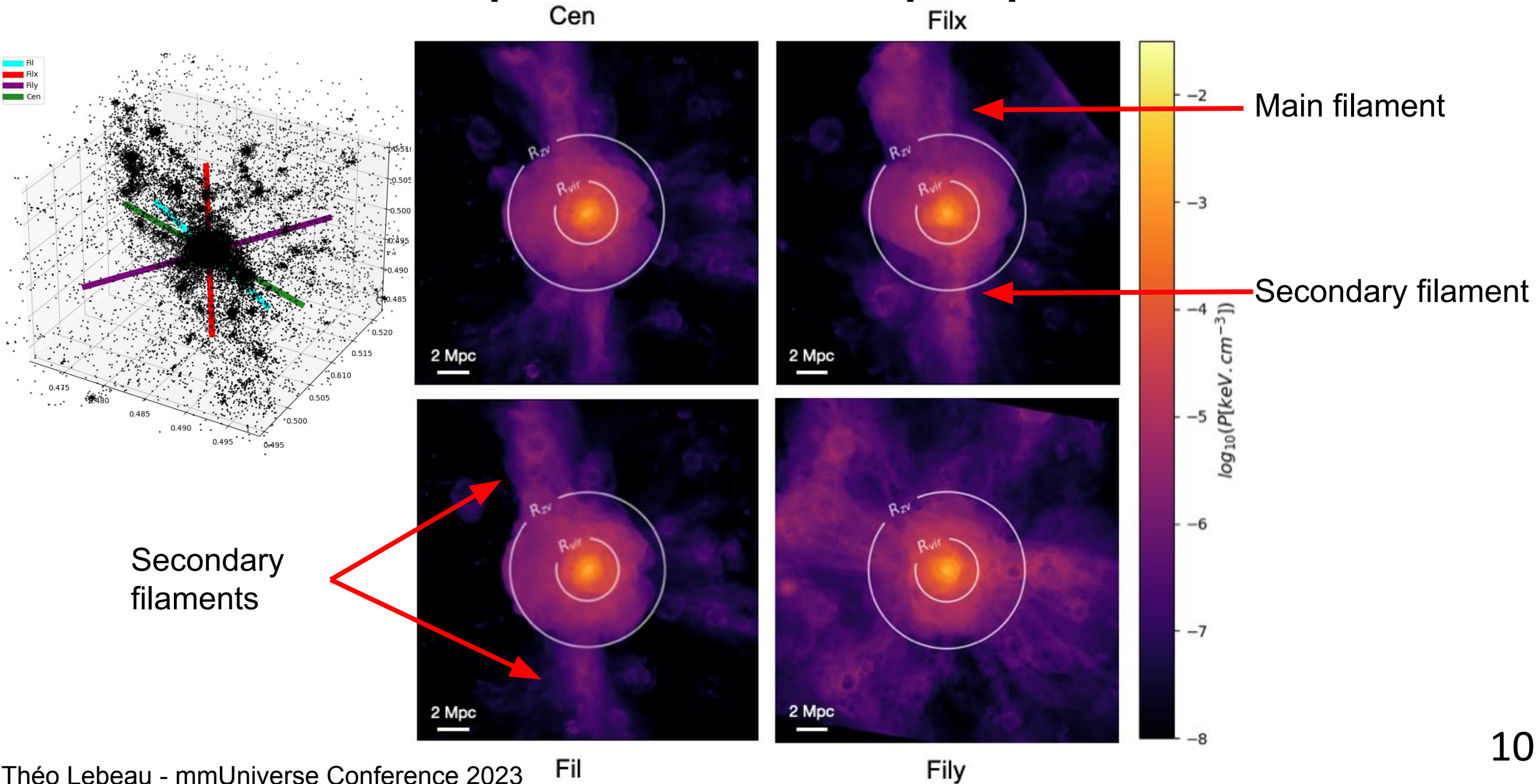
Pressure maps in several projections



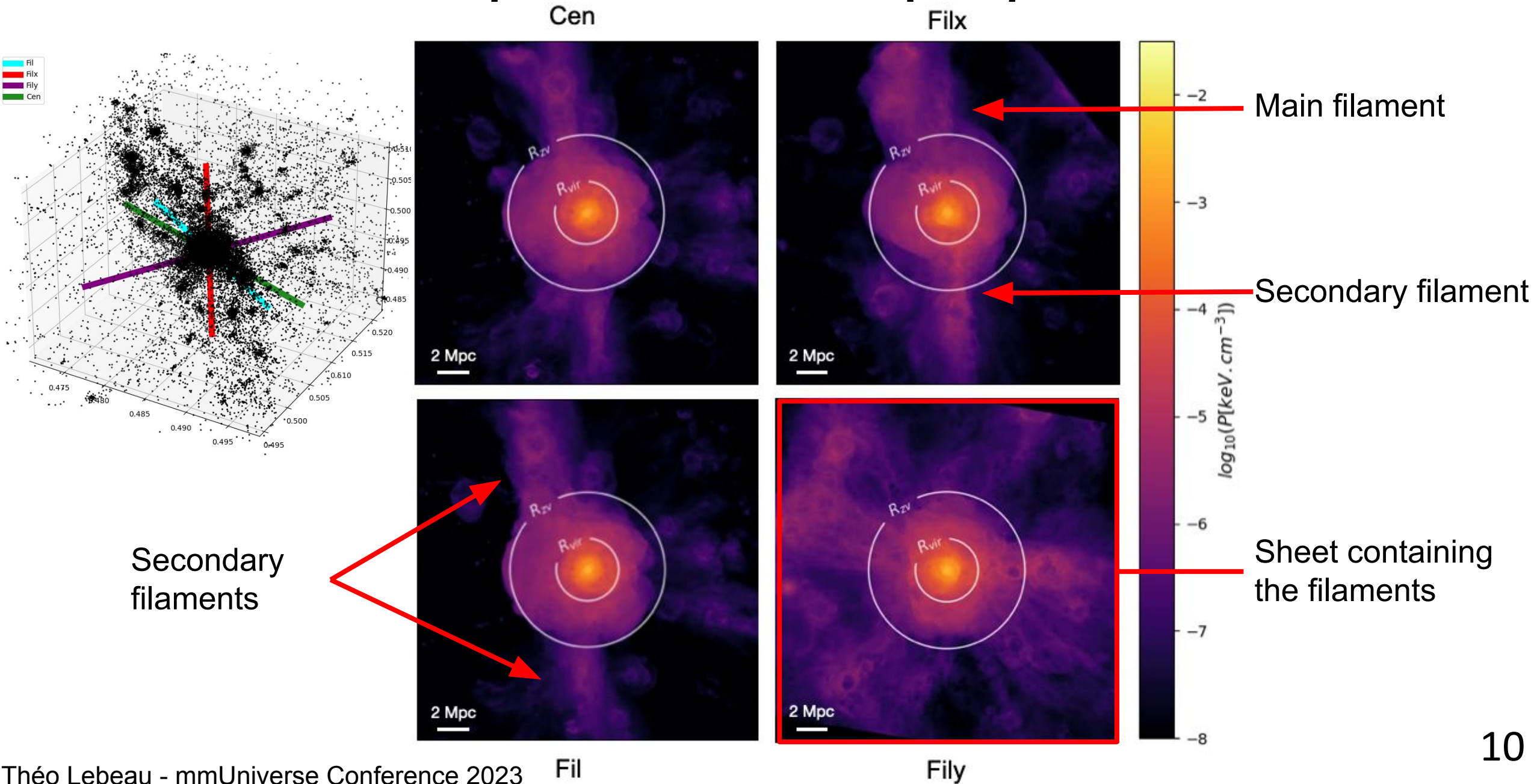
Pressure maps in several projections



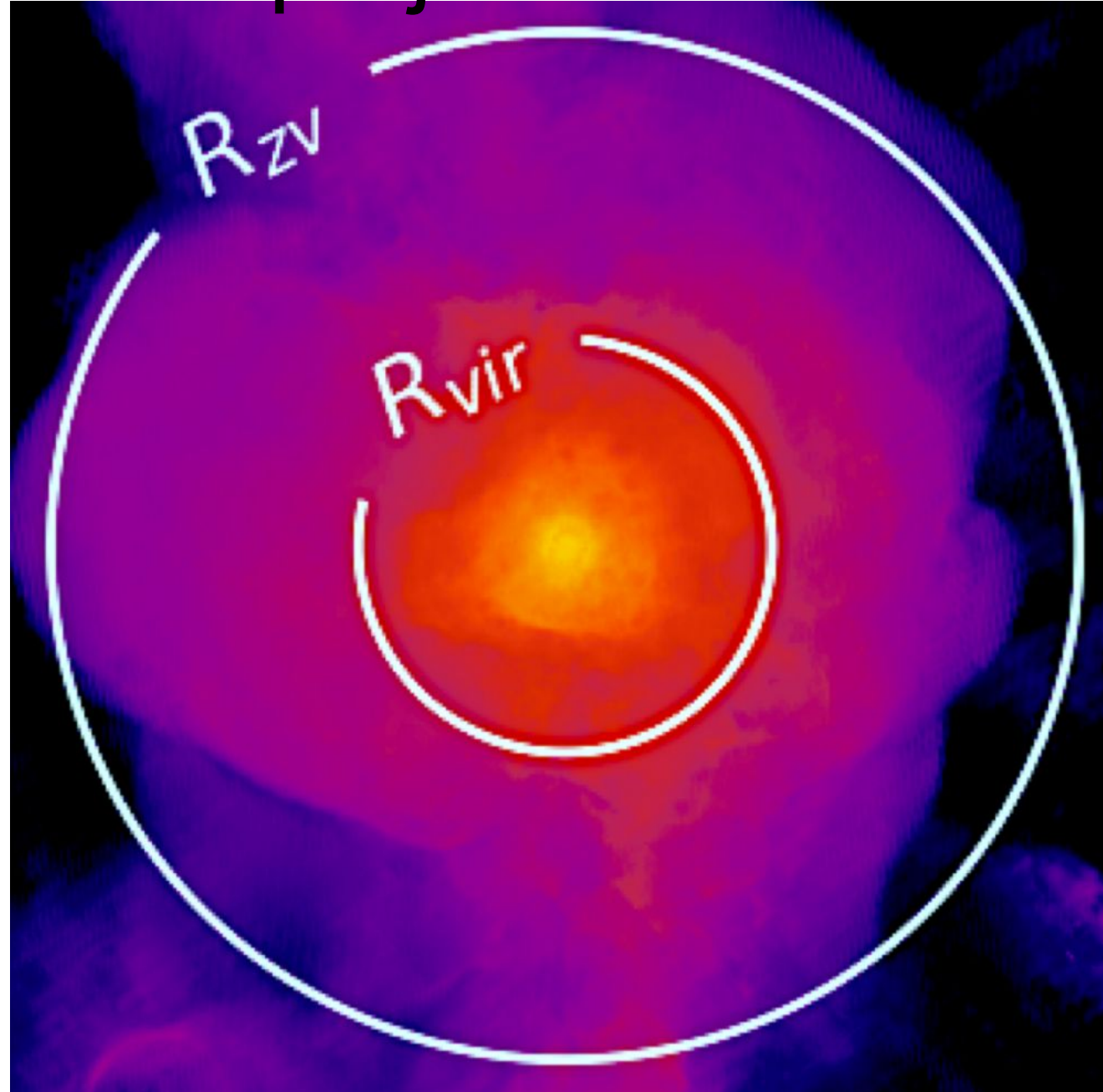
Pressure maps in several projections



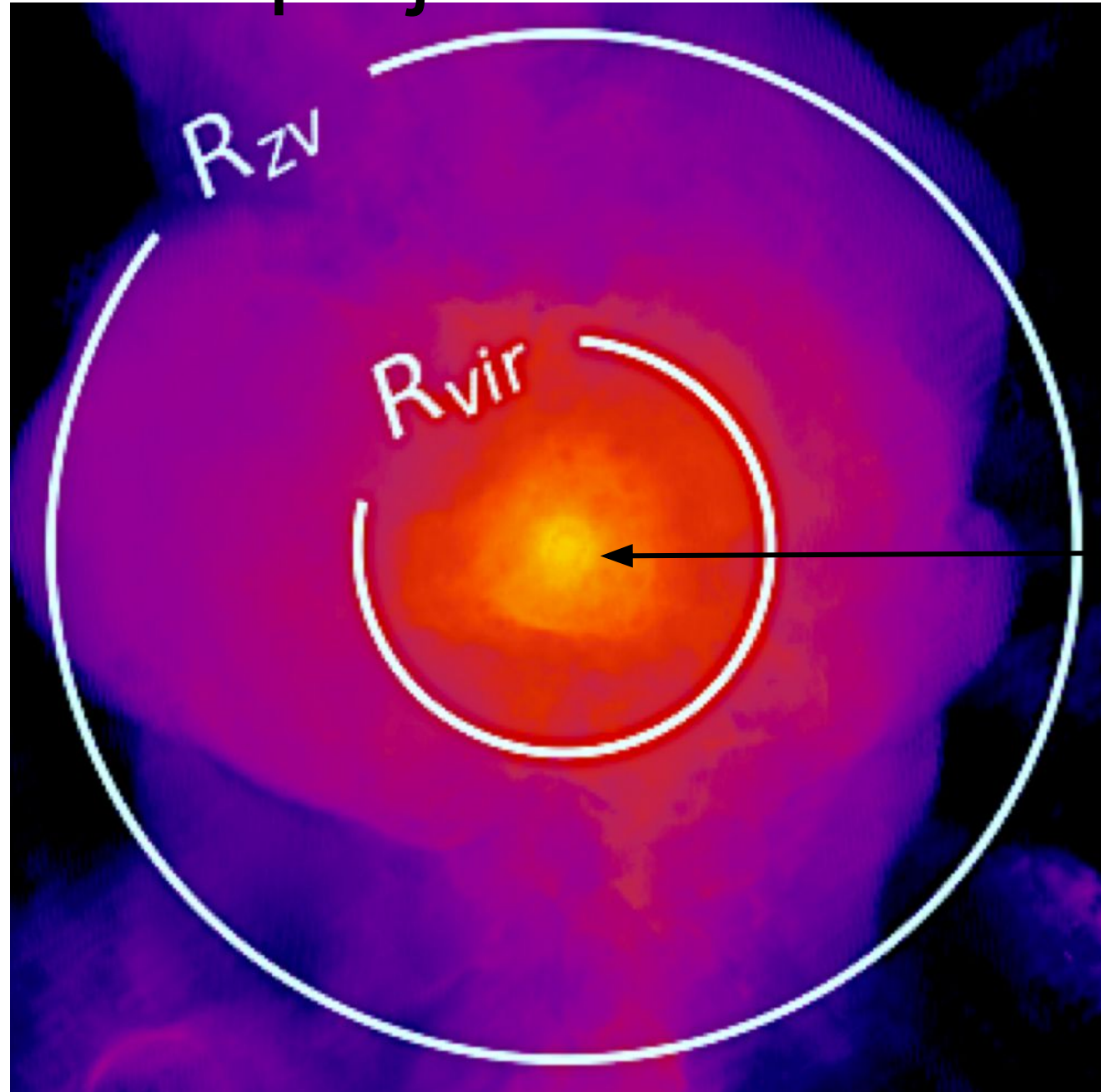
Pressure maps in several projections



Zoom on the Filx projection



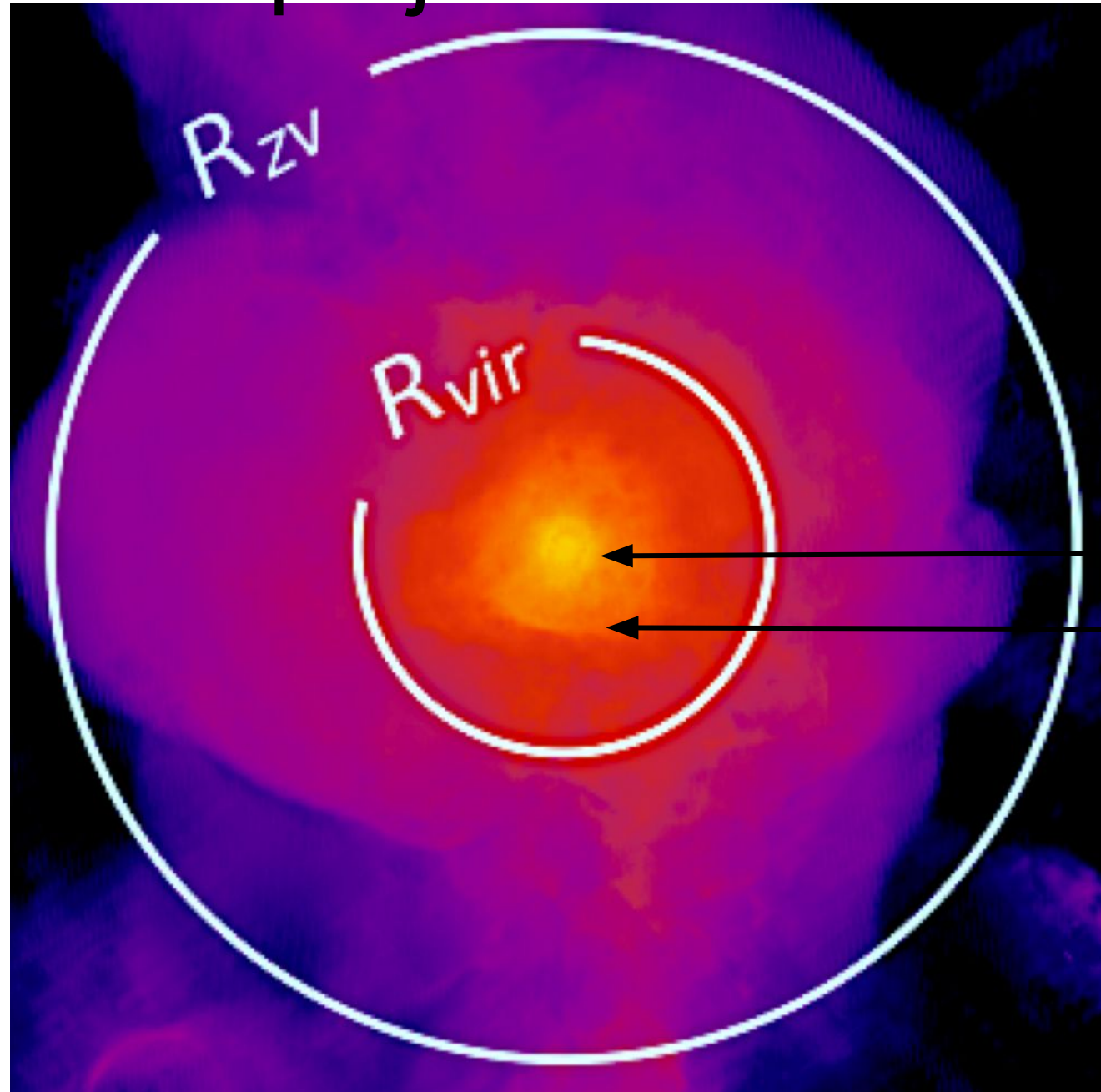
Zoom on the Filx projection



Pressure discontinuities

AGN feedback

Zoom on the Filx projection



Pressure discontinuities

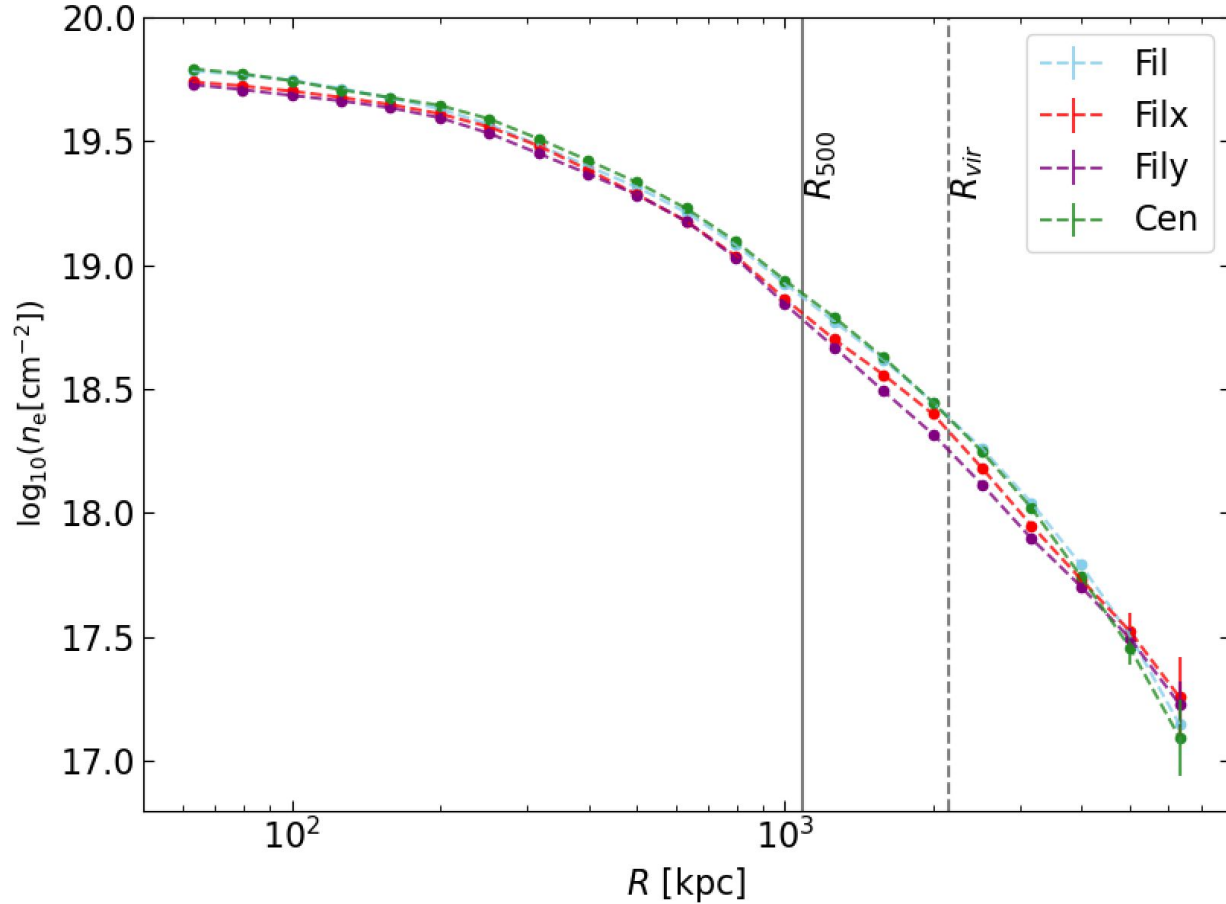
AGN feedback

Matter infall from the filament

(see Gouin et al. 2022)

Projected radial profiles

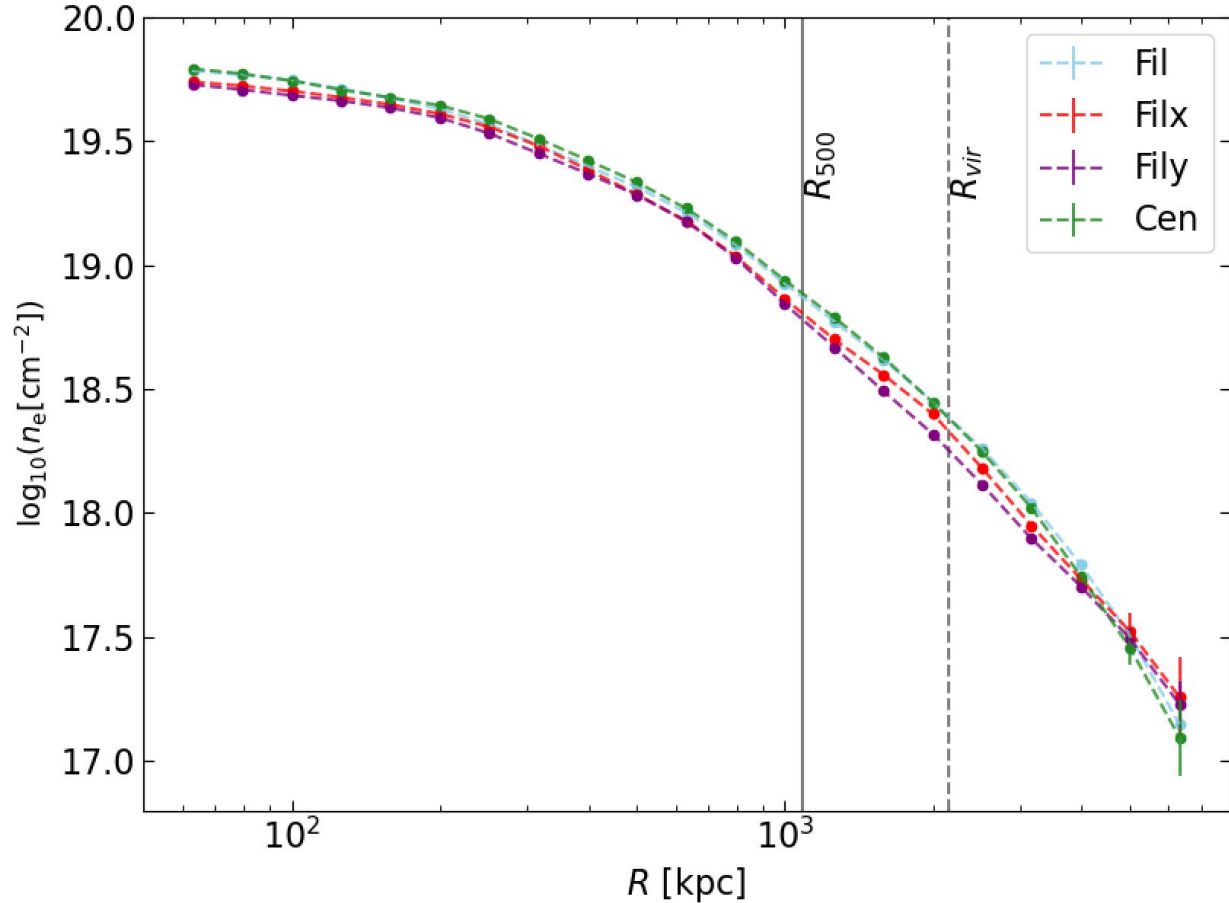
Electron Density (column density)



More mass (associated to hot gas) outside the cluster along the LoS induces **higher column density**

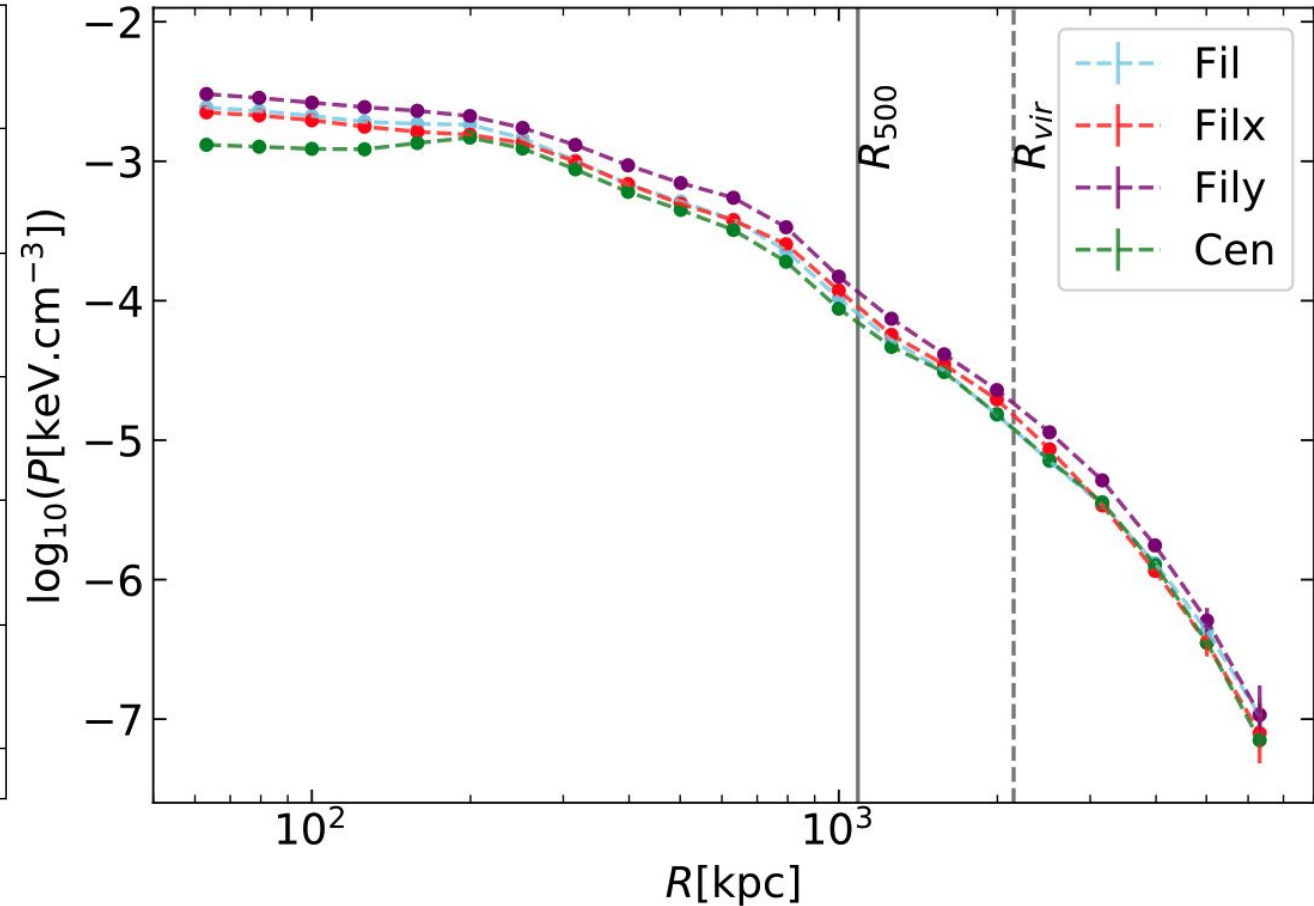
Projected radial profiles

Electron Density (column density)



More mass (associated to hot gas) outside the cluster along the LoS induces **higher column density**

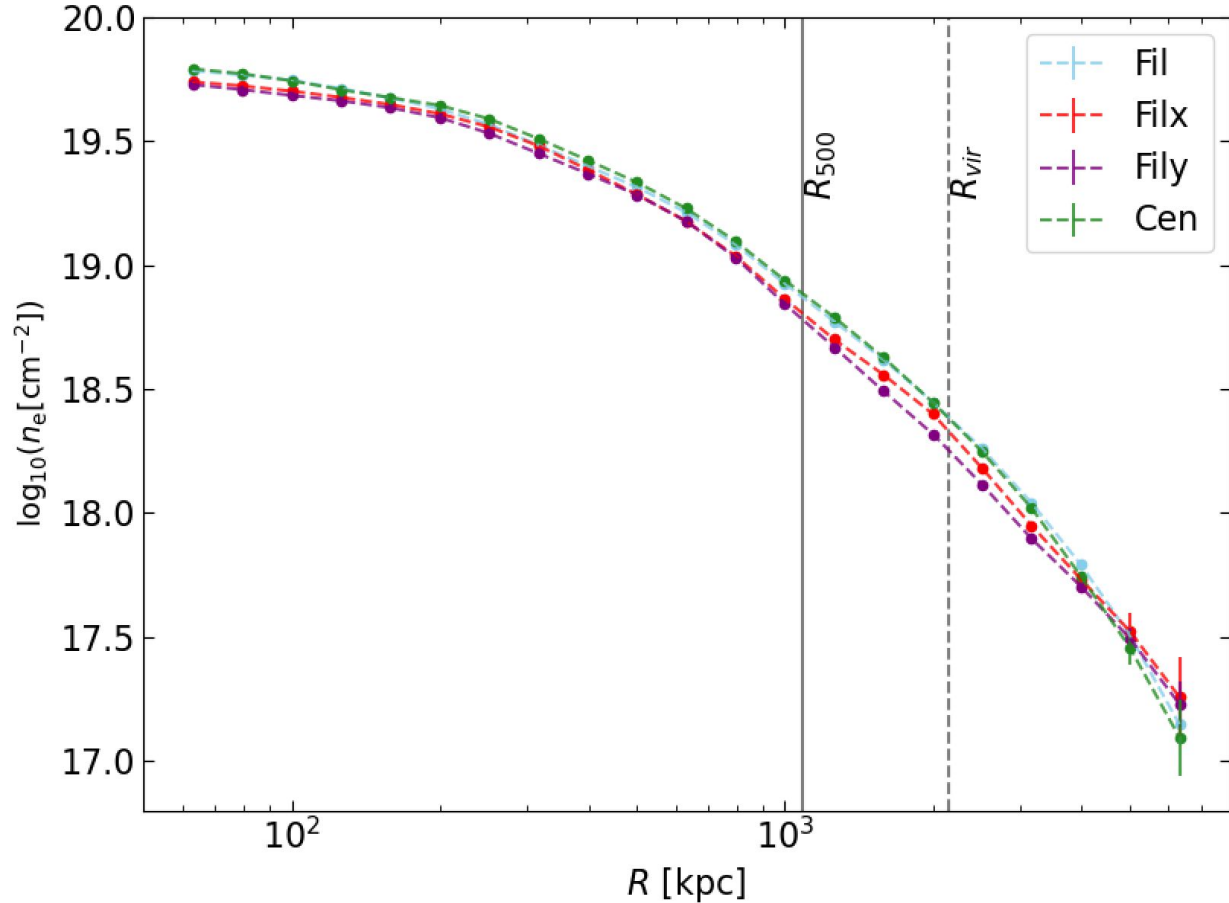
Pressure (mass-weighted mean)



Mass (associated to hot gas) outside the cluster along the LoS induces **lower mean pressure** (contribution from the foreground and background)

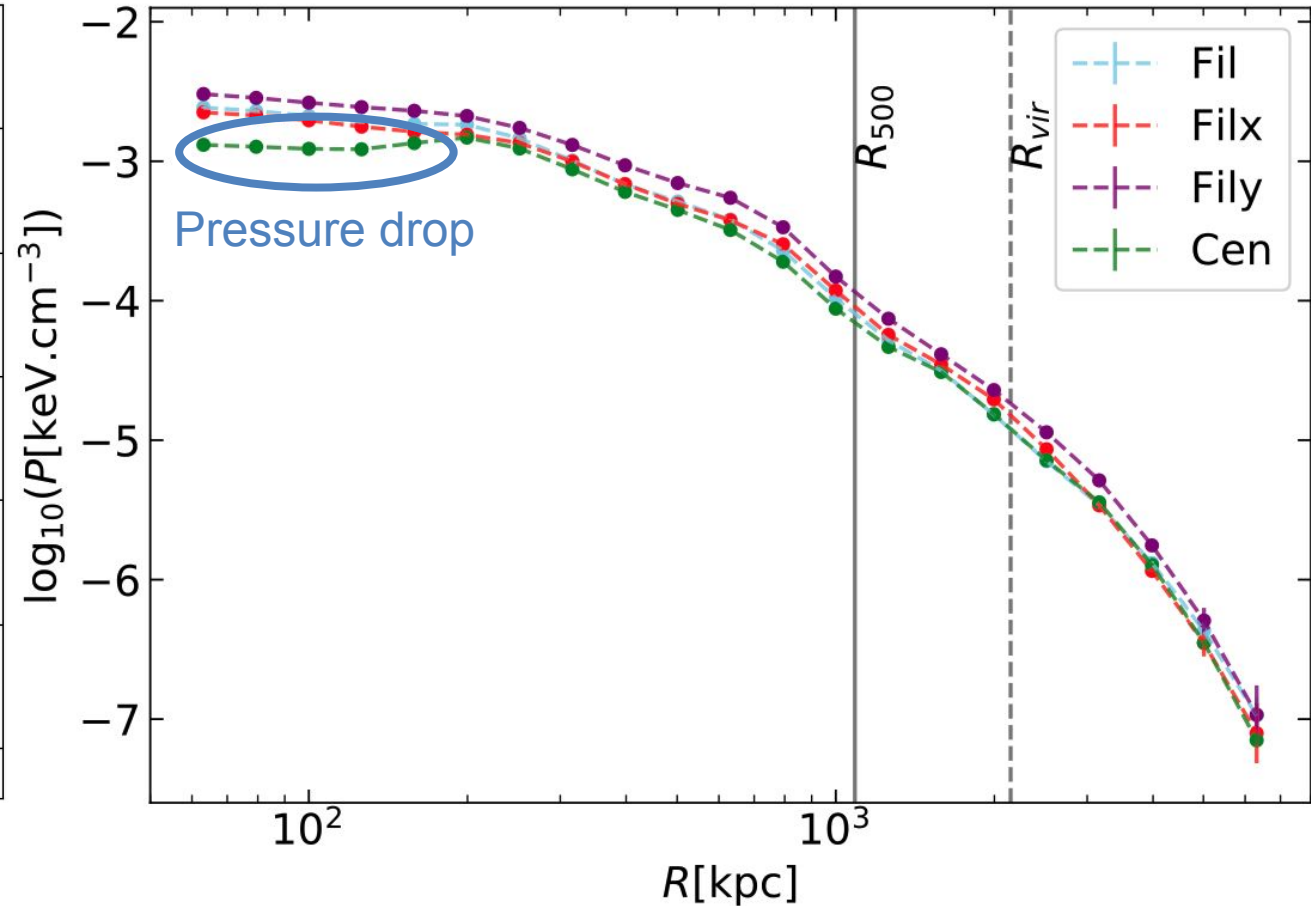
Projected radial profiles

Electron Density (column density)



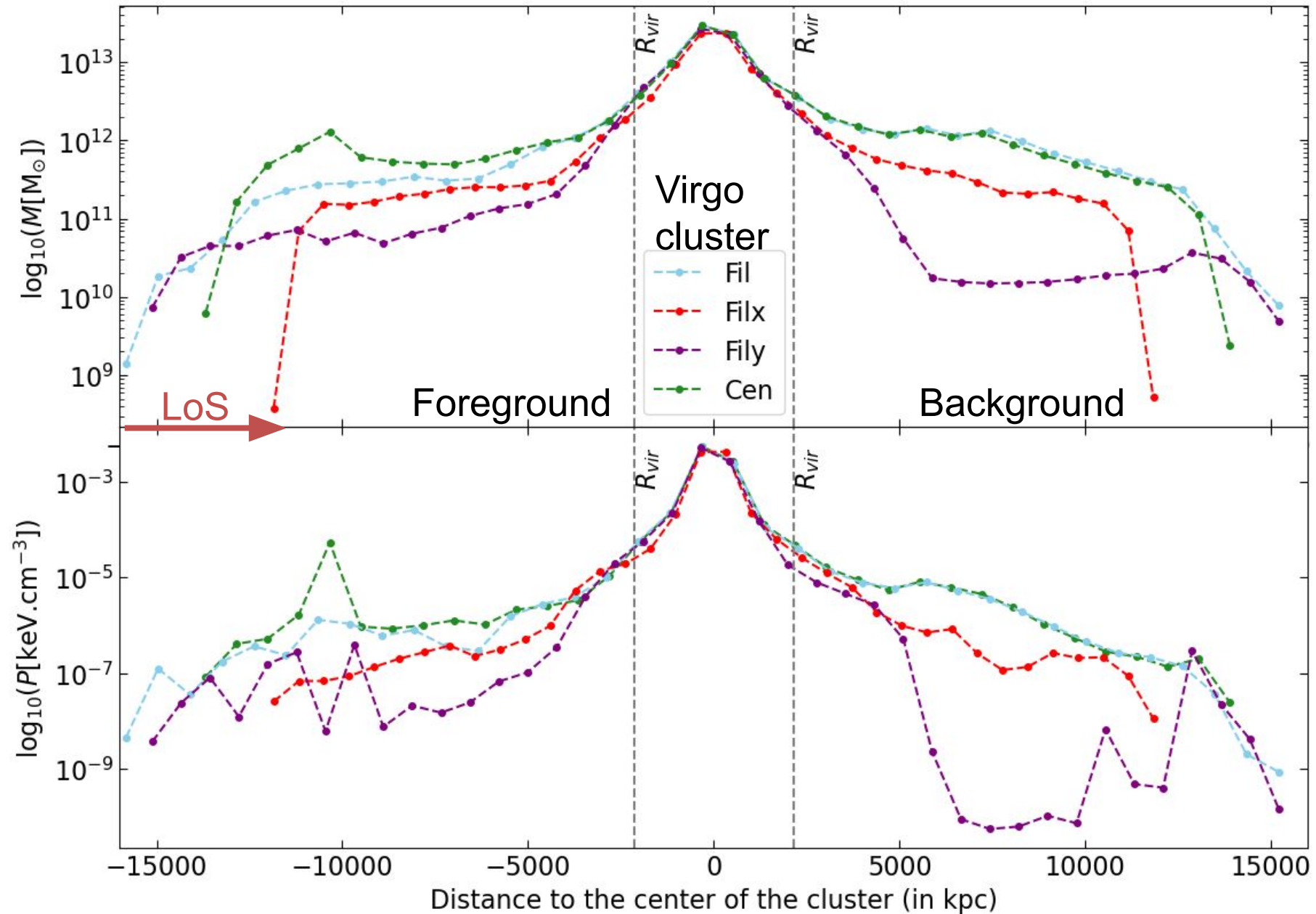
More mass (associated to hot gas) outside the cluster along the LoS induces **higher column density**

Pressure (mass-weighted mean)

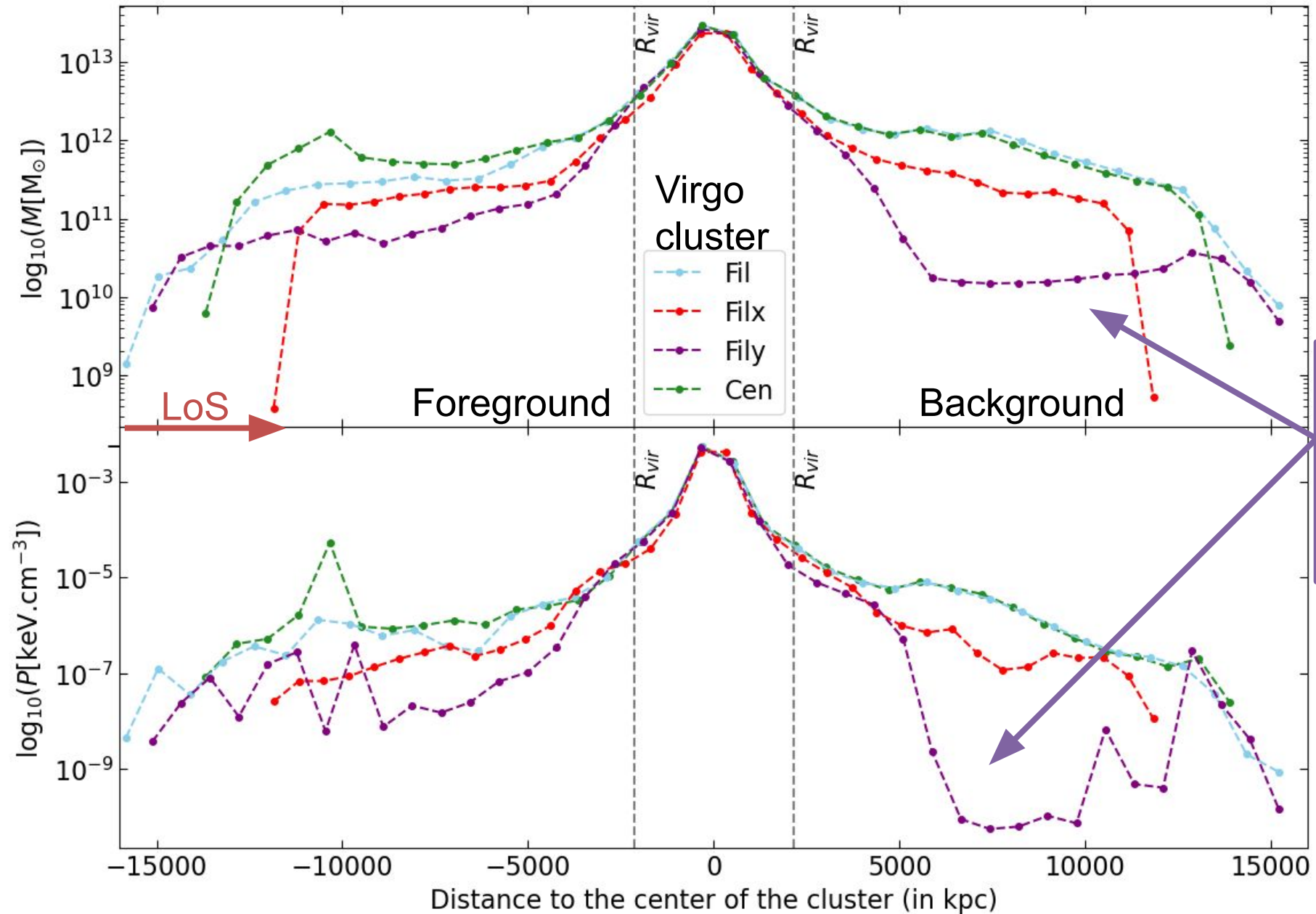


Mass (associated to hot gas) outside the cluster along the LoS induces **lower mean pressure** (contribution from the foreground and background)

Mass/pressure distribution along the line of sight

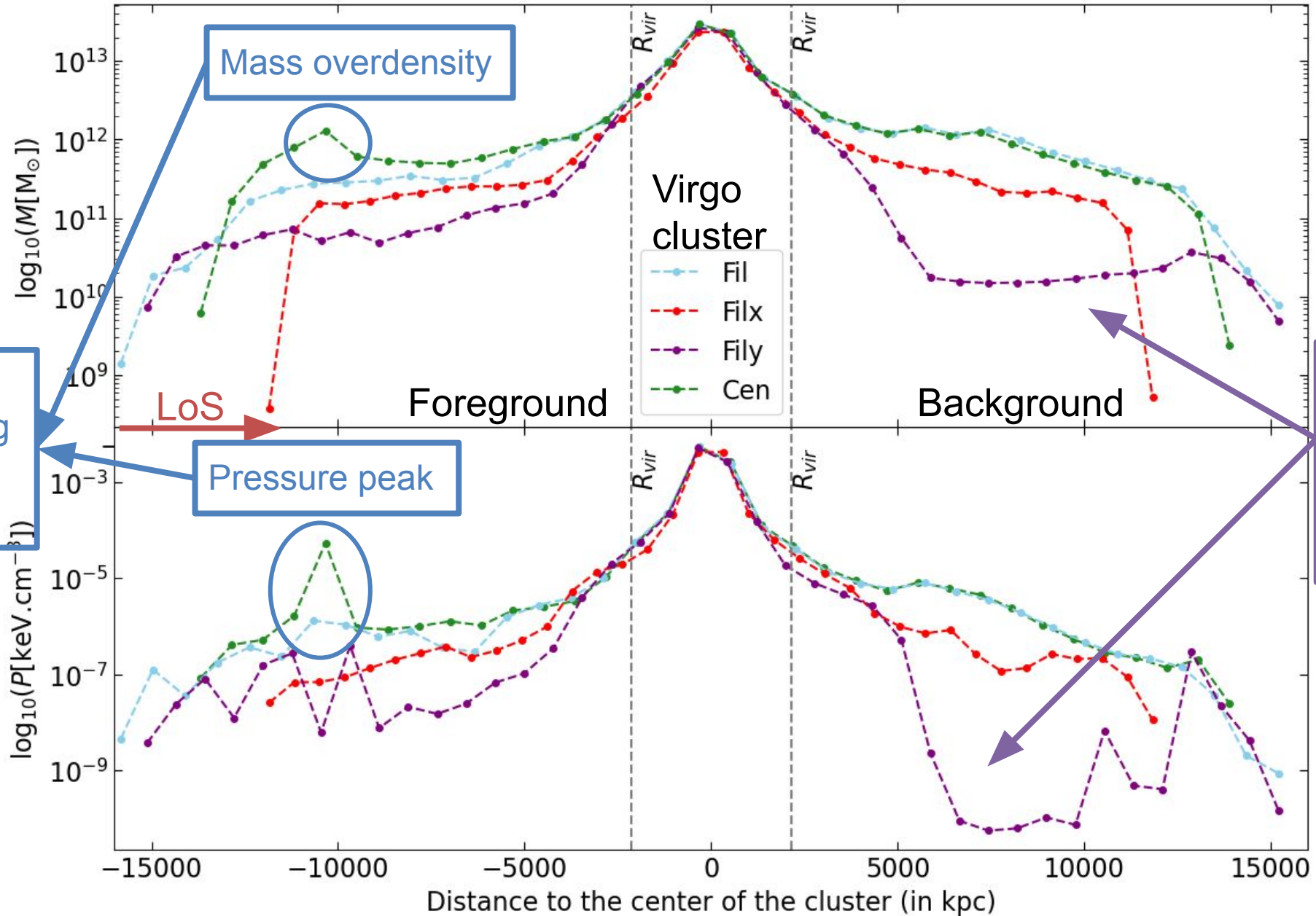


Mass/pressure distribution along the line of sight



The **Fily** line of sight contains the least mass and pressure outside the cluster

Mass/pressure distribution along the line of sight

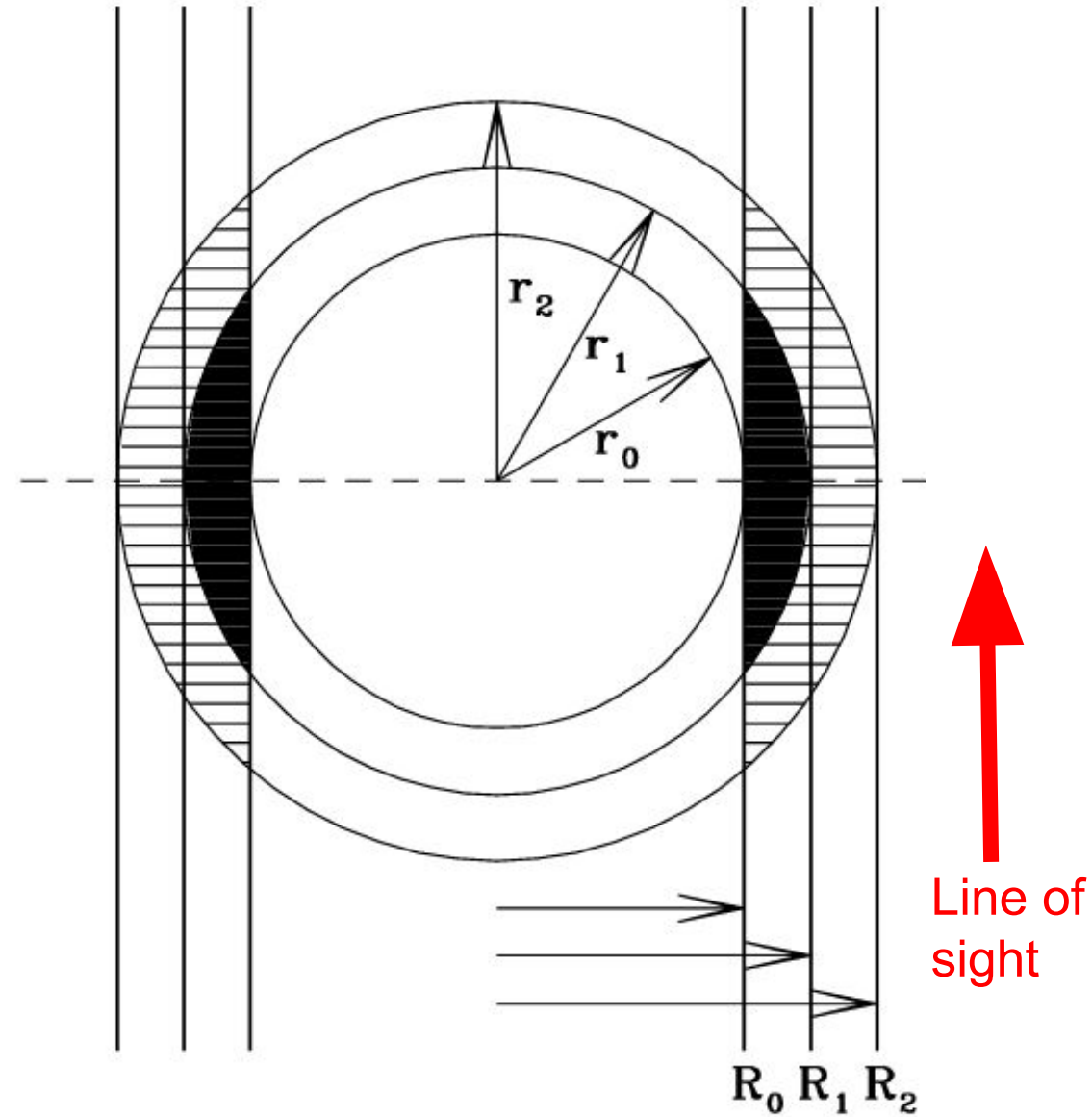


The **Fily** line of sight contains the least mass and pressure outside the cluster

Group of galaxies along this line of sight

Deprojection method

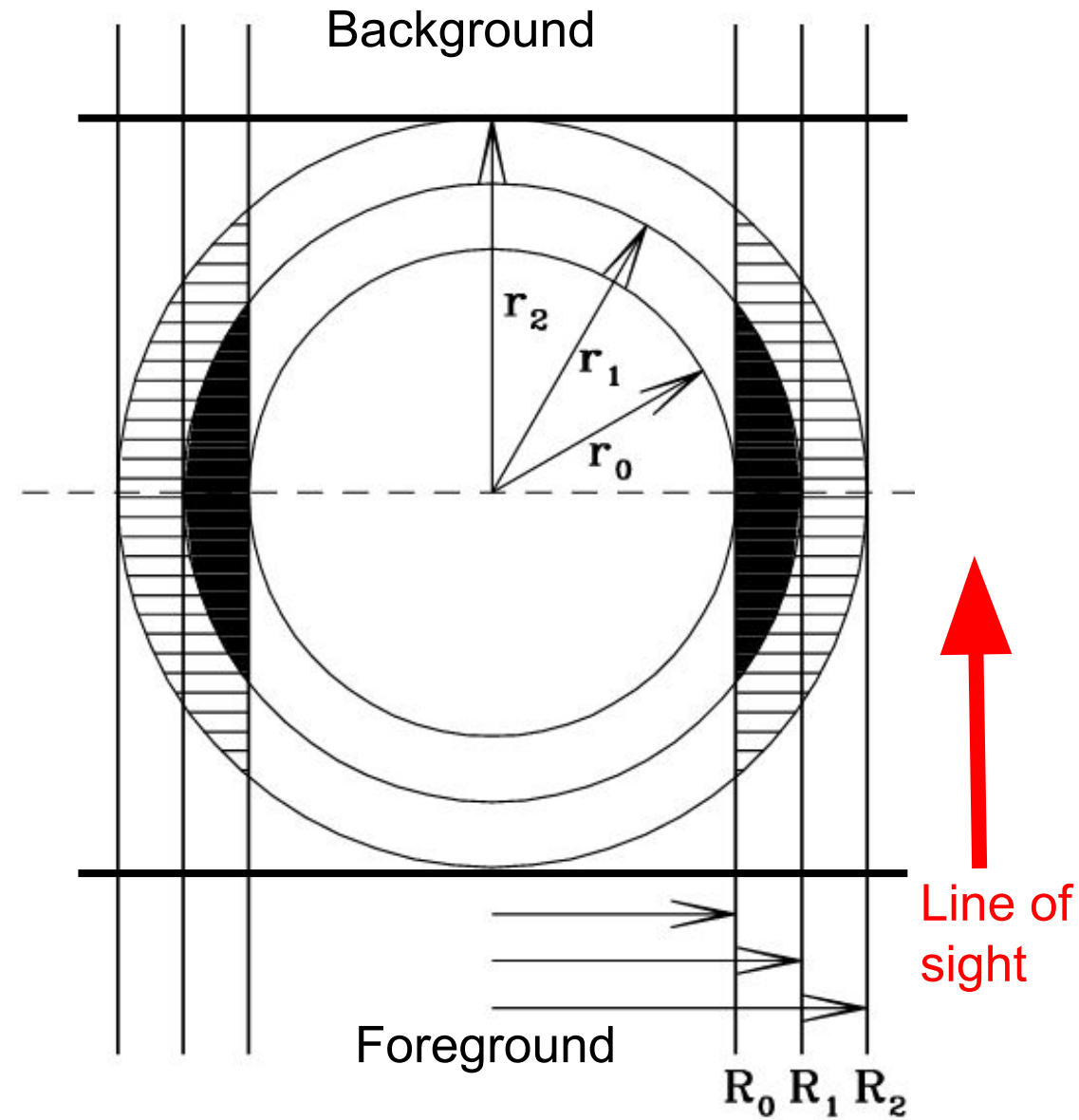
- Iterative geometrical process (“onion rings method”) : from the outskirts to the center of the cluster → model-free



McLaughlin et al. (1999)

Deprojection method

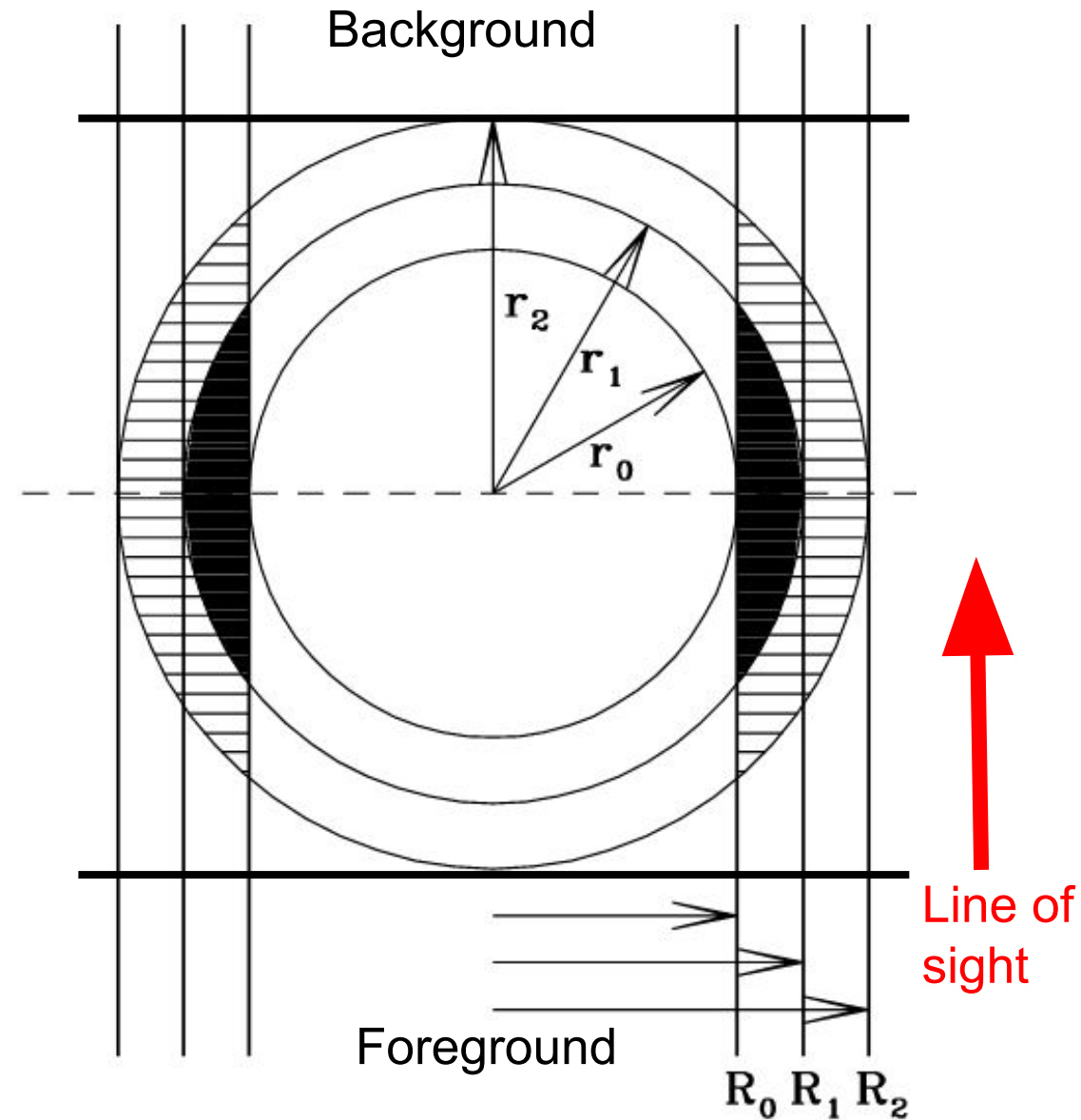
- Iterative geometrical process (“onion rings method”) : from the outskirts to the center of the cluster → model-free
- Background and foreground are accounted for



McLaughlin et al. (1999)

Deprojection method

- Iterative geometrical process (“onion rings method”) : from the outskirts to the center of the cluster → model-free
- Background and foreground are accounted for
- Circular annuli on maps = Cylinders along the LoS
- Signal in circular annuli : contributions of spherical shells along the LoS



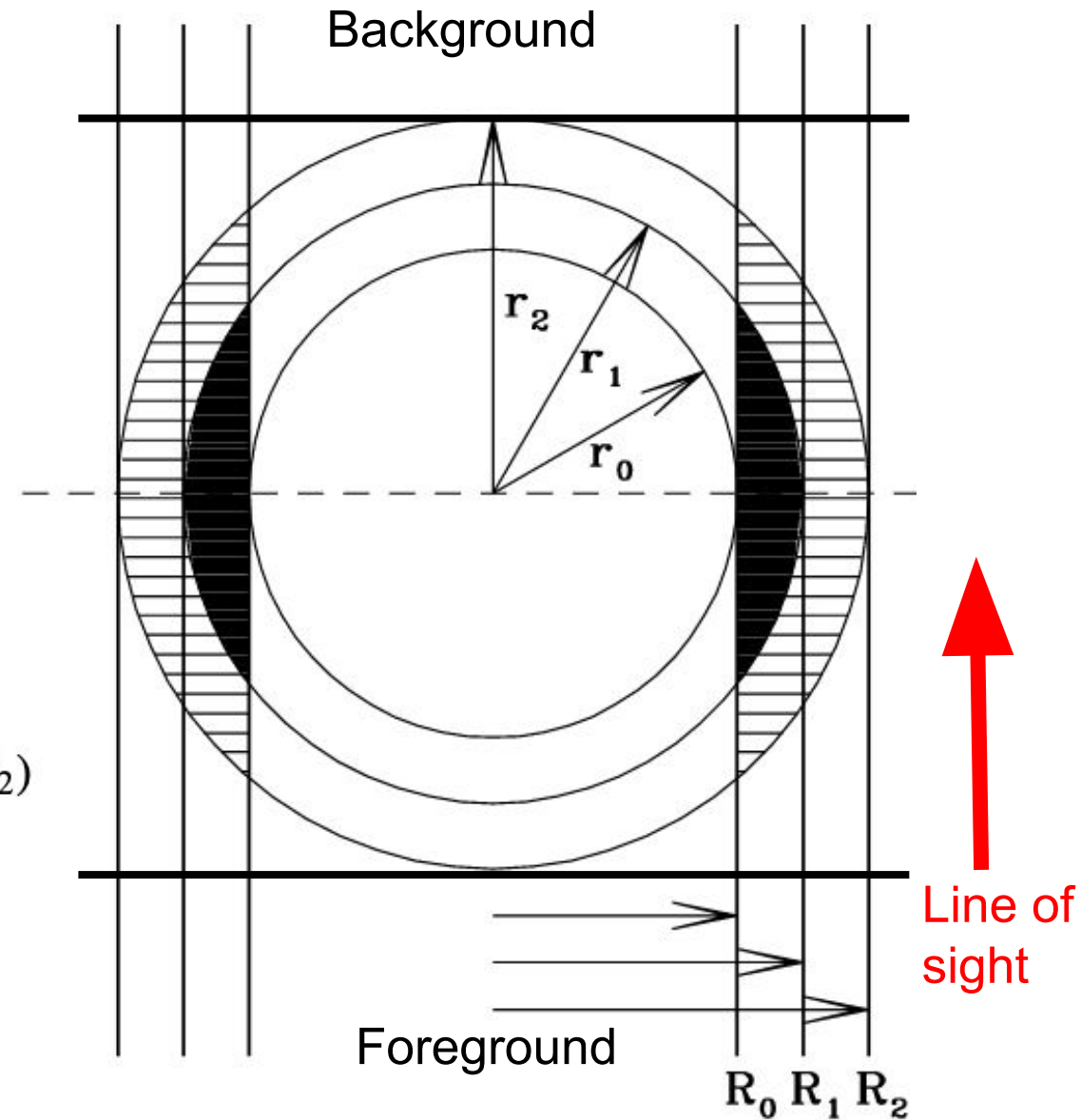
McLaughlin et al. (1999)

Deprojection method

- Iterative geometrical process (“onion rings method”) : from the outskirts to the center of the cluster → model-free
- Background and foreground are accounted for
- Circular annuli on maps = Cylinders along the LoS
- Signal in circular annuli : contributions of spherical shells along the LoS

P : projected pressure, P' : deprojected pressure

Furthest annulus: $P(R_1, R_2) * \pi(R_2^2 - R_1^2)L = P'(r_1, r_2) * V_{int}(r_1, r_2, R_1, R_2)$



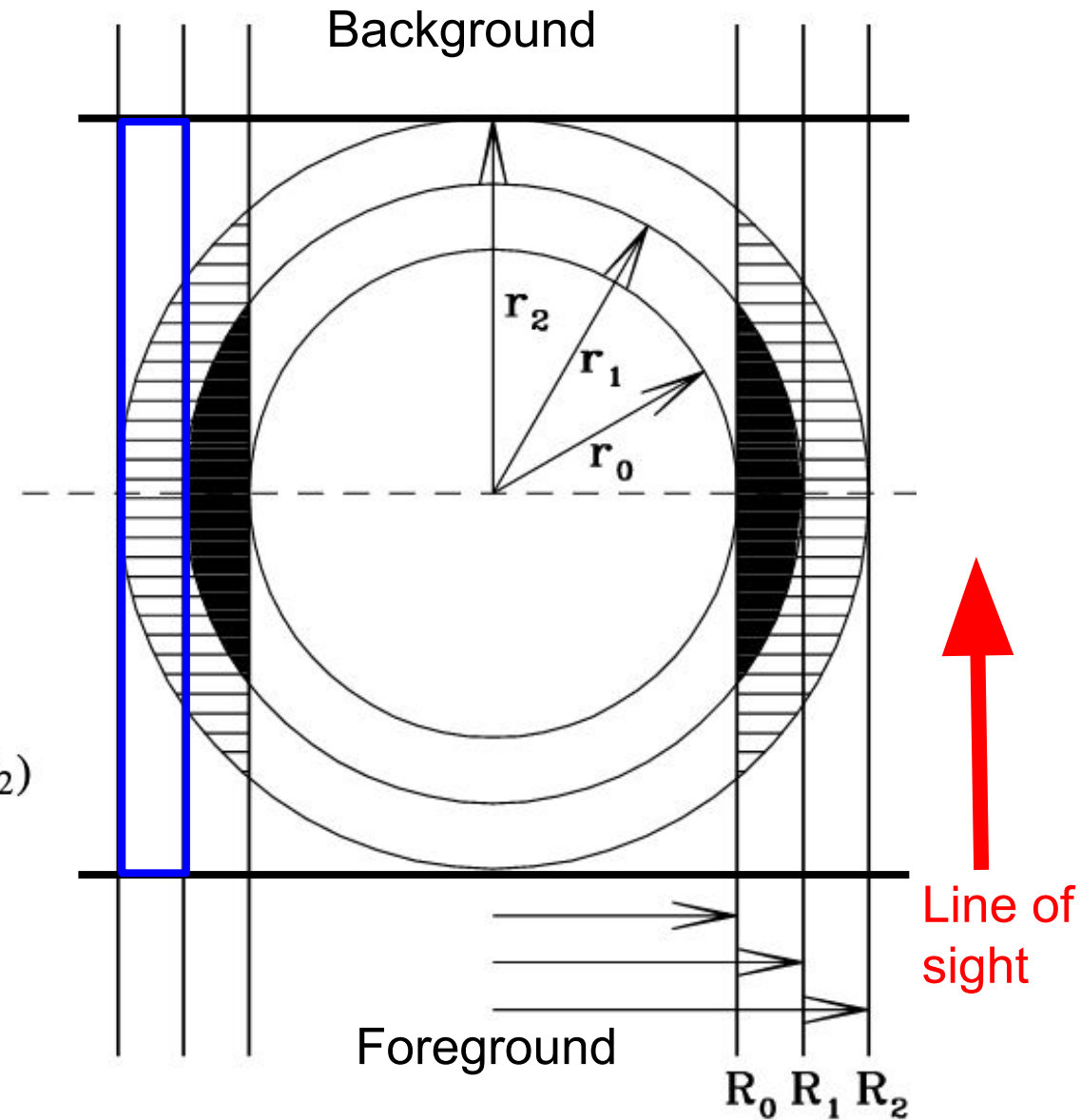
McLaughlin et al. (1999)

Deprojection method

- Iterative geometrical process (“onion rings method”) : from the outskirts to the center of the cluster → model-free
- Background and foreground are accounted for
- Circular annuli on maps = Cylinders along the LoS
- Signal in circular annuli : contributions of spherical shells along the LoS

P : projected pressure, P' : deprojected pressure

Furthest annulus: $P(R_1, R_2) * \pi(R_2^2 - R_1^2)L = P'(r_1, r_2) * V_{int}(r_1, r_2, R_1, R_2)$



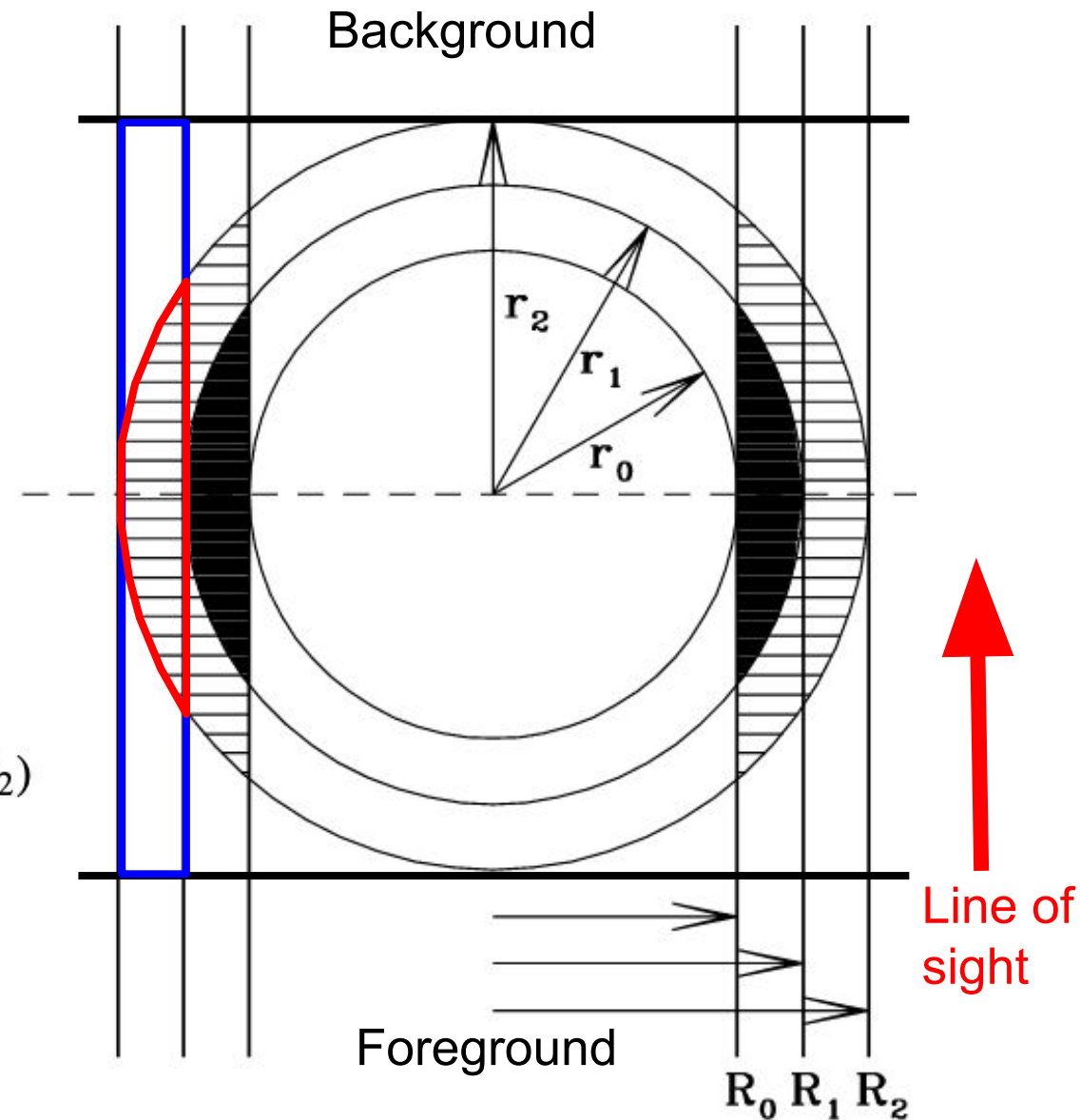
McLaughlin et al. (1999)

Deprojection method

- Iterative geometrical process (“onion rings method”) : from the outskirts to the center of the cluster → model-free
- Background and foreground are accounted for
- Circular annuli on maps = Cylinders along the LoS
- Signal in circular annuli : contributions of spherical shells along the LoS

P : projected pressure, P' : deprojected pressure

Furthest annulus: $P(R_1, R_2) * \pi(R_2^2 - R_1^2)L = P'(r_1, r_2) * V_{int}(r_1, r_2, R_1, R_2)$



McLaughlin et al. (1999)

Deprojection method

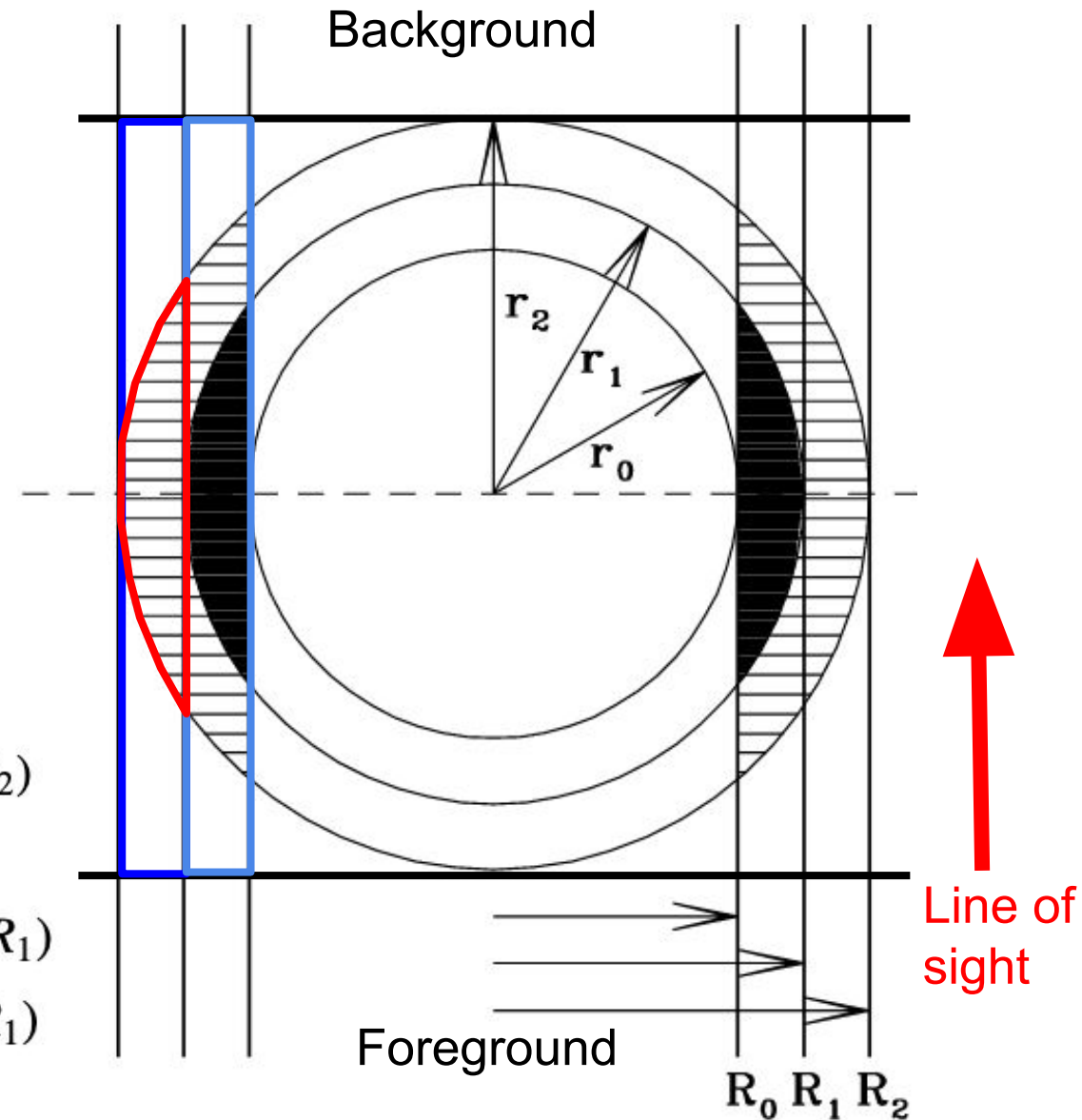
- Iterative geometrical process (“onion rings method”) : from the outskirts to the center of the cluster → model-free
- Background and foreground are accounted for
- Circular annuli on maps = Cylinders along the LoS
- Signal in circular annuli : contributions of spherical shells along the LoS

P : projected pressure, P' : deprojected pressure

Furthest annulus: $P(R_1, R_2) * \pi(R_2^2 - R_1^2)L = P'(r_1, r_2) * V_{int}(r_1, r_2, R_1, R_2)$

Second furthest annulus:

$$P(R_0, R_1) * \pi(R_1^2 - R_0^2)L = P'(r_0, r_1) * V_{int}(r_0, r_1, R_0, R_1) + P'(r_1, r_2) * V_{int}(r_1, r_2, R_0, R_1)$$



McLaughlin et al. (1999)

Deprojection method

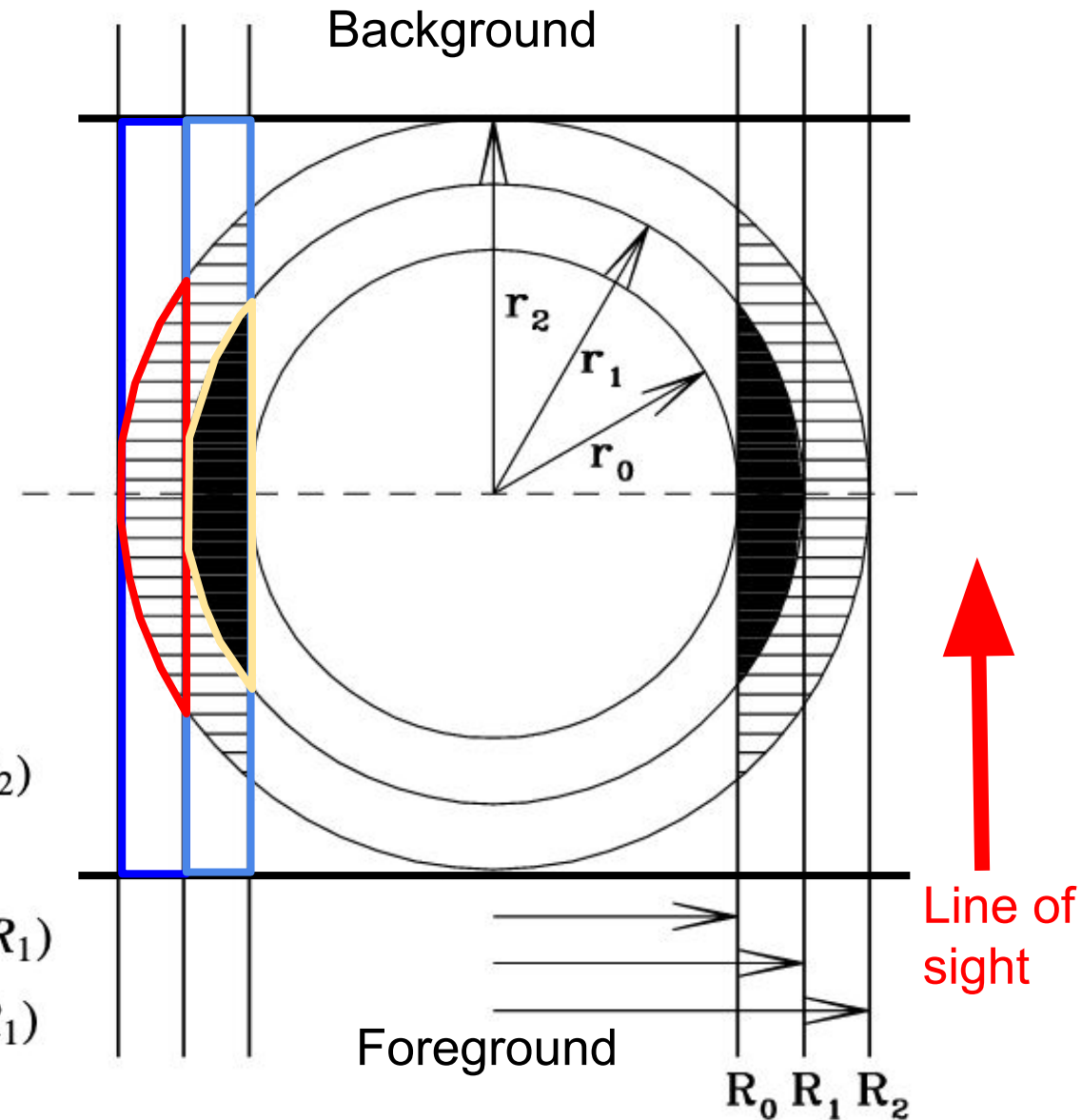
- Iterative geometrical process (“onion rings method”) : from the outskirts to the center of the cluster → model-free
- Background and foreground are accounted for
- Circular annuli on maps = Cylinders along the LoS
- Signal in circular annuli : contributions of spherical shells along the LoS

P : projected pressure, P' : deprojected pressure

Furthest annulus: $P(R_1, R_2) * \pi(R_2^2 - R_1^2)L = P'(r_1, r_2) * V_{int}(r_1, r_2, R_1, R_2)$

Second furthest annulus:

$$P(R_0, R_1) * \pi(R_1^2 - R_0^2)L = P'(r_0, r_1) * V_{int}(r_0, r_1, R_0, R_1) + P'(r_1, r_2) * V_{int}(r_1, r_2, R_0, R_1)$$



McLaughlin et al. (1999)

Deprojection method

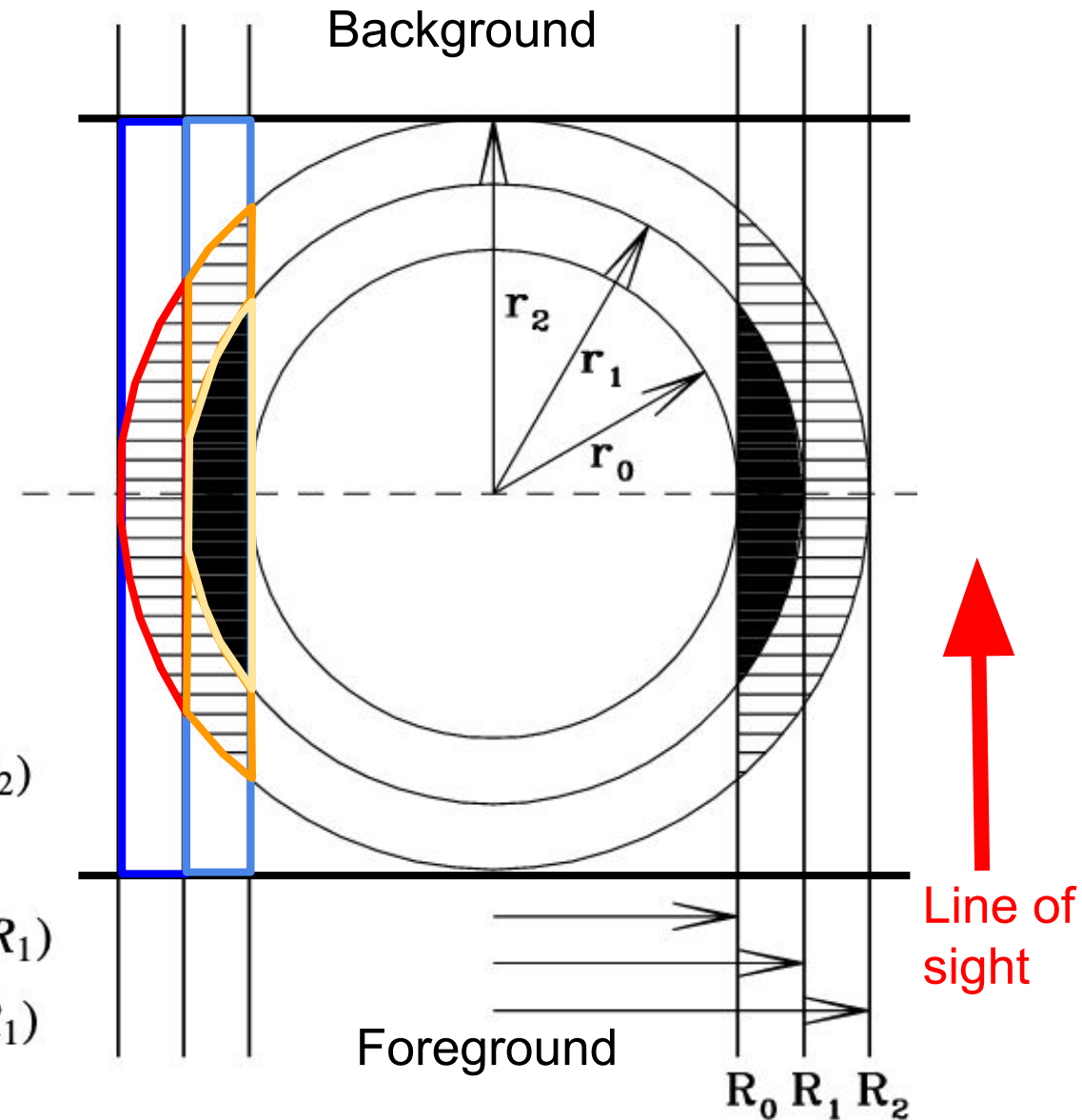
- Iterative geometrical process (“onion rings method”) : from the outskirts to the center of the cluster → model-free
- Background and foreground are accounted for
- Circular annuli on maps = Cylinders along the LoS
- Signal in circular annuli : contributions of spherical shells along the LoS

P : projected pressure, P' : deprojected pressure

Furthest annulus: $P(R_1, R_2) * \pi(R_2^2 - R_1^2)L = P'(r_1, r_2) * V_{int}(r_1, r_2, R_1, R_2)$

Second furthest annulus:

$$P(R_0, R_1) * \pi(R_1^2 - R_0^2)L = P'(r_0, r_1) * V_{int}(r_0, r_1, R_0, R_1) + P'(r_1, r_2) * V_{int}(r_1, r_2, R_0, R_1)$$



McLaughlin et al. (1999)

Deprojection method

- Iterative geometrical process (“onion rings method”) : from the outskirts to the center of the cluster → model-free
- Background and foreground are accounted for
- Circular annuli on maps = Cylinders along the LoS
- Signal in circular annuli : contributions of spherical shells along the LoS

P : projected pressure, P' : deprojected pressure

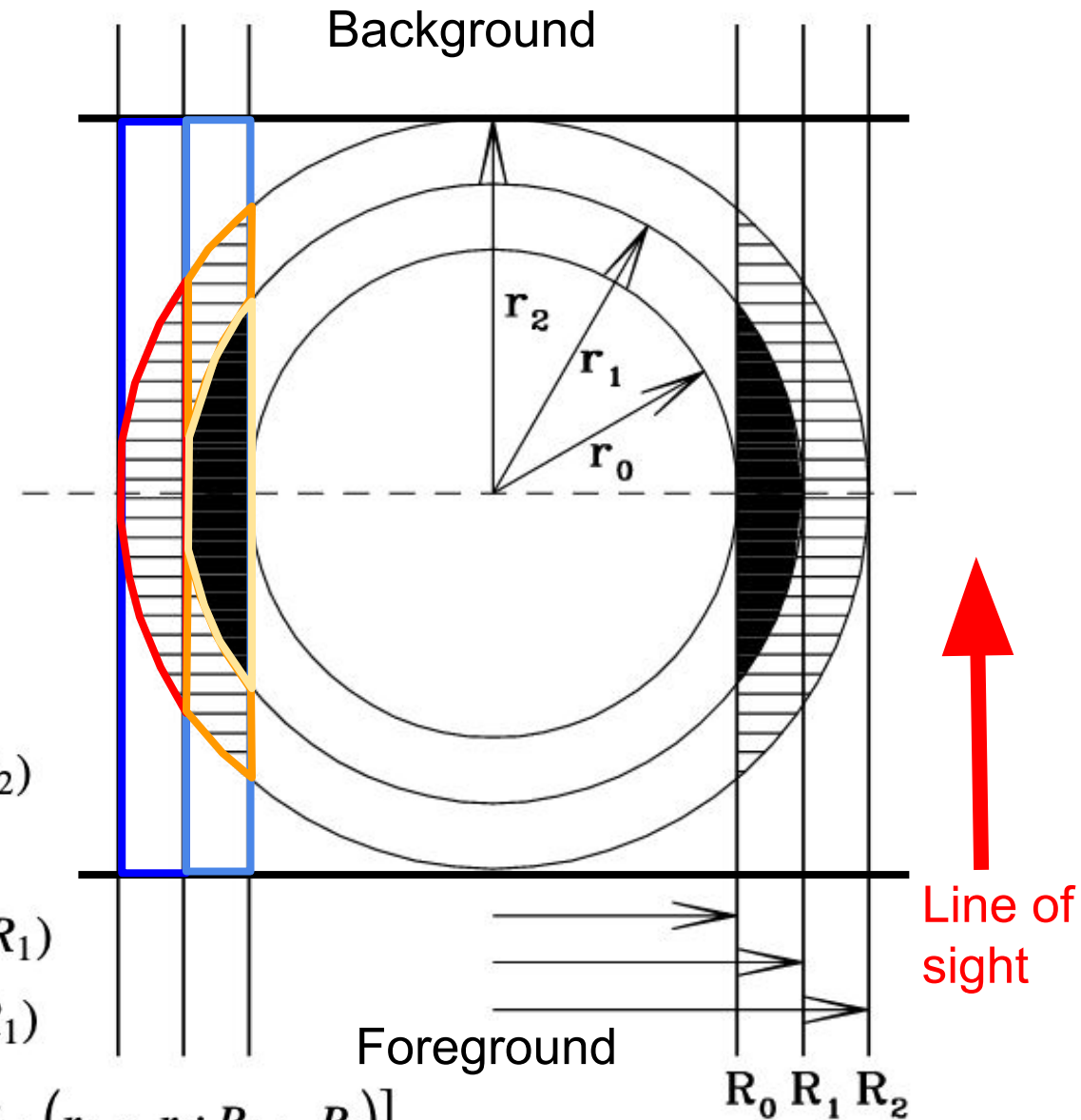
Furthest annulus: $P(R_1, R_2) * \pi(R_2^2 - R_1^2)L = P'(r_1, r_2) * V_{int}(r_1, r_2, R_1, R_2)$

Second furthest annulus:

$$P(R_0, R_1) * \pi(R_1^2 - R_0^2)L = P'(r_0, r_1) * V_{int}(r_0, r_1, R_0, R_1) + P'(r_1, r_2) * V_{int}(r_1, r_2, R_0, R_1)$$

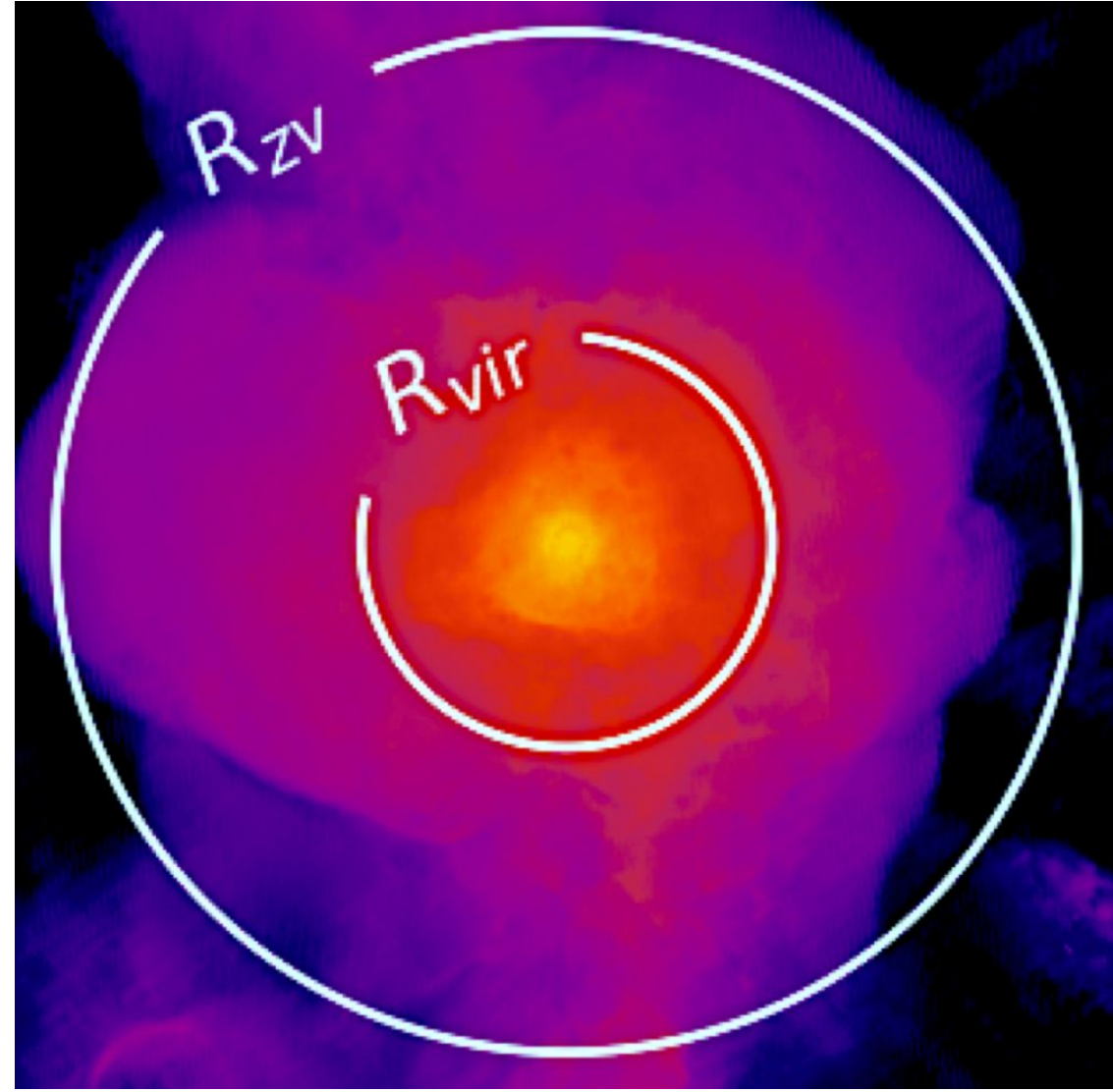
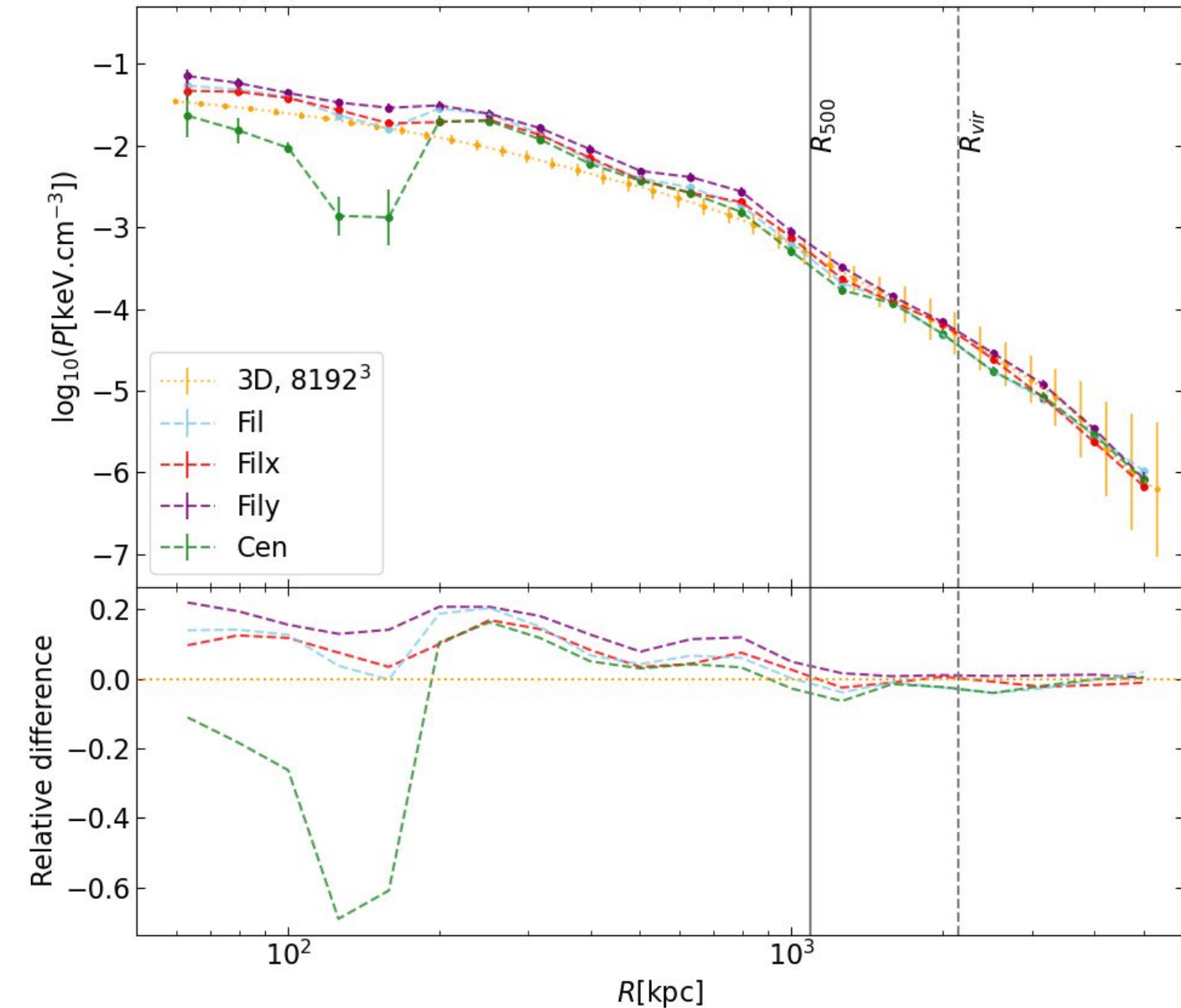
Generalisation :

$$P'(r_{i-1}, r_i) = \frac{P(R_{i-1}, R_i) \pi(R_i^2 - R_{i-1}^2)L - \sum_{j=i+1}^m [P'(r_{j-1}, r_j) V_{int}(r_{j-1}, r_j; R_{i-1}, R_i)]}{V_{int}(r_{i-1}, r_i; R_{i-1}, R_i)}$$

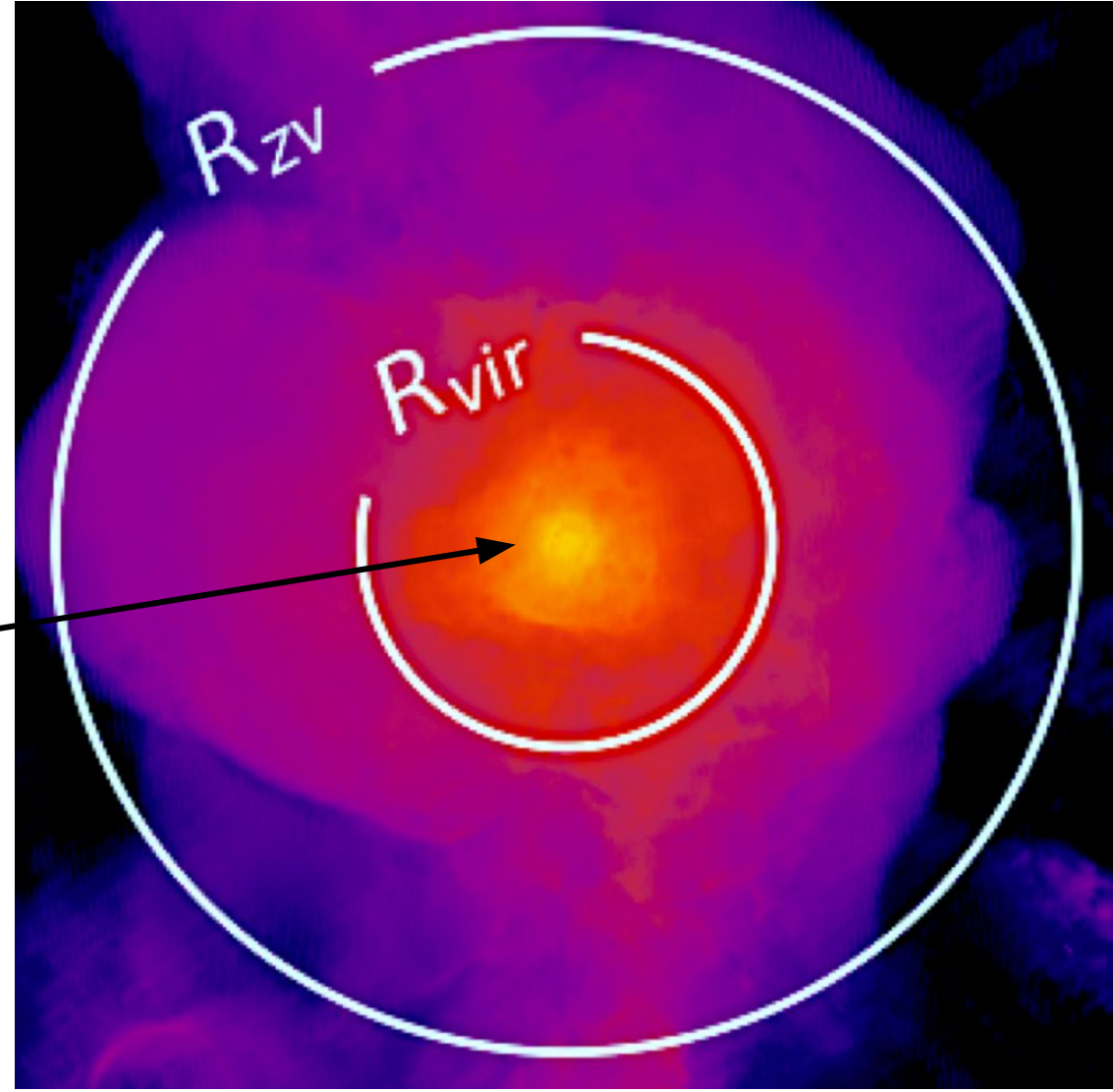
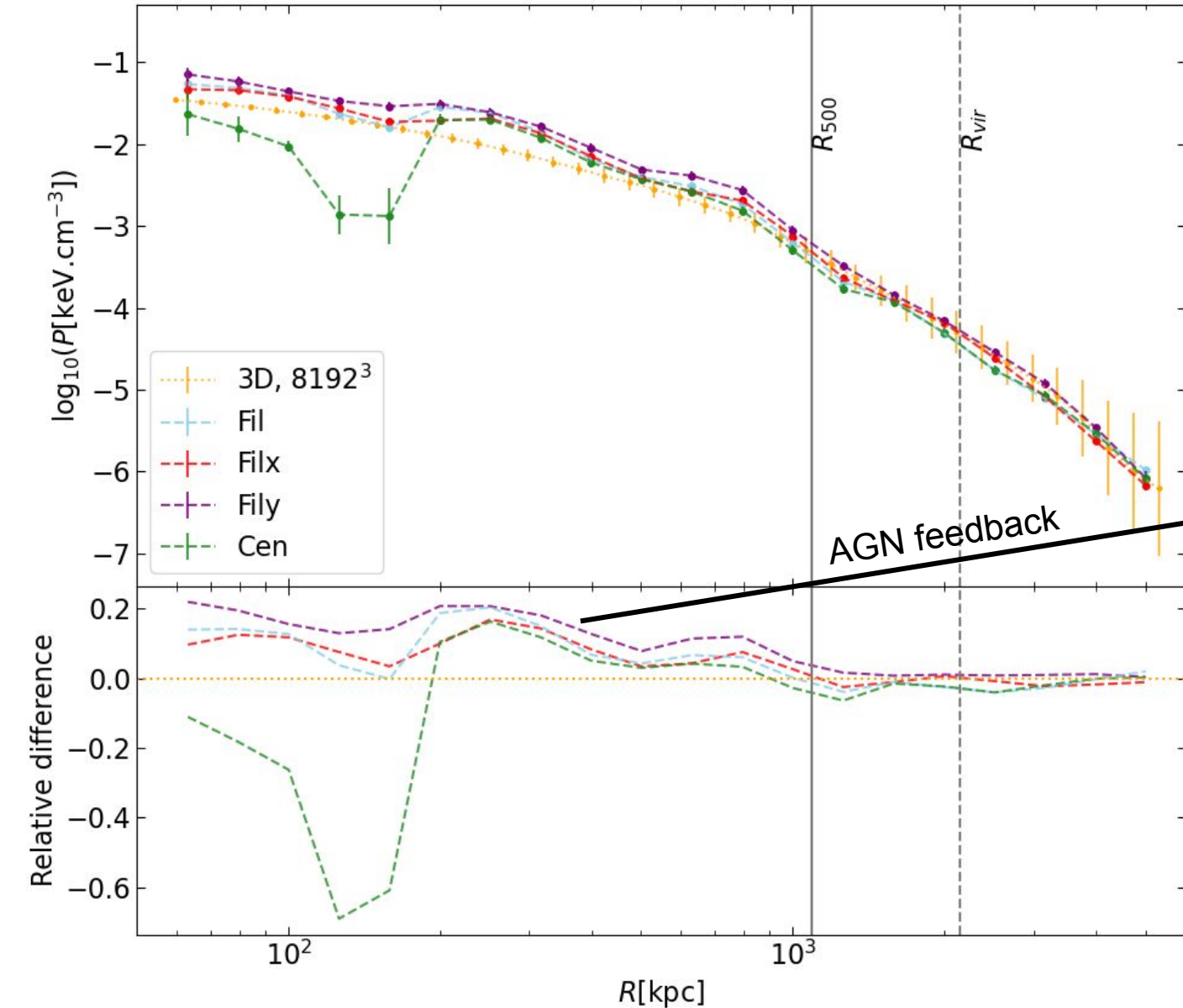


McLaughlin et al. (1999)

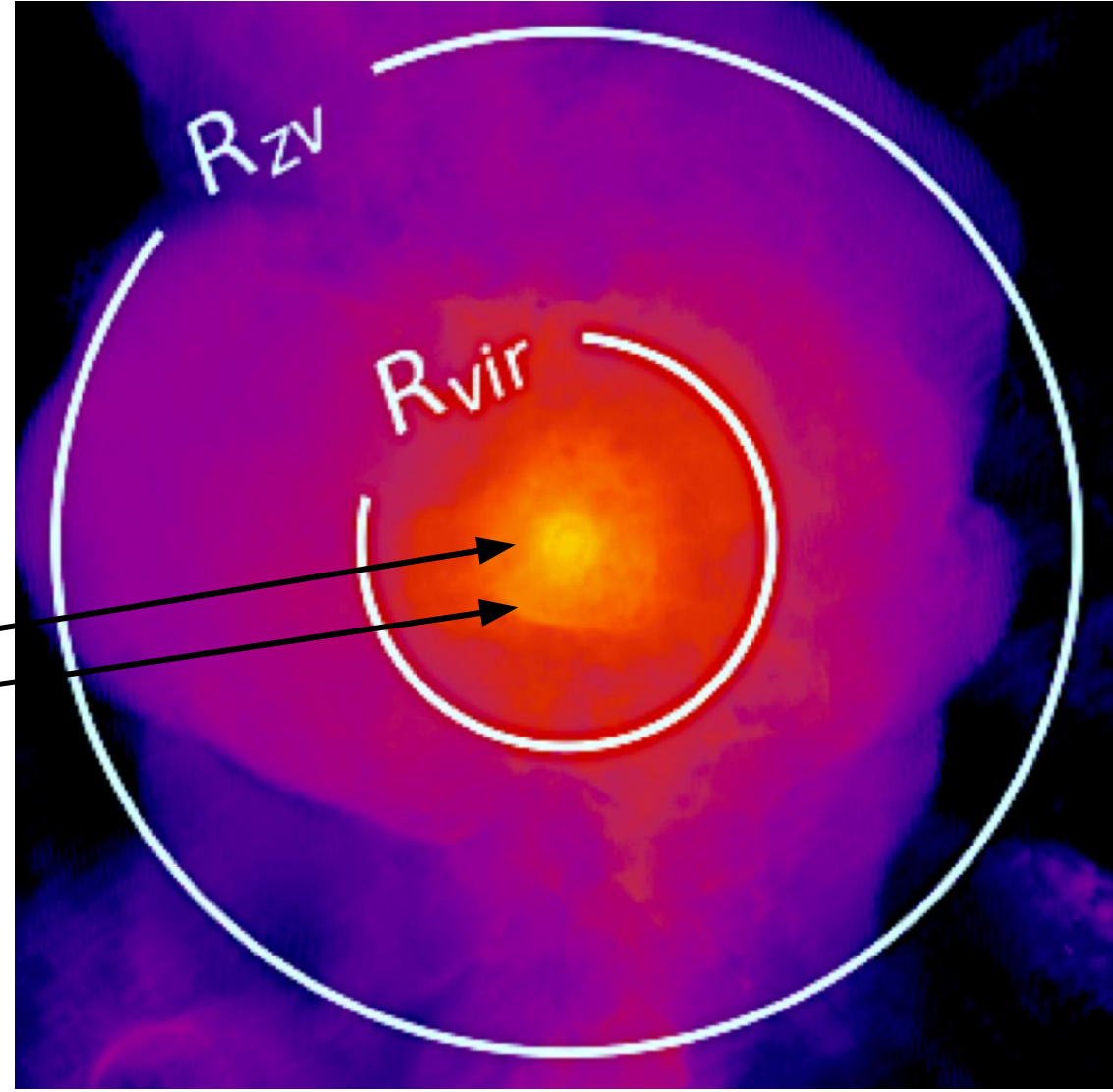
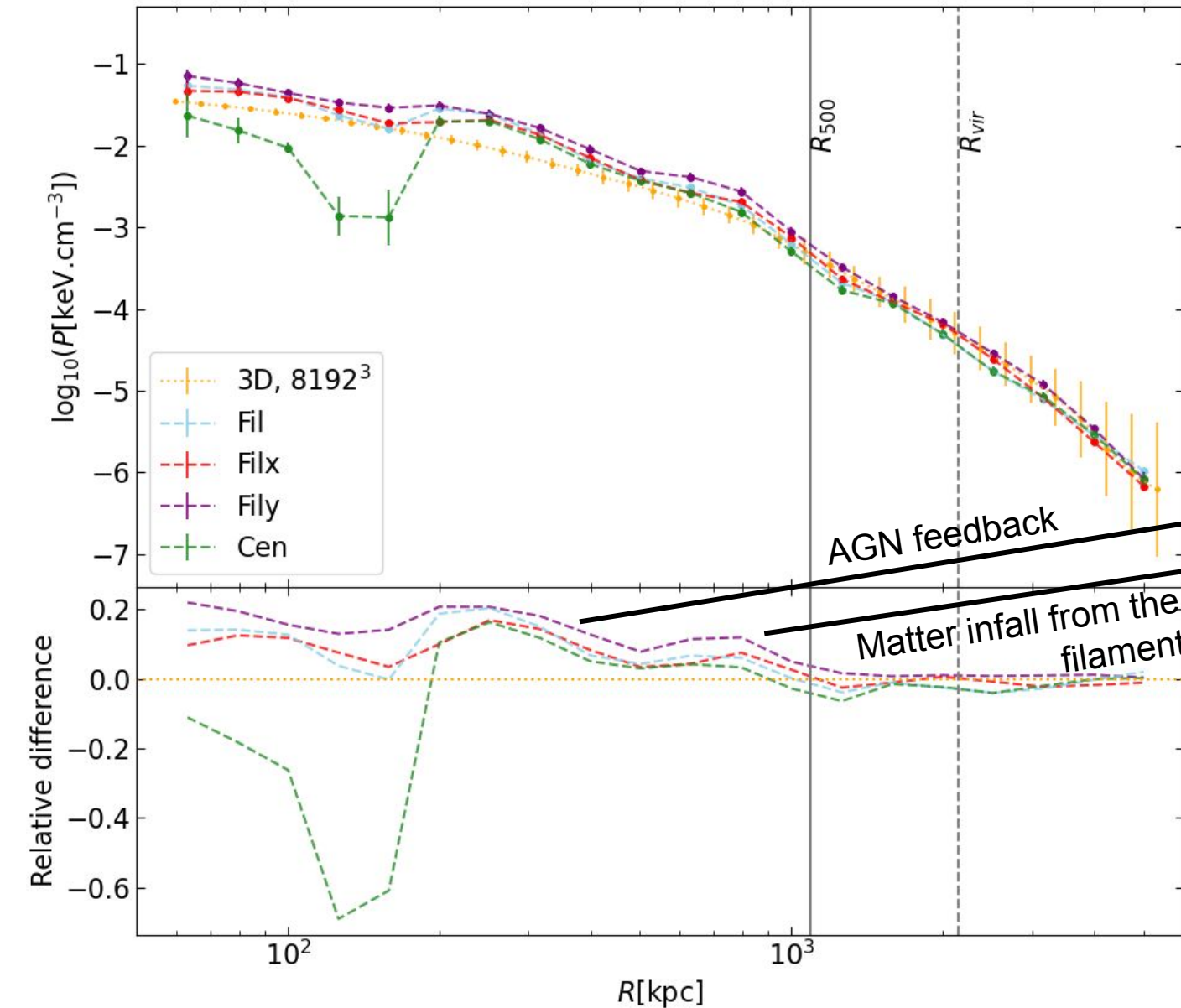
Deprojected pressure profiles



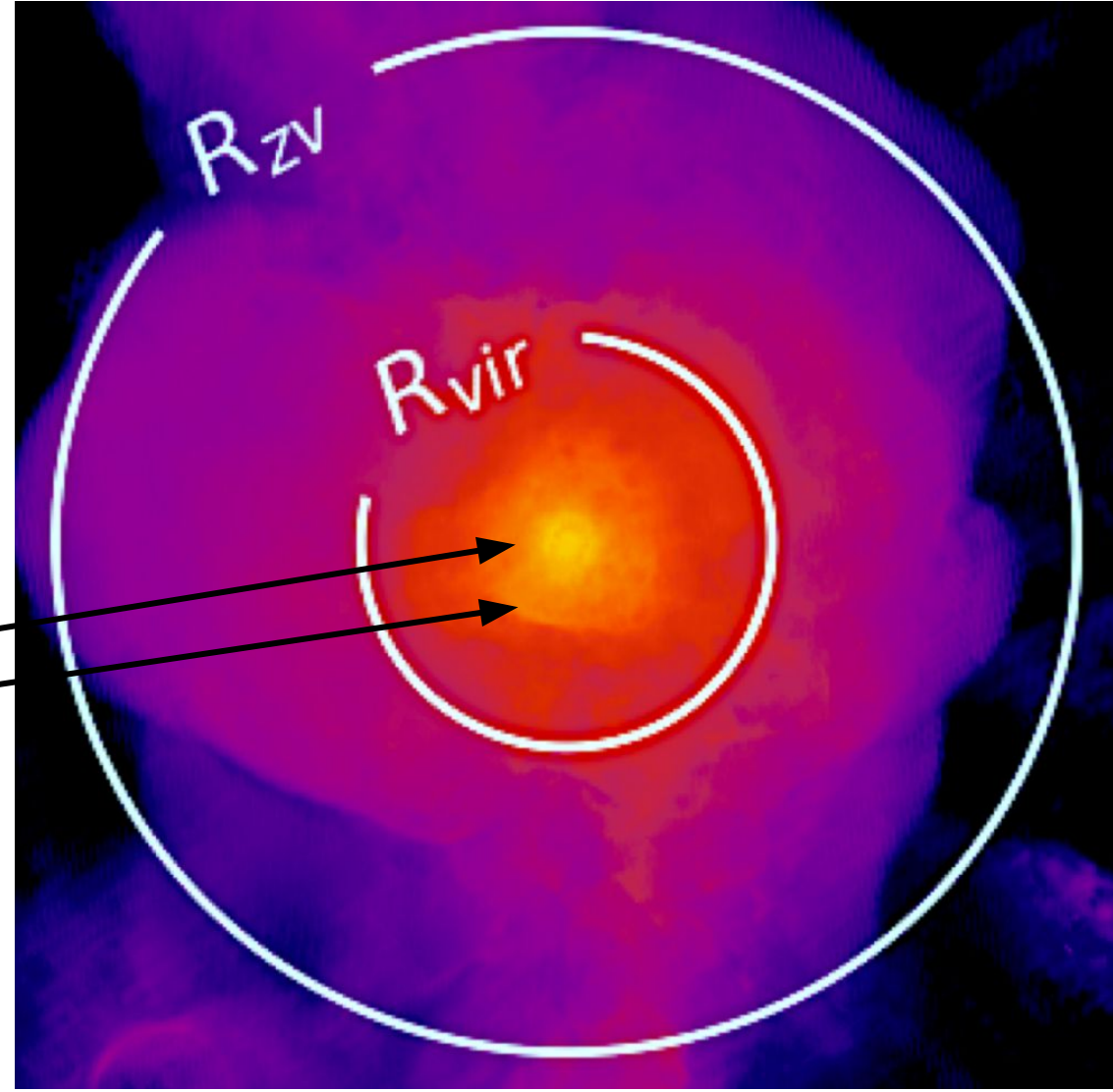
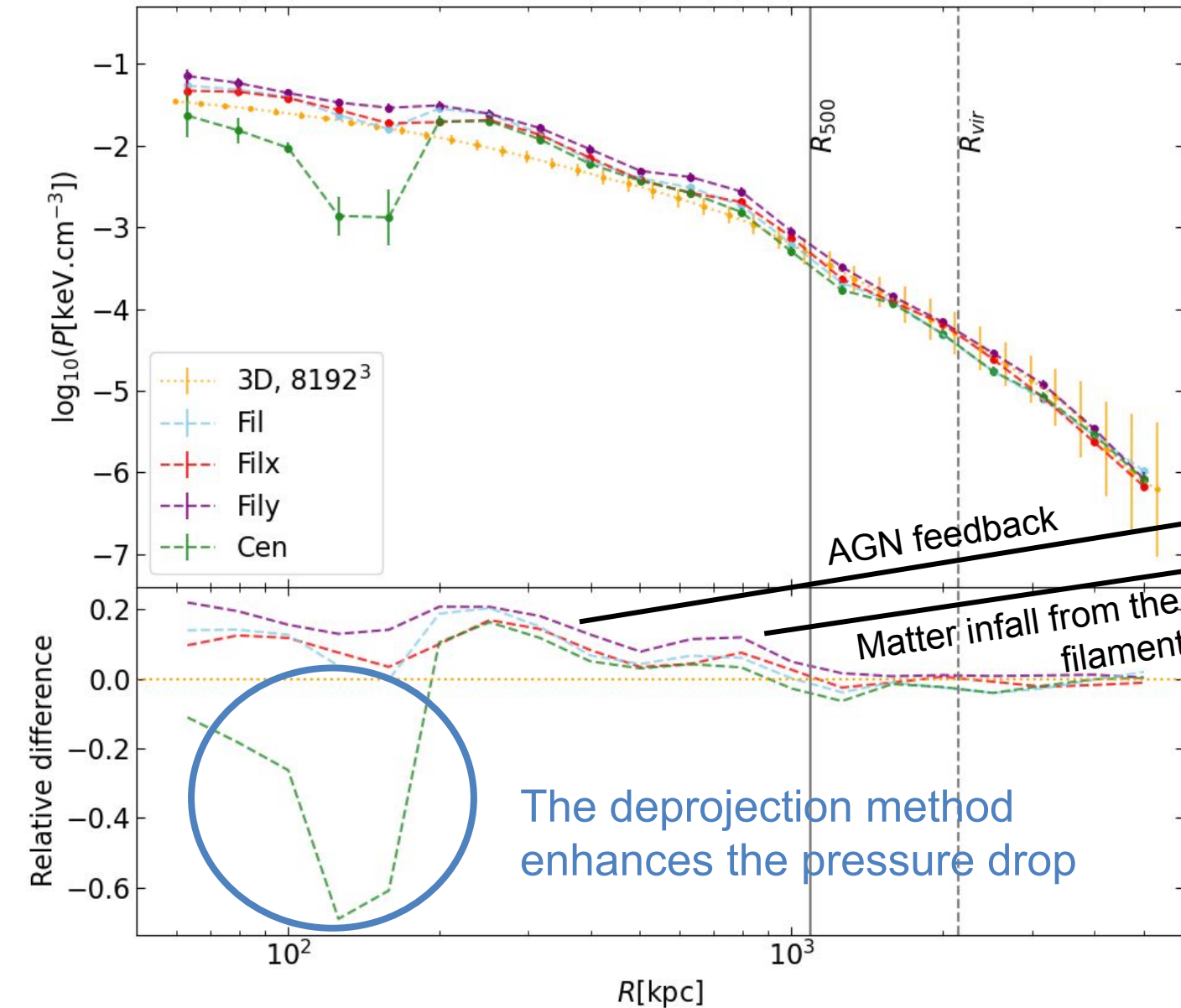
Deprojected pressure profiles



Deprojected pressure profiles

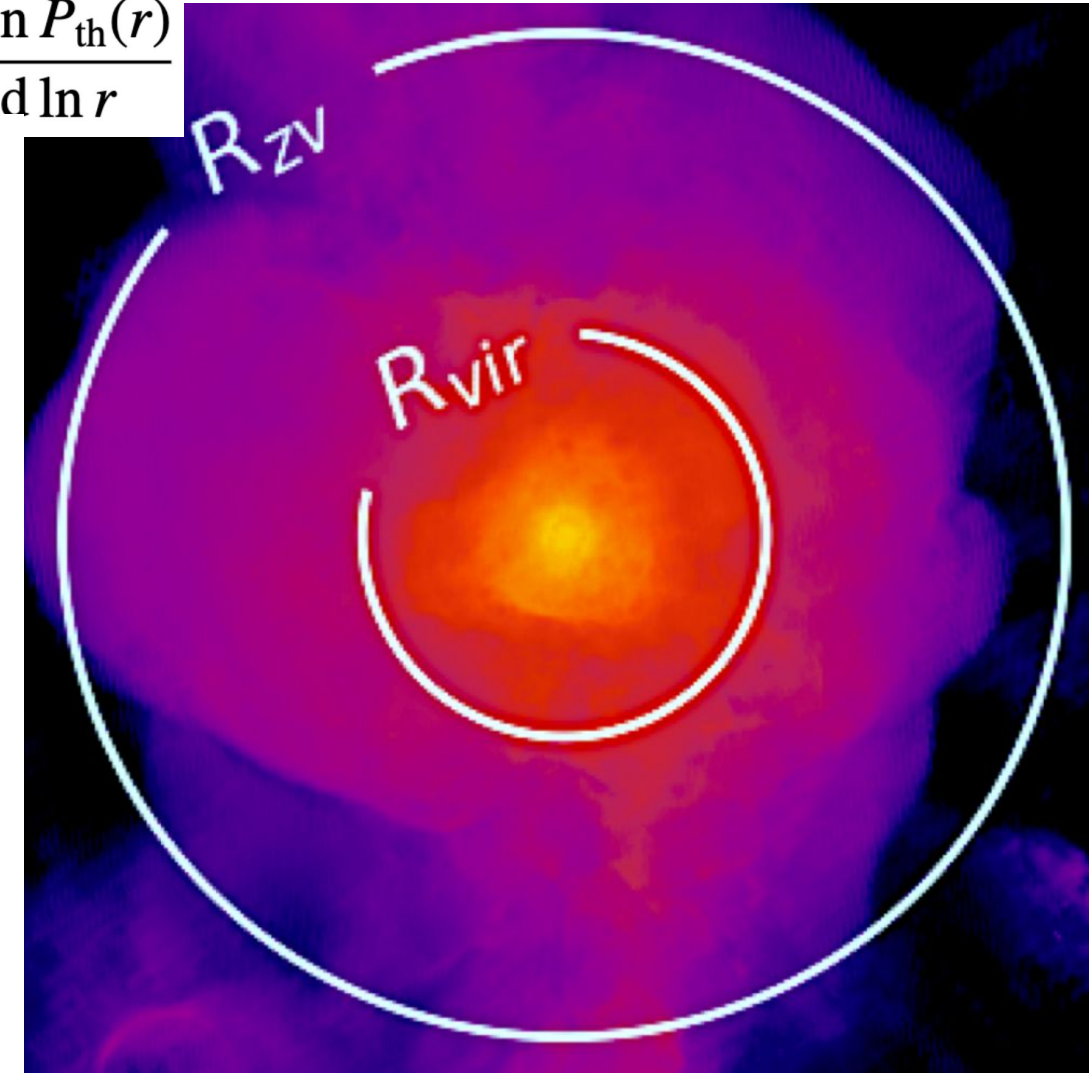
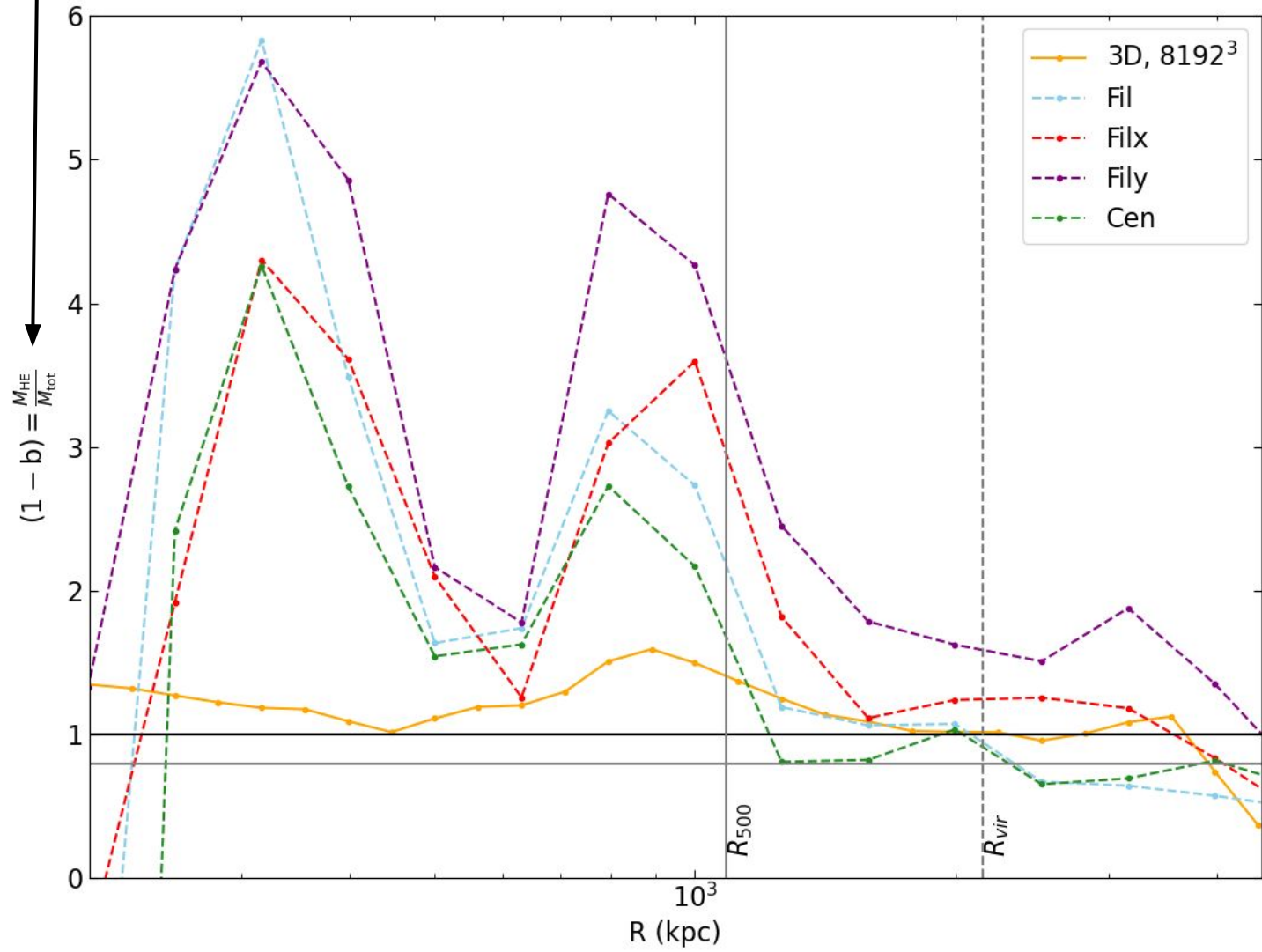


Deprojected pressure profiles



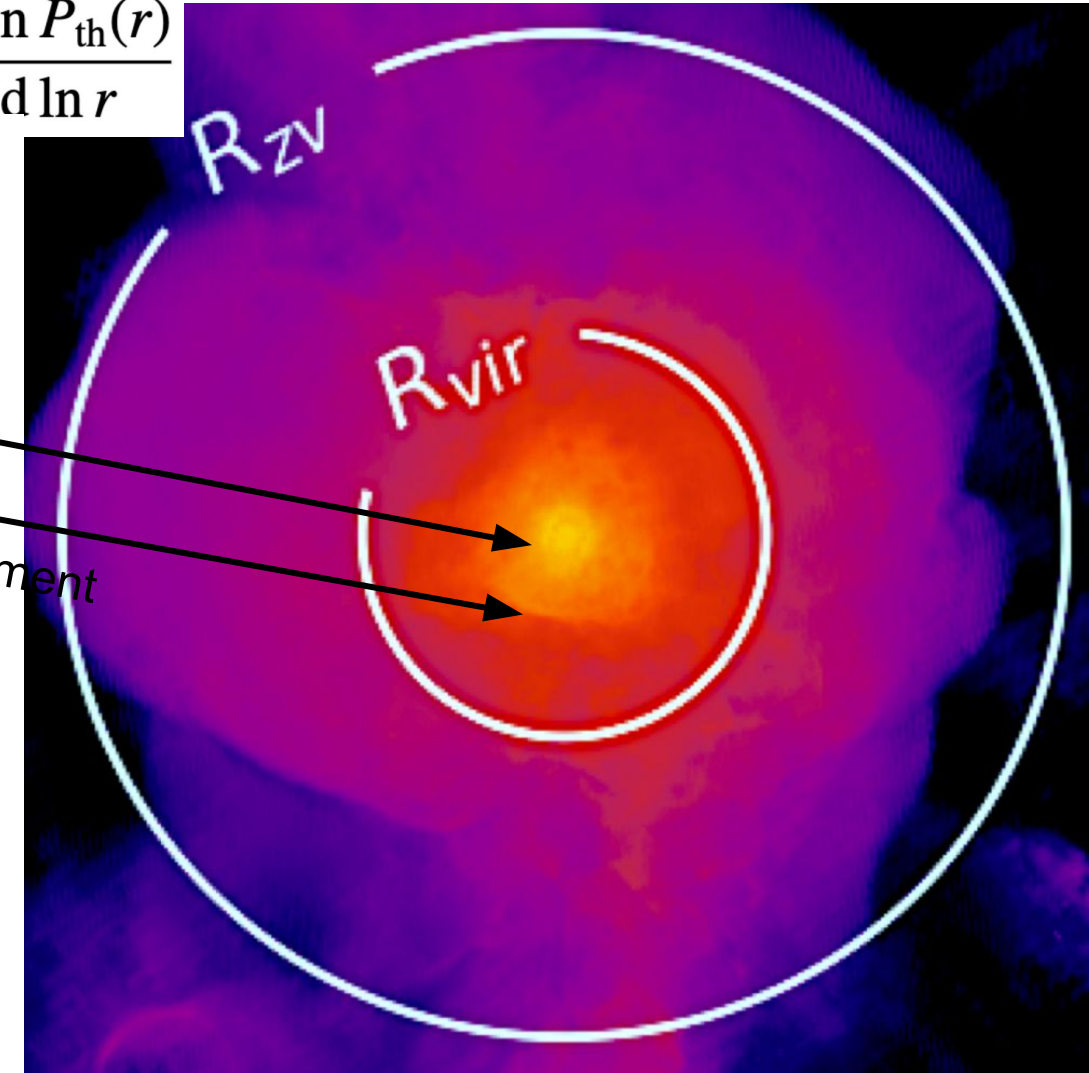
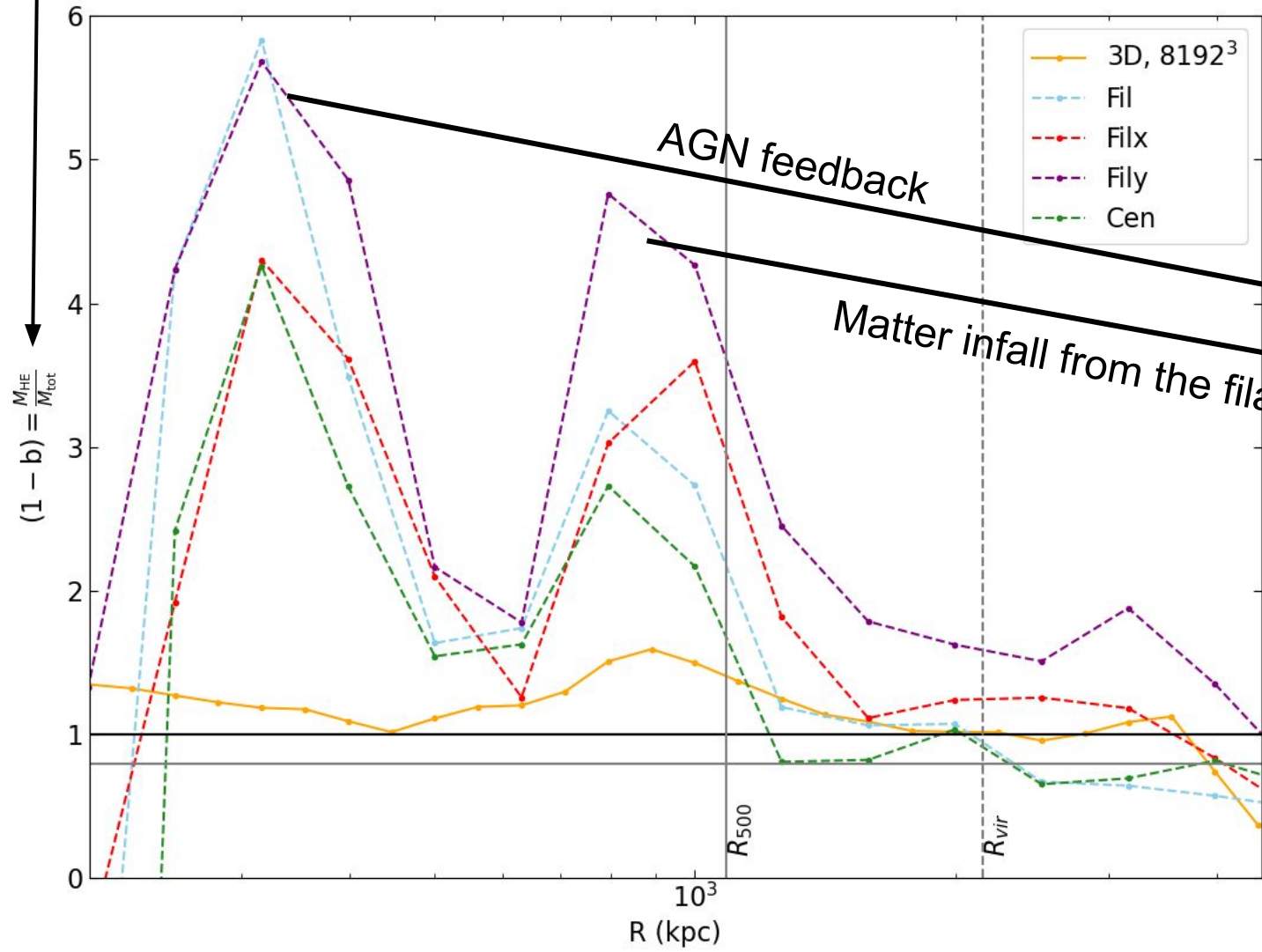
Hydrostatic mass bias from deprojected profiles

$$(1 - b) = \frac{M_{HE}(< r)}{M_{tot}(< r)} \quad M_{HE}(< r) = - \frac{r P_{th}(r)}{G \mu_n n_a(r)} \frac{d \ln P_{th}(r)}{d \ln r}$$



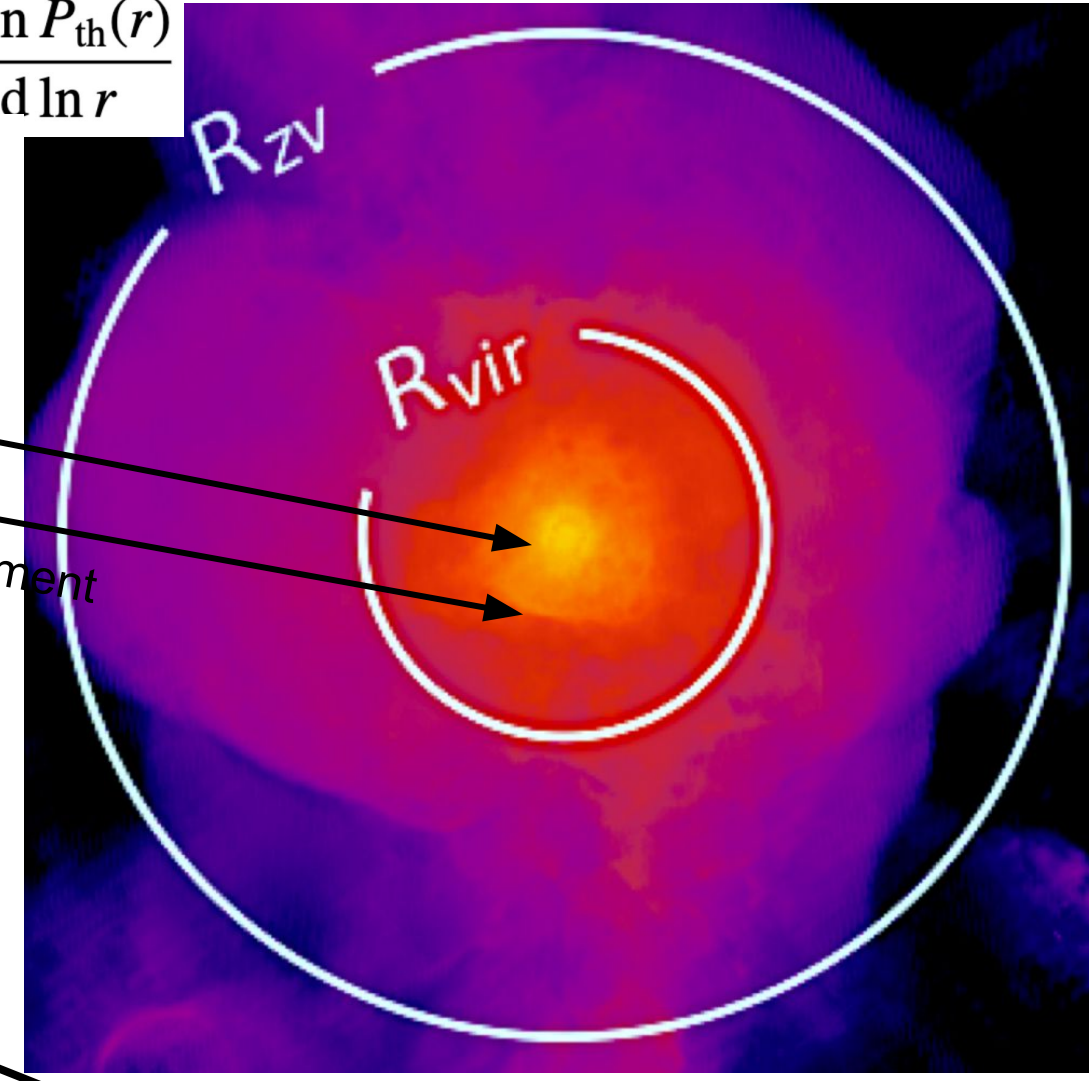
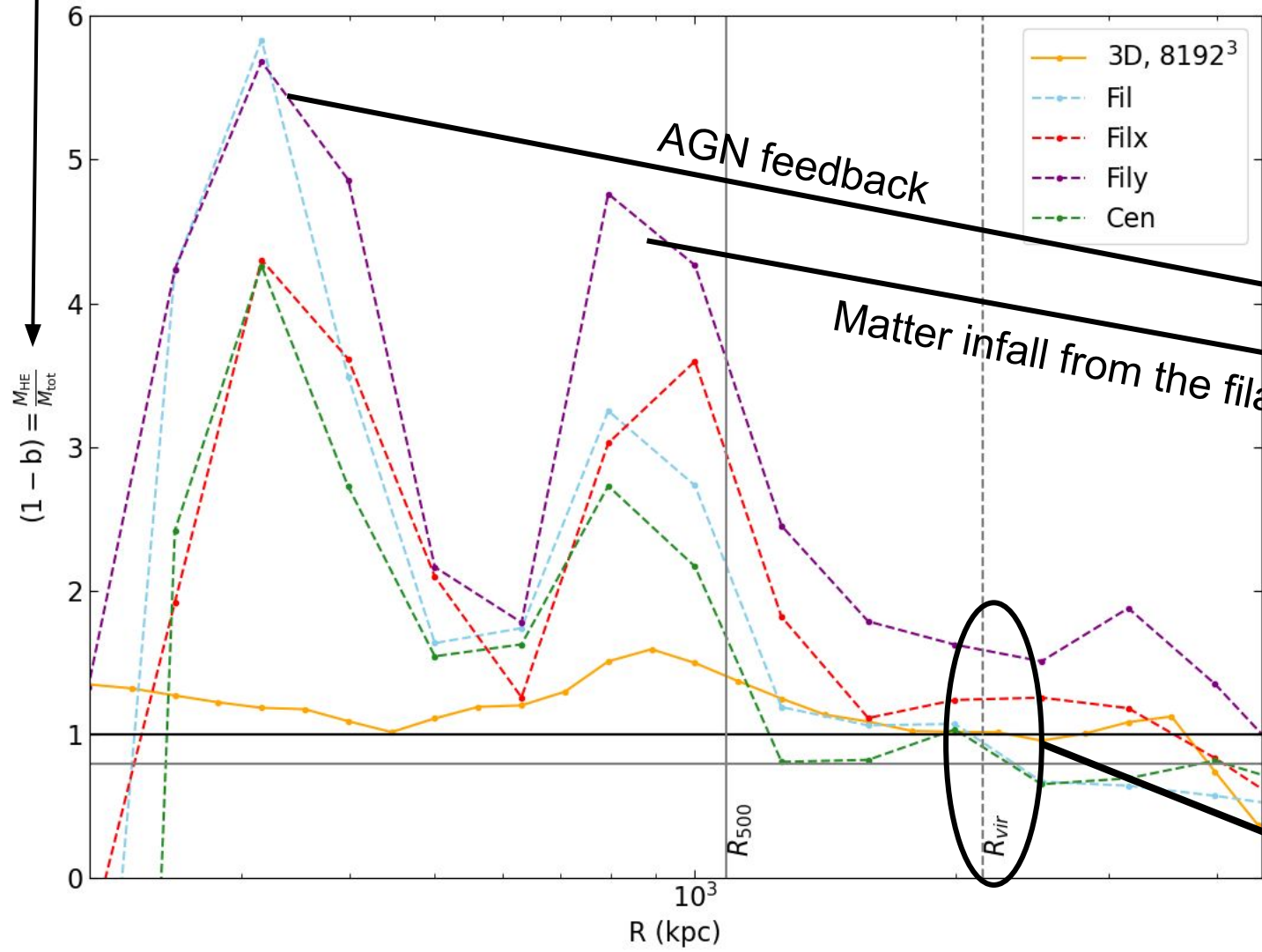
Hydrostatic mass bias from deprojected profiles

$$(1 - b) = \frac{M_{HE}(< r)}{M_{tot}(< r)} \quad M_{HE}(< r) = - \frac{r P_{th}(r)}{G \mu_n n_b(r)} \frac{d \ln P_{th}(r)}{d \ln r}$$



Hydrostatic mass bias from deprojected profiles

$$(1 - b) = \frac{M_{HE}(< r)}{M_{tot}(< r)} \quad M_{HE}(< r) = - \frac{r P_{th}(r)}{G \mu_n n_o(r)} \frac{d \ln P_{th}(r)}{d \ln r}$$



Contribution of the integrated mass to the hydrostatic mass estimation

Conclusions

- Unreliable hydrostatic mass biases derived from deprojected profiles in the cluster core, large scatter at R_{vir} :
 - Major role of the mass along the LoS on derived radial profiles and bias
 - Hydrostatic mass estimation strongly impacted by shocks in the cluster

Conclusions

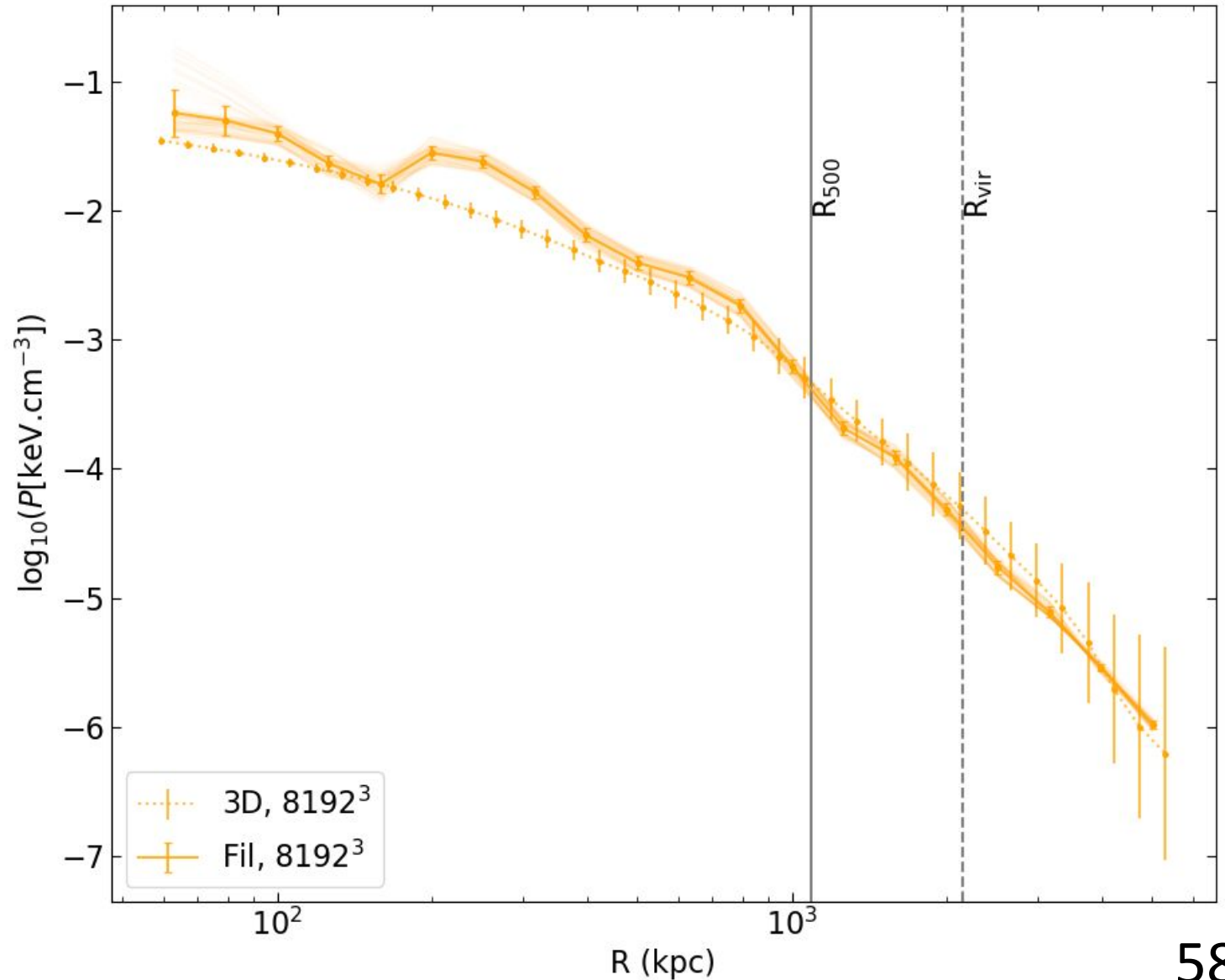
- Unreliable hydrostatic mass biases derived from deprojected profiles in the cluster core, large scatter at R_{vir} :
 - Major role of the mass along the LoS on derived radial profiles and bias
 - Hydrostatic mass estimation strongly impacted by shocks in the cluster

Perspectives and future work:

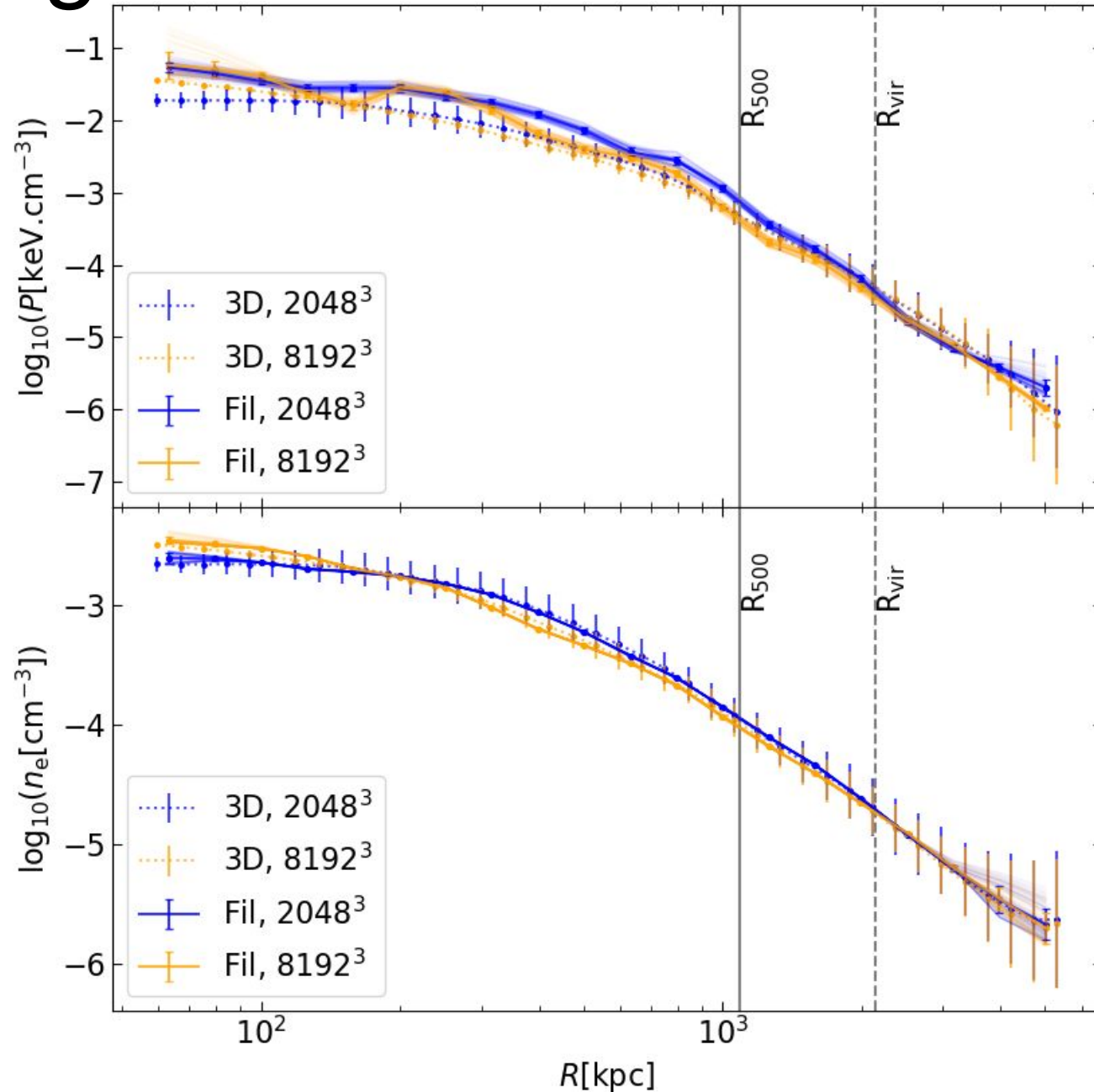
- The Virgo cluster: physical model of the cluster (shocks, dynamical state,...) and comparison to observations
- The upcoming large scale simulation : statistical study of different sources of bias

Smoothing the deprojected profiles

- Monte Carlo method: random selection of the lower and upper bounds of the deprojection process
 - Lower limit in the [50,100]kpc range
 - Upper limit in the [4000,6000]kpc range
 - 100 realizations
- Interpolation and extrapolation of the profiles in order to calculate the mean profile



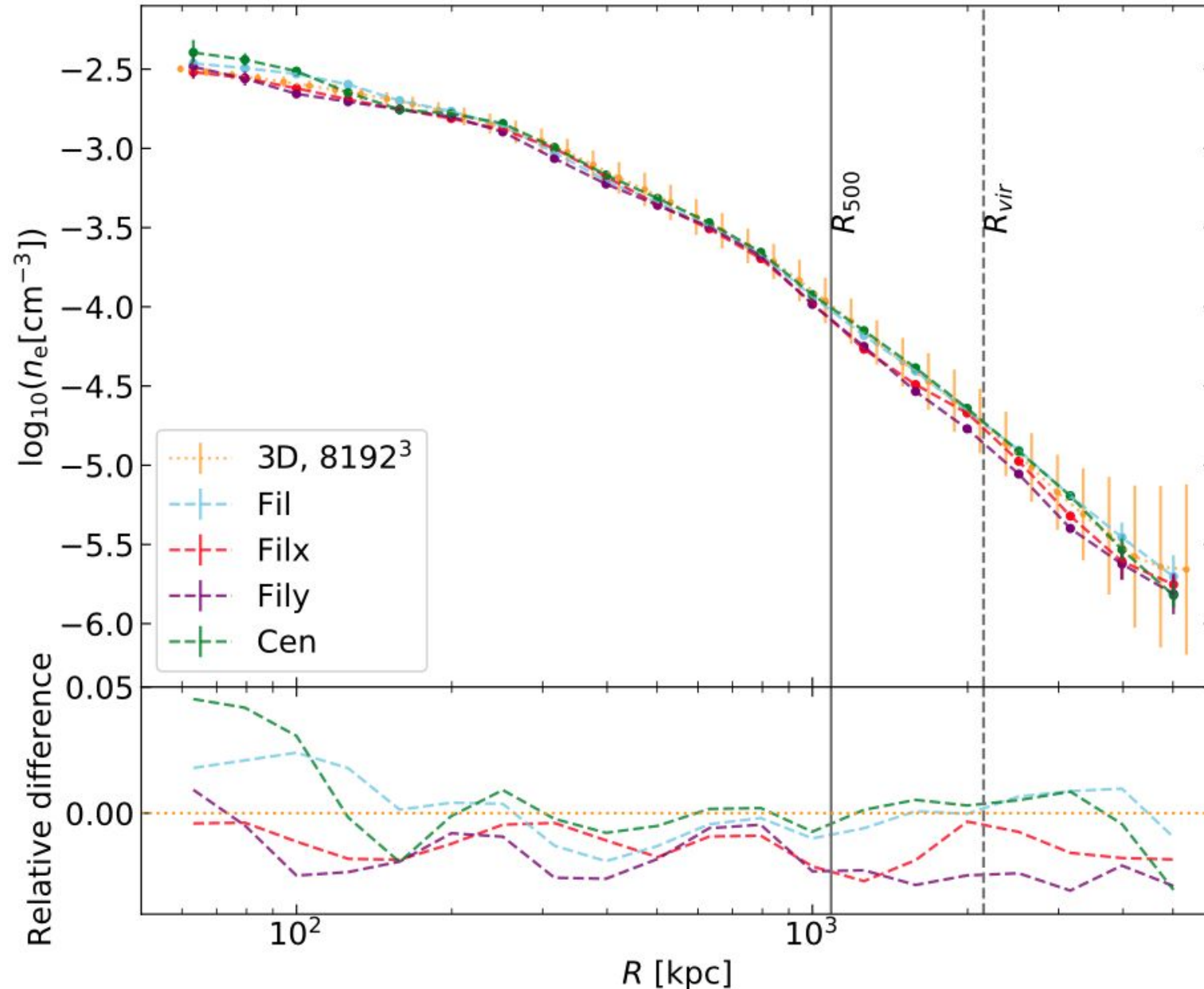
High and low resolution comparisons



The deprojected pressure profiles deviate from the 3D profiles within R_{500}

The deprojected electron density profiles are similar to their respective 3D profiles

Deprojected electron density profiles

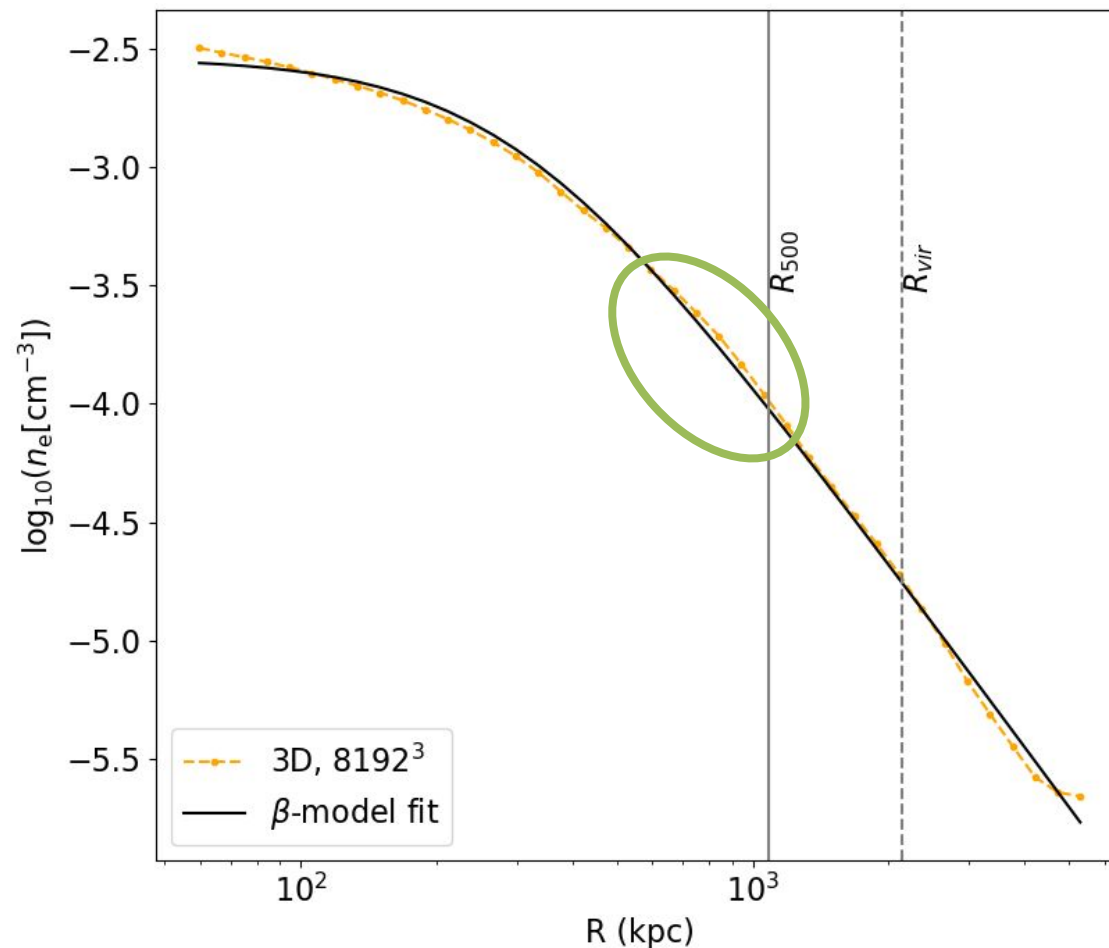
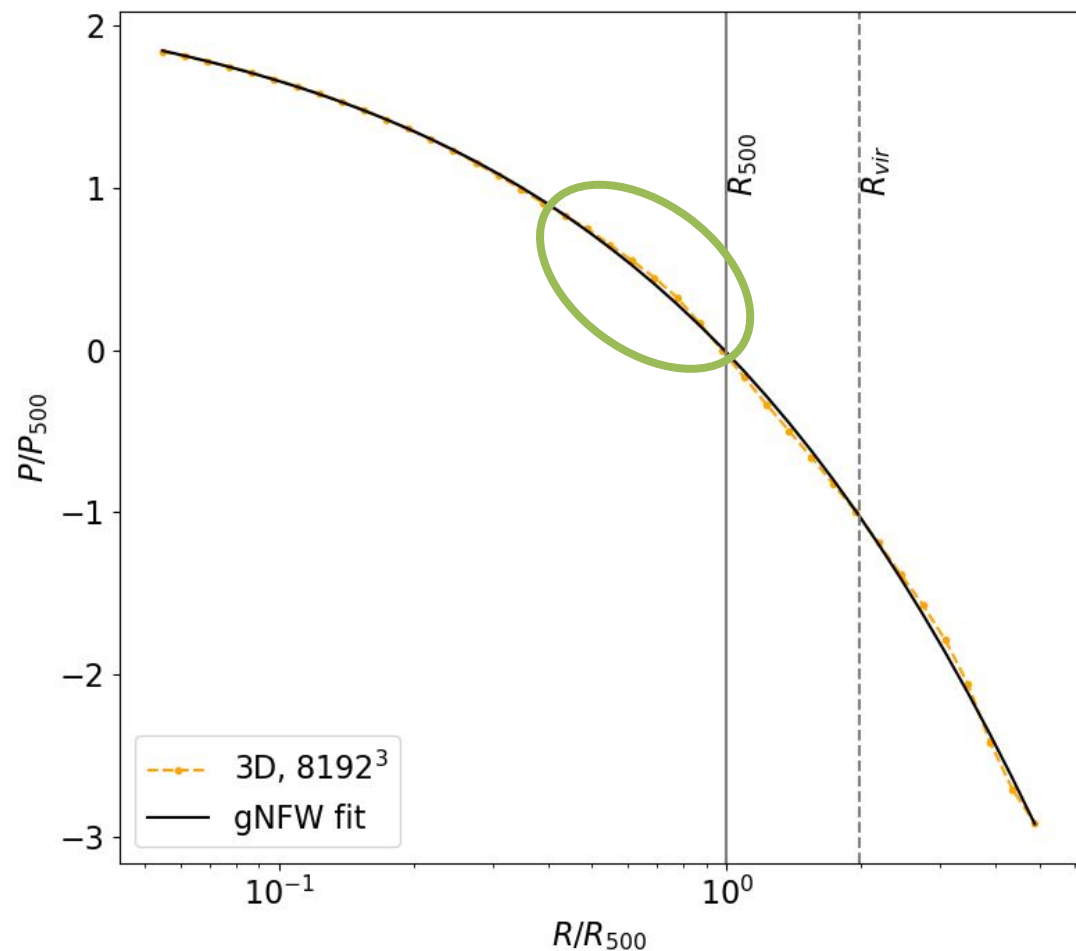


Same trend as for the projected profiles: **more mass** along the line of sight induces **higher** deprojected electron density profile

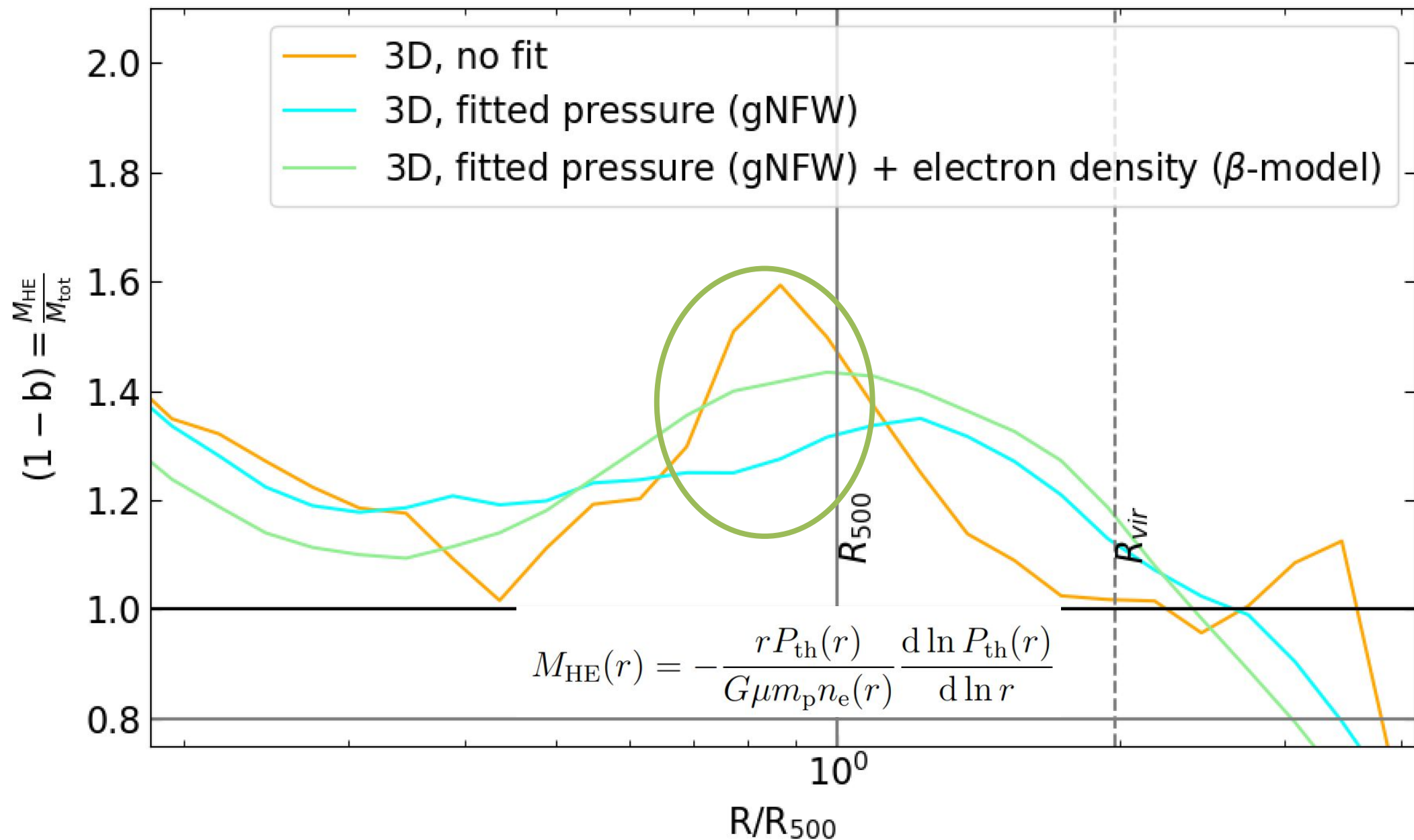
Numerical VS fitted profiles gradient (*preliminary*)

$$\text{gNFW} : \frac{P(r)}{P_{500}} = \frac{P_0}{x^c (1 + x^a)^{\frac{b-c}{a}}}$$

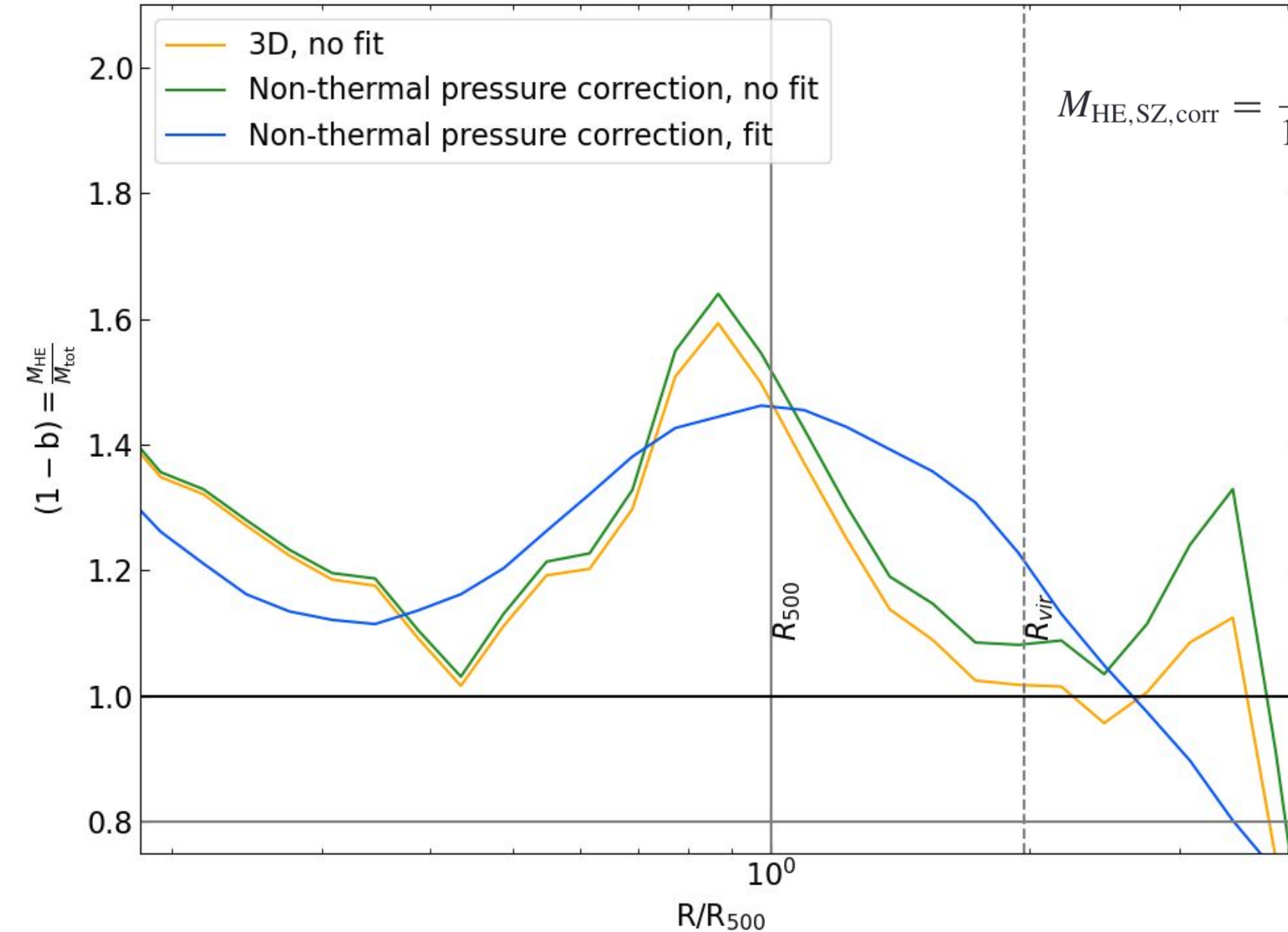
$$\beta\text{-model} : n_{\text{gas}}(r) = n_{\text{gas}}(0) \left[1 + \left(\frac{r}{r_c} \right)^2 \right]^{-3\beta/2}$$



Numerical VS fitted profiles gradient (*preliminary*)



Non-thermal pressure correction (*preliminary*)



$$M_{\text{HE,SZ,corr}} = \frac{1}{1 - \alpha} \left[M_{\text{HE,SZ}} - \frac{\alpha}{1 - \alpha} \frac{r P_{\text{th}}}{G \mu m_p n_e} \frac{d \ln \alpha}{d \ln r} \right]$$

Pearce et al. (2020)

$$P_{\text{tot}} = P_{\text{th}} + P_{\text{nth}}$$

$$P_{\text{nth}} = \rho \sigma^2$$

$$P_{\text{nth}} = \alpha(r) P_{\text{tot}}$$

Deprojection method: Electron Density

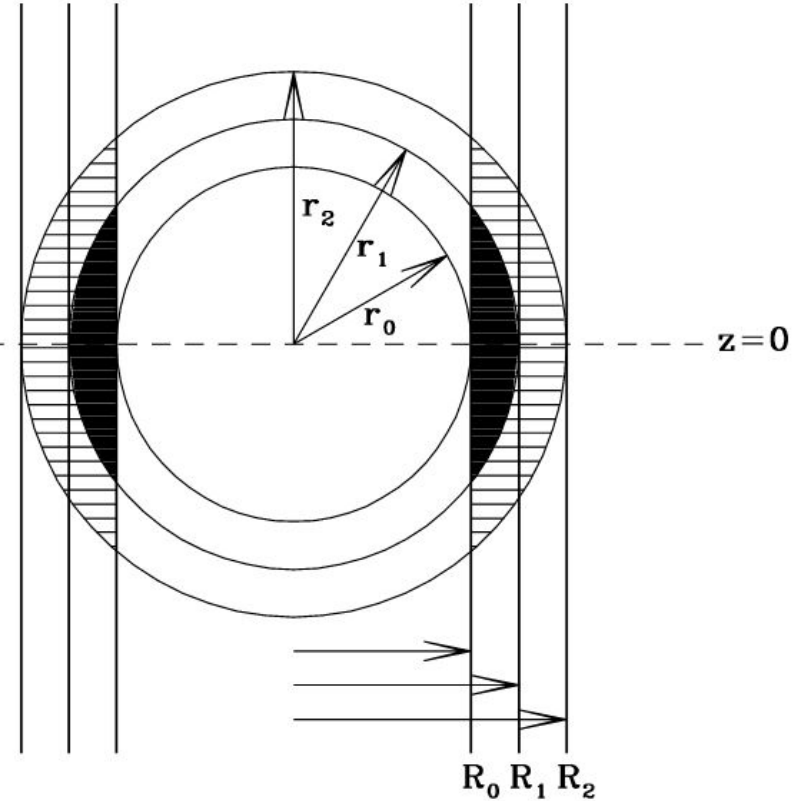
Basic example: n_e : projected electron density (in cm^{-2})
 n'_e : deprojected electron density (in cm^{-3})

Furthest annulus:

$$n_e(R_1, R_2) * \pi(R_2^2 - R_1^2) = n'_e(r_1, r_2) * V_{int}(r_1, r_2, R_1, R_2) + n_e^{back} * (\pi(R_2^2 - R_1^2) * L_{los} - V_{int}(r_1, r_2, R_1, R_2))$$

Second furthest annulus:

$$n_e(R_0, R_1) * \pi(R_1^2 - R_0^2) = n'_e(r_0, r_1) * V_{int}(r_0, r_1, R_0, R_1) + n'_e(r_1, r_2) * V_{int}(r_1, r_2, R_0, R_1) + n_e^{back} * (\pi(R_1^2 - R_0^2) * L_{los} - V_{int}(r_0, r_2, R_0, R_1))$$



Background : Mean electron density of the local environment (mean electron density in a circular annulus between 8 and 10 Mpc)

Generalisation : $V_{int}(r_{j-1}, r_j; R_{i-1}, R_i) = \frac{4\pi}{3} \left[(r_j^2 - R_{i-1}^2)^{3/2} - (r_j^2 - R_i^2)^{3/2} + (r_{j-1}^2 - R_i^2)^{3/2} - (r_{j-1}^2 - R_{i-1}^2)^{3/2} \right]$ server

$$n'_e(r_{i-1}, r_i) = \frac{n_e(R_{i-1}, R_i) \pi(R_i^2 - R_{i-1}^2) - n_e^{back} * (\pi(R_i^2 - R_{i-1}^2) * L_{los} - V_{int}(r_{i-1}, R_{amas}, R_{i-1}, R_i)) - \sum_{j=i+1}^m [n'_e(r_{j-1}, r_j) V_{int}(r_{j-1}, r_j; R_{i-1}, R_i)]}{V_{int}(r_{i-1}, r_i; R_{i-1}, R_i)}$$

Deprojection method: Pressure

Basic example: P: projected pressure
P': deprojected pressure

Furthest annulus:

$$P(R_1, R_2) * \pi(R_2^2 - R_1^2)L = P'(r_1, r_2) * V_{int}(r_1, r_2, R_1, R_2)$$

$$\Rightarrow P'(r_1, r_2) = P(R_1, R_2) * \frac{\pi(R_2^2 - R_1^2)L}{V_{int}(r_1, r_2, R_0, R_1)}$$

Ratio of the cylindrical annulus over the fraction of the sphere

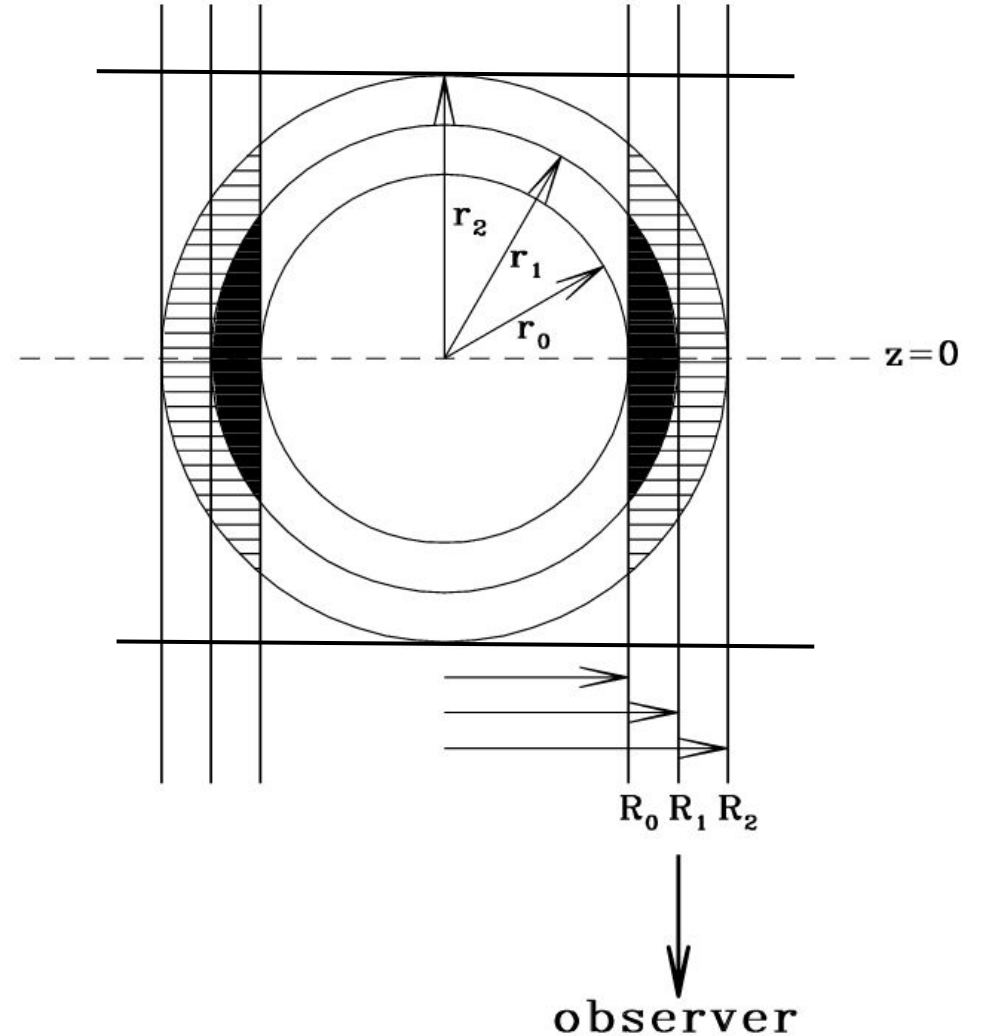
Second furthest annulus:

$$P(R_0, R_1) * \pi(R_1^2 - R_0^2)L = P'(r_0, r_1) * V_{int}(r_0, r_1, R_0, R_1) + P'(r_1, r_2) * V_{int}(r_1, r_2, R_0, R_1)$$

Background subtraction: Subtract the mean pressure of the local environment (mean pressure in a circular annulus between 8 and 10 Mpc)

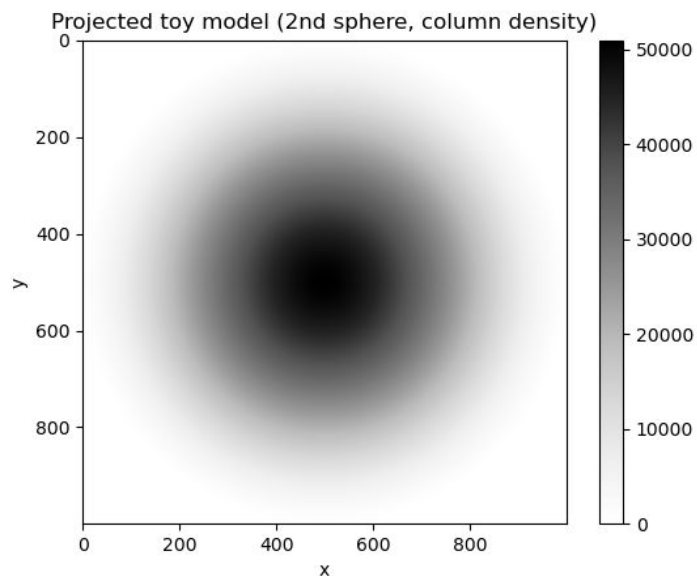
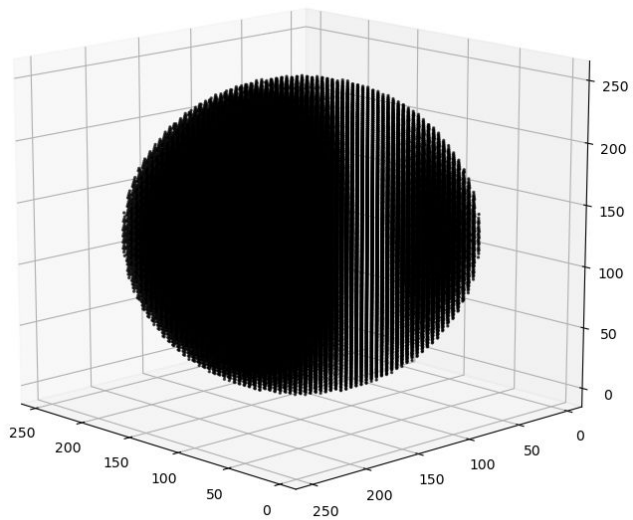
Generalisation :

$$P'(r_{i-1}, r_i) = \frac{P(R_{i-1}, R_i) \pi(R_i^2 - R_{i-1}^2)L - \sum_{j=i+1}^m [P'(r_{j-1}, r_j) V_{int}(r_{j-1}, r_j; R_{i-1}, R_i)]}{V_{int}(r_{i-1}, r_i; R_{i-1}, R_i)}$$

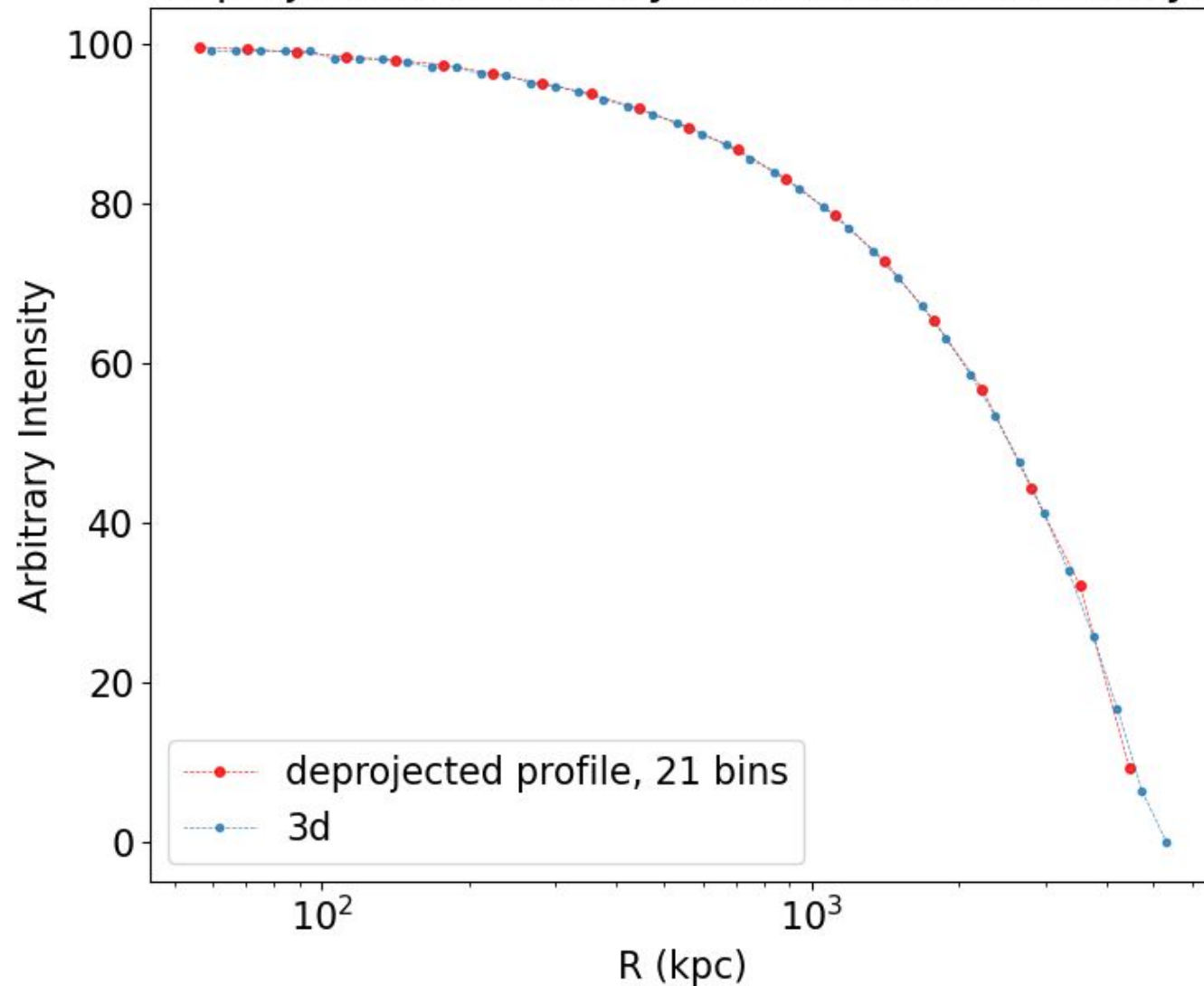


Test of the method: column density maps

Perfect sphere, values in cells varying from 100 in the center to 1 in the outskirts

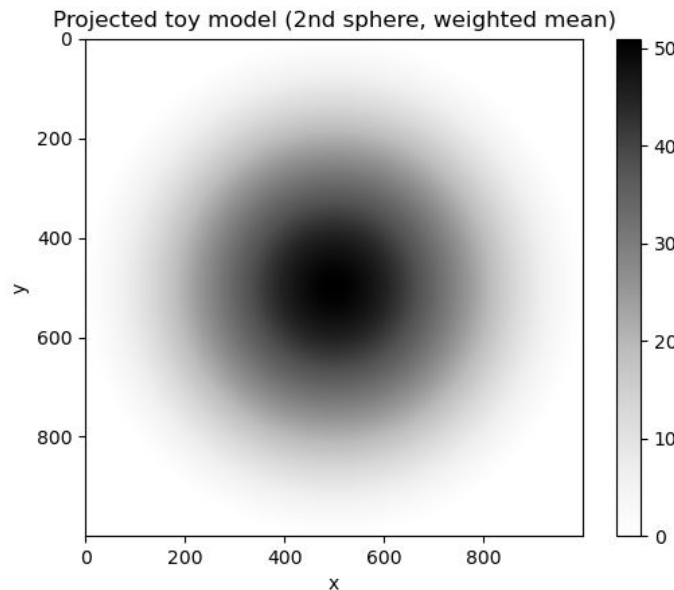
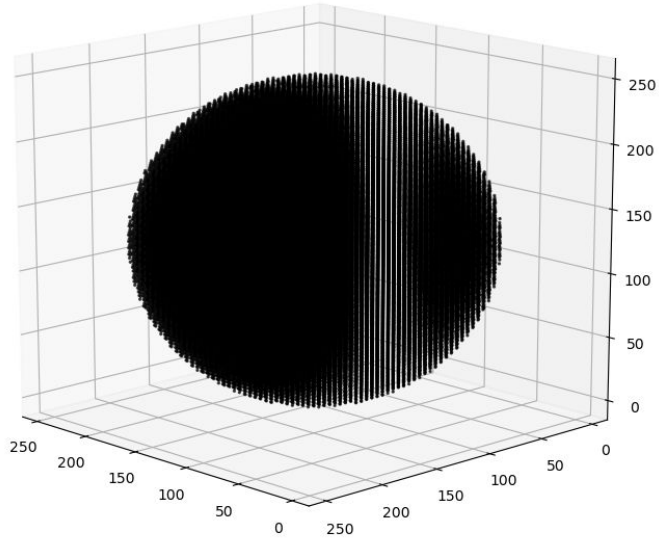


Deprojection of 2nd toy model (column density)

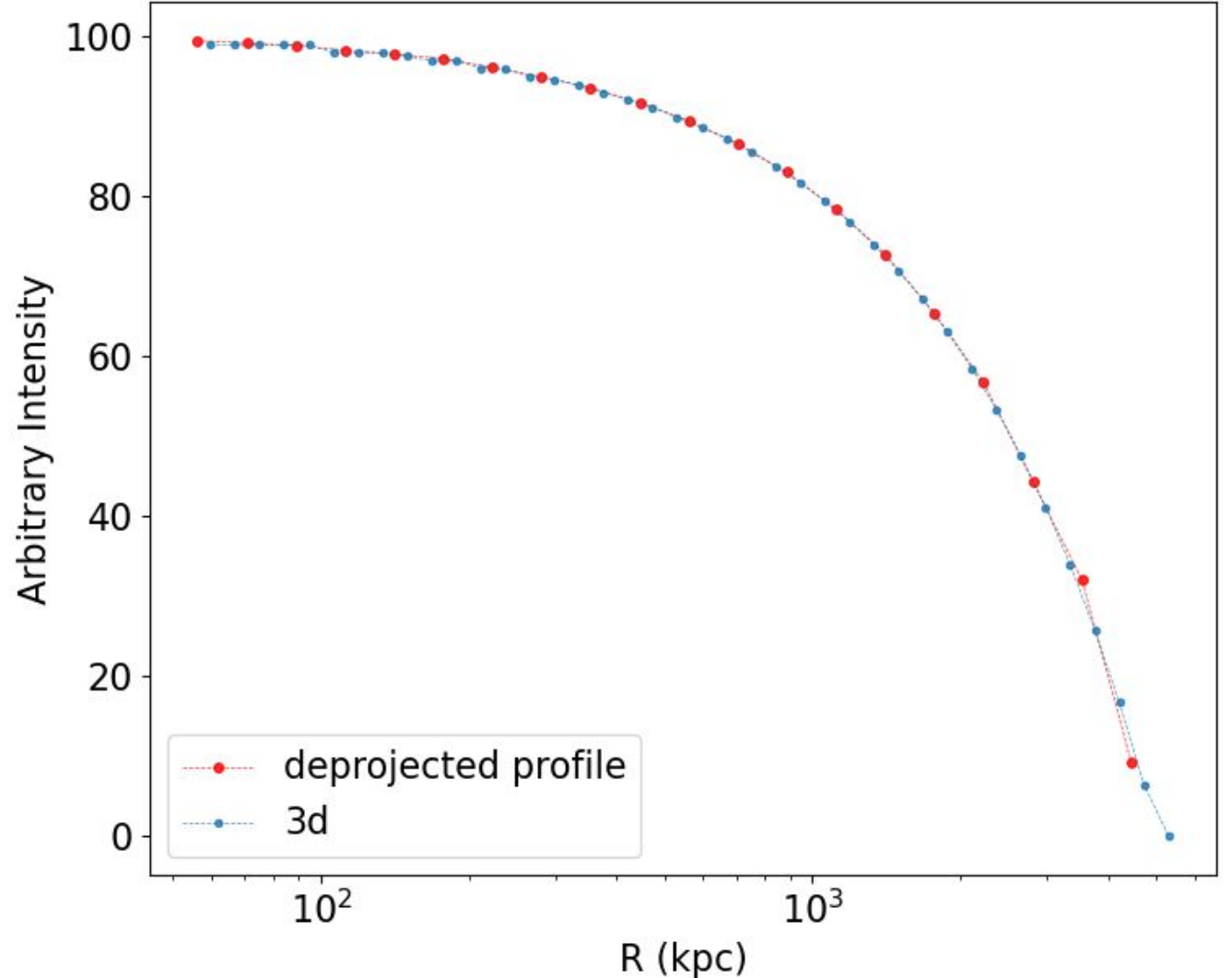


Test of the method: weighted mean maps

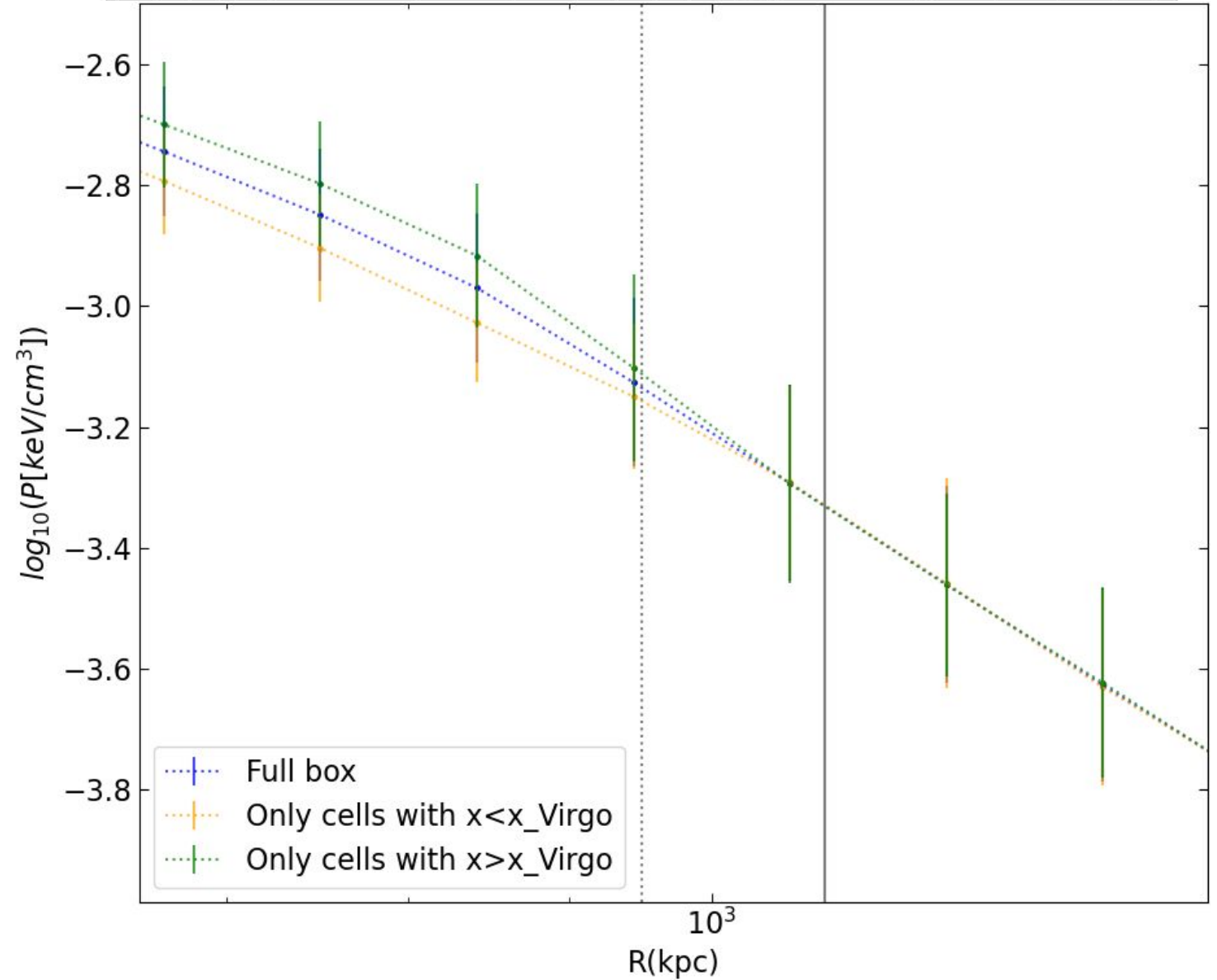
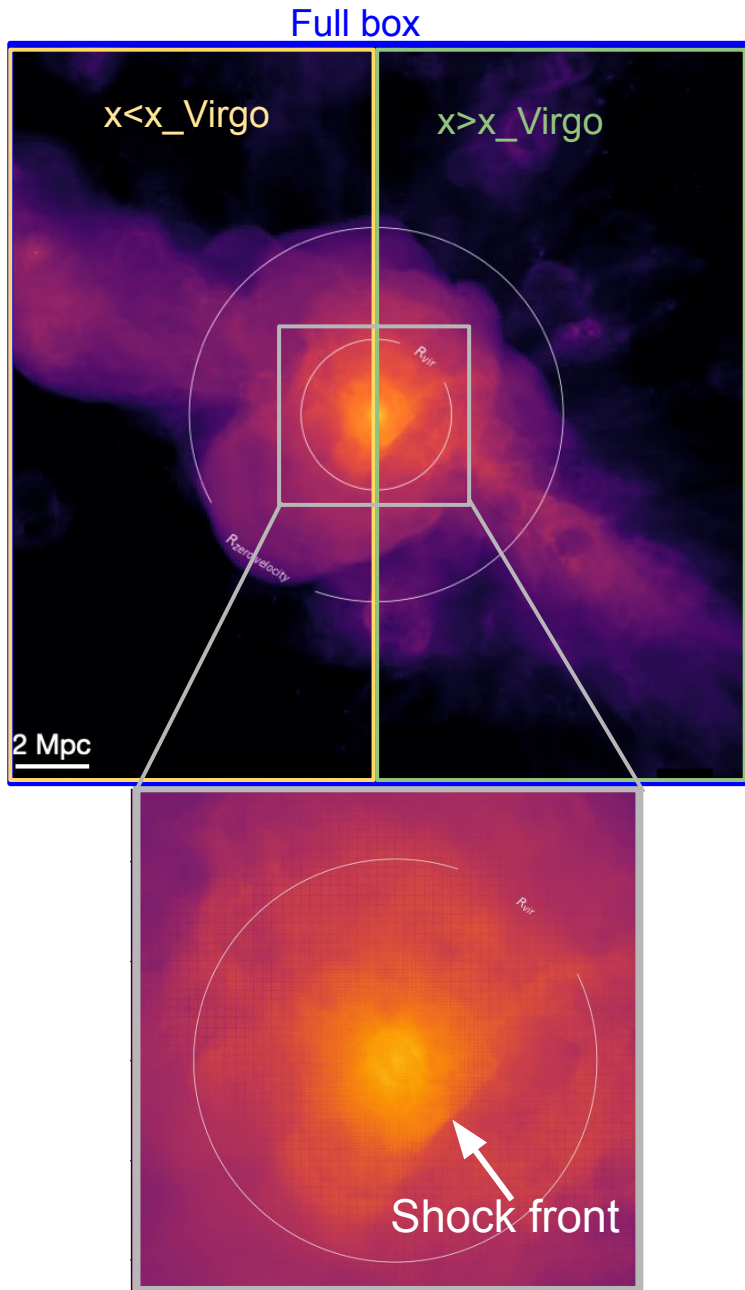
Perfect sphere, values in cells varying from 100 in the center to 1 in the outskirts



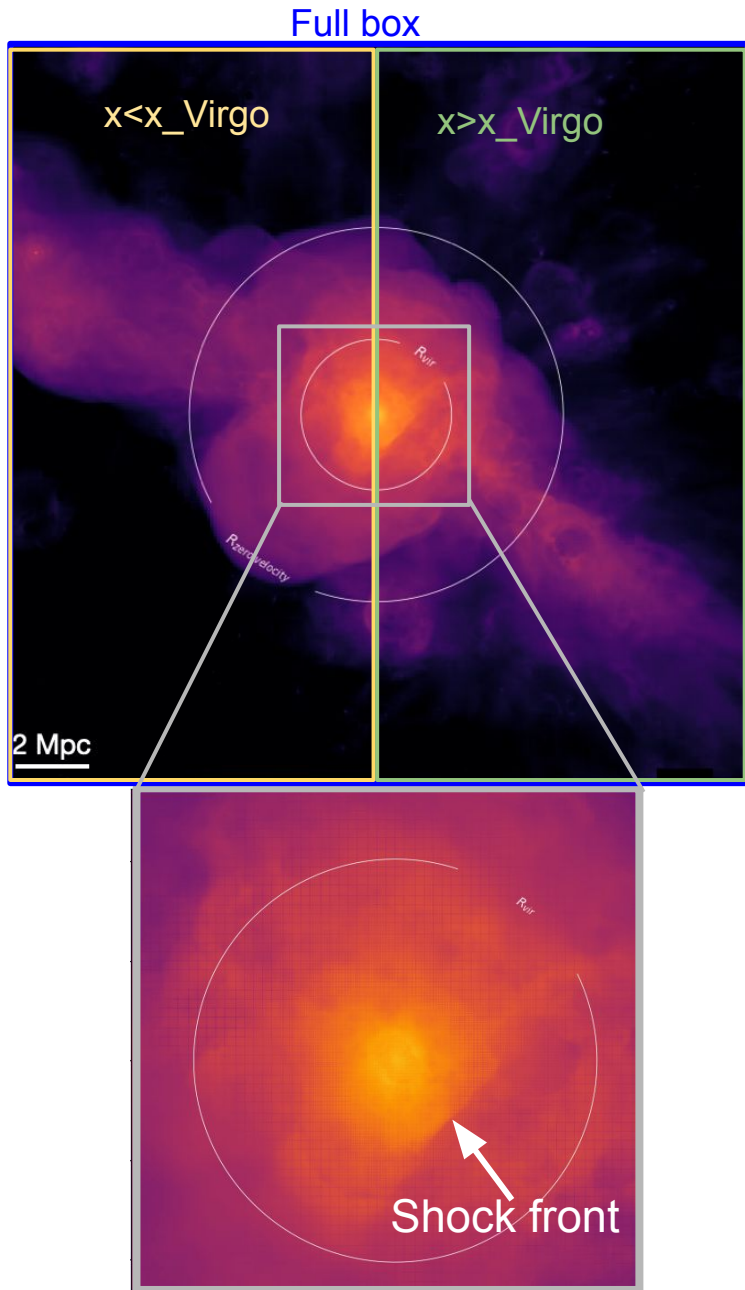
Deprojection of the 2nd toy model (weighted mean), 21 bins



Hydrostatic mass using only a fraction of the simulation box



Hydrostatic mass using only a fraction of the simulation box



simulation box

